Facial ageing and rejuvenation modeling including lifestyle behaviours, using biometrics-based approaches

Elham Farazdaghi

THÈSE

présentée par

Elham Farazdaghi

pour l'obtention de
GRADE DE DOCTEUR

de

L'UNIVERSITÉ PARIS-EST

Ecole Doctorale MSTIC

Spécialité: Signal. Images. Automatique

Facial Ageing and Rejuvenation Modeling Including Lifestyle Behaviours, Using Biometrics-based Approaches

le 6 Decembre 2017 devant le jury composé de

Prof. Liming Chen	École Centrale de Lyon	Rapporteur
Prof. Christophe Rosenberger	ENSICAEN	Rapporteur
Prof. Bernadette Dorizzi	Télécom SudParis	Présidente du jury
Dr. Régis Fournier	Université Paris-Est Créteil (UPEC)	Examinateur
Prof. Amine Nait-ali	Université Paris-Est Créteil (UPEC)	Directeur

. . . to my lovely mother
whose constant love, supports and encouragements
have sustained me throughout my life.

Abstract

The main focus of this thesis is to model the evolution trajectory of human face from infancy to senility using the biometric facial features.

The manifestation of facial changes caused by ageing depends on different factors such as genetic, ethnicity and lifestyle. Nevertheless, individuals in the same age group share some facial similarities. These resemblances can be employed to approximate the facial appearance of an individual in the bygone or the forthcoming years.

Unlike numerous studies dealing with predictive face ageing models, for the first time, this thesis proposes the first Backward Facial Ageing Model aiming at digitally rejuvenate an adult face appearance down to its early childhood. We also present the Forward Facial Ageing Model to predict the adult face appearance in its future by taking into account the natural ageing trajectory. The main purpose of Forward Facial Ageing Model is to have a base model for the supplementary ageing models such as behavioural models.

In this thesis for the first time in face ageing studies, the effects of different lifestyle behaviours are integrated into the facial ageing models. The Behavioural Facial Ageing Models predict the feature of a young face in case of having the high-risk lifestyle habits. The main attempt of these models is to illustrate the adverse effects of unsafe lifestyle behaviours on the senility of the face, aiming to prevent the youth from becoming involved in these habits. The Facial Ageing Modeling Database, contains over 1600 facial images, is collected to construct the models and 30 Face Templates for the purpose of the face ageing studies. Besides, the Face Time-Machine Database from 120 subjects is created and published to test and evaluate the results. For the proposed approach face contour and different components are modified non-linearly based on an estimated geometrical model related to the trajectory of growth or ageing. Moreover, the face texture is adapted by mapping a Face Template to the estimated geometrical model. Then, the effects of each lifestyle habit are set up to the primal predictive model.

The evaluations of the results indicate that the proposed models are remarkably accurate to estimate the correct face appearance of an individual in the target age. While the simulated facial images are realistic and have the appearance, geometrical and textural characteristics of the target age, the personal identity and details of the input face images are preserved.

Keywords

biometrics, face ageing, ageing modeling, behavioural model, geometrical model, textural model, digital rejuvenation, digital ageing, anthropology

Résumé

Cette thèse a pour objectif de modéliser, par approches biométriques, l'évolution dans le temps du visage humain, en partant de l'âge enfant, jusqu'à un âge adulte. Ces travaux sur le vieillissement rentrent dans le cadre des activités de recherche du groupe biométrie du laboratoire LiSSi (UPEC).

Comme il est connu, l'évolution des traits dues au vieillissement dépend de plusieurs facteurs intrinsèques ou extrinsèques, dont : la génétique, l'origine ethnique, le mode de vie, etc. En considérons les modèles paramétriques proposés dans cette thèse, nous exploitons entre autres, les similitudes des caractéristiques extraites chez des individus d'une même catégorie d'âge. Ces similitudes sont intégrées dans nos modèles afin de pouvoir estimer l'apparence faciale à un âge spécifique.

Contrairement aux nombreuses études traitant les modèles prédictifs de vieillissement facial, cette thèse propose pour la première fois un modèle réversible permettant également le rajeunissement numérique de l'apparence du visage que nous appellerons, modèle de prédiction arrière d'apparence. Quant à la prédiction avant, notre contribution s'est orientée vers la proposition d'un modèle non-linaire paramétrique de vieillissement permettant de prendre en considération les facteurs accélérateurs de vieillissements liés au mode de vie des individus. De manière générale, nous nous sommes intéressés aux conséquences de certaines addictions de type (drogues, alcool, exposition au soleil, etc.), sur le vieillissement prématuré du visage. Par conséquent, nous avons proposé des modèles sensibles à certains de ces facteurs en se basant sur des analyses statistiques. Comme retombés socio-économiques, cette étude a pour objectif de sensibiliser les jeunes personnes par rapport aux dangers liés à la consommation excessives de certaines substances, voire à l'addiction à certaines pratiques.

Les études que nous avons menées durant cette thèse, ont nécessité la constitution d'une base de données contenant plus de 1600 images faciales. Cette base de données a permis le développement 30 modèles de visages «Face Templates». Suite à cela, nous avons créé une base de données d'évaluation, appelée «Face Time-Machine (FaceTiM)». Constituée à partir de 120 sujets, cette base de données est mise à disposition des chercheurs afin qu'ils puissent reproduire les résultats que nous avons obtenus, évaluer les performances, et enfin contribuer à l'amélioration des modèles proposés.

Mots clés

vieillissement facial, modélisation de vieillissement, modèle géométrique facial, modèle de Texture, rajeunissement numérique, vieillissement numérique, anthropologie, biométrie.

Publications

Journal publications

E. Farazdaghi and A. Nait-ali, "Backward Face Ageing Model (B-FAM) for Digital Face Image Rejuvenation," *IET Biometrics*, DOI:10.1049/iet-bmt.2016.0079, May 2017.

E. Farazdaghi and A. Nait-ali, "Predictive Facial Ageing Model Considering Melanin and UV Exposure Factors," *IEEE Transactions on NanoBioscience*, 2018 (Under correction).

International Conferences

E. Farazdaghi, F. M. Z. Heravi, L. Chatelain, and A. Nait-ali,, "Reverse Facial Ageing Model For Youthful Appearance Restoration From Adult Face Images," *in 2016 6th European Workshop on Visual Information Processing (EUVIP)*, 2016, pp. 1–6.

E. Farazdaghi and A. Nait-Ali, "Face Ageing Predictive Model Due to Methamphetamine Addiction," *in 2016 International Conference on Bio-engineering for Smart Technologies (BioSMART)*, 2016, pp. 1–4.

F. M. Z. Heravi, M. Eslahi, E. Farazdaghi, and A. Nait-Ali, "A Morphable Model to Simulate Rejuvenation Trajectory of 3d Face Images: Preliminary Results," *in 2016 International Conference on Bio-engineering for Smart Technologies (BioSMART)*, 2016, pp. 1–4.

E. Farazdaghi and A. Nait-Ali, "Facial Ageing Model Considering Sun Exposure Effects" *in 2nd International Conference on Bio-engineering for Smart Technologies (BioSMART)*, 2017.

Book chapters

E. Farazdaghi, F. Majid Zadeh Heravi, A. Nait-Ali, "Backward Facial Ageing Modeling", in *Biometrics under Biomedical Considerations*, (Amine Nait-Ali, editor), Springer, 2018 (Under press).

F. Majid Zadeh Heravi, E. Farazdaghi, A. Nait-Ali, "Forward Facial Ageing Modeling", in *Biometrics under Biomedical Considerations*, (Amine Nait-Ali, editor), Springer, 2018 (Under press).

E. Farazdaghi, A. Nait-Ali, “Behavioural Facial Ageing Modeling”, in *Biometrics under Biomedical Considerations*, (Amine Nait-Ali, editor), Springer, 2018 (Under press).

Acknowledgements

I cordially thank Professor Christophe Rosenberger and Professor Liming Chen for accepting to review this work. Many thanks to Professor Bernadette Dorizzi and Doctor Régis Fournier for being part of my thesis jury.

I would like to express my thanks to Professor Amine Nait-Ali, my thesis director, for his consistent supports, meticulous comments, and advices throughout this long way. He is not merely a wise mentor but a great human being.

I would like to thank all my friends, Mahsa khalili, Afrooz Behroozi, Neda Ghavidel, Ashkan Noroozkhani, and Laurent Chatelain, these wonderful and lovely people whose companionship and supports empowered me.

I would like to express my appreciation to Doctor Maryam Najafi, for editing my work, despite her limited time.

My other special thanks would go to my lovely Sara Bigdeli Shamloo for decorating my thesis with her stunning digital art paintings.

And my profound appreciations belong to my companion, emotional and spiritual mate, Mehran Kordi. He has always been there, has kindly helped me, has wisely encouraged me, and his patient and gentle behaviour have made life delightful to me.

My pure thanks and appreciations to my family. My lovely parents, for their love, immense support and encouragements over the years. My beloved sisters, without the supports of whom I could not continue this journey. No words can ever be enough to tell them what they mean to me and how thankful I am to them. I am grateful to my elder sister, Arezoo, for her kindness, advices, and making me feel strong each time I felt weak. I owe thanks to my younger sister, Afsoon, for supporting and soothing me. For being a great console for all of our family, though she is the youngest one; for being strong, patient and wise. My adorable grandmother, who always motivated me and she has left a very deep impact on my life with her love and tact. There is a special corner in my heart, which will always hold gratitude for her.

And last but not the least, over and over again, for every single moments of my life, I owe appreciation and sincere thanks to my incredible mother who has stood by me through all life's storms. Mom! Whatever I am is because of you and all I have in my life is you, your endless love and supports.

And to every person who has been there. Thank you ...

Table of contents

List of figures

List of tables

Acronyms

2D	Two Dimentional
3D	Three Dimentional
AAM	Active Appearance Model
AGES	AGing pattErn Subspace
API	Application Program Interface
ASM	Active Shape Models
BFAC	Backward Facial Ageing Collection
B-FAM	Backward Facial Ageing Model
CEA	Conformal Embedding Analysis
CLM	Constrained Local Model
DET	Detection Error Trade-off
DHEA	Dehydroepiandrosterone
DWT	Discrete Wavelet Transform
EER	Equal Error Rate
FaceTiM	Face Time-Machine Database
FAMD	Facial Ageing Modeling Database
FAR	False Acceptance Rate
FERET	Facial Recognition Technology
FFAC	Forward Facial Ageing Collection
F-FAM	Forward Facial Ageing Model
FFPD	Facial Feature Points Detection
FG-NET	Face and Gesture Recognition Network
FRR	False Rejection Rate
GH	Growth Hormone
HOIP	The Human and Object Interaction Processing
ICP	Iterative Closest Point
IDWT	Inverse Discrete Wavelet Transform
IFDB	Iranian Face Database
LDA	Linear Discriminant Analysis
LK	Lucas–Kanade
LPP	Locality Preserving Projections
LTP	Local Ternary Patterns
MLS	Iterative Closest Point
MRF	Markov Random Field

MRI	Magnetic Resonance Imaging
OLPP	Orthogonal Locality Preserving Projections
PAL	Park Ageing Mind Laboratory
PCA	Principal Component Analysis
PDM	Point Distribution Models
ROC	Receiver Operating Characteristic
SBSH	Sun Behavioural Score History
SDP	Sun Damage Percentage
S-P	Sun-Phobic
SR	Spectral Regression
S-S	Sun-Seeking
SVM	Support Vector Machines
SVR	Support Vector Regression
UV	Ultraviolet Radiation
WIT-DB	Waseda human-computer Interaction Technology Database
YGA	Yamaha Gender and Age
SMAS	Superficial Muscular Aponeurotic System

Introduction

Human face is a mystery, an extraordinary combination of uniqueness and resemblances. It is a gate into the human's inner nature; an indicative of each individual's biological, anatomical, and psychological characteristics; a complex structure composed of diverse soft and hard tissue layers, contoured with complex yet delicate components and capable of demonstrating a wealth of information about ethnicity, gender, age and emotional states. However, human face is still not as mysterious as its ageing trajectory from birth to senility.

Very few things in life are as certain as ageing. We are all affected by ageing, and there is no escape. Although ageing is a definite and imminent process, it is neither uniform nor linear, and its pattern varies in different individuals. The facial ageing pattern of each individual is linked with several intrinsic factors like genetic, ethnic, gender and extrinsic factors such as gravity, geographical area, working environment, lifestyle, and many other factors that may change the health condition and consequently the ageing pattern. On the other hand, in spite of the fact that the ageing pattern generally differs from one person to another, people belonging to the same age class share certain facial similarities.

The study of these patterns and variations can improve the understanding of the ageing process. Accordingly, new branches of different fields of science and technology can be derived in order to improve the quality of human life. For example, age estimation and facial ageing modeling in the field of computer science. As a matter of fact, the common fundamental characteristics in different age classes help to classify individuals into distinct age groups as well as modeling the facial ageing process.

Concisely, age estimation aims to determine a person's chronological age based on the facial features. While, facial ageing modeling is the illustration of an individual's facial appearance in the bygone or the forthcoming years, by simulating the alterations caused by facial ageing trajectory and by using the biometric facial features.

The course of life can be divided into two broad periods; growth and ageing, respectively from infancy to youth and from youth to senescence. During the growth process, most of the facial changes are geometrical, while texture undergoes minor alterations. In contrast, in ageing trajectory, since the face and its components find their adult size and shape while entering adulthood, most of the alterations occur in texture and geometry does not undergo drastic changes.

Accordingly, a reliable model for facial ageing should be able to estimate the face in its past or future, in the different ages from each of the two foregoing periods. Thus, two kinds of models can be considered for facial ageing:

- Reconstructive Models that rejuvenate the face image down to its earlier age (young adulthood or early childhood) by providing their current facial appearance. These models have not received proper attention in the literature, and there are no existing works on adult to child digital face image rejuvenation. For the first time, a Reconstructive Facial Ageing Model has been proposed by this thesis in the biometrics research group of LiSSi laboratory.

- Predictive Models that previse the individual's facial appearance in the forthcoming years up to its 80s using their current facial image. The majority of the models proposed in previous researches are concerned with the prediction of face appearance in the future.

A complex set of external factors, including lifestyle behaviours, interact with facial ageing pattern in an individual. Therefore, besides the generic model for the natural process of facial ageing, more specific models can be conceived based on different lifestyle behaviours' effects. For example, drug and alcohol abuse, smoking and sun exposure are some of the high-risk behaviours that considerably affect face ageing and can be serious concerns for Behavioural Facial Ageing Models.

The effects of lifestyle habits are not considered so far in the ageing studies. This study for the first time integrates these influences into the ageing models.

Behavioural Models are Predictive Models that demonstrate a person's face in the future in case of having the high-risk lifestyle behaviours, such as drug abuse, sun exposure, alcohol intake, smoking, etc. These models can visually notify that although chronological age cannot be changed and internal factors cannot easily be influenced, healthy lifestyle and supervising the external factors can greatly impact the individual's appearance age.

A reliable model of facial ageing trajectory in its different modes such as Reconstructive, Predictive or Behavioural has many and diverse applications. Some of these applications are: forensics, criminal investigation, finding missing people, modeling suspects' faces, face recognition (age normalisation), movie special effects in the film industry, visual arts and entertainment, computer graphics, cosmetic surgery, planning the facial transplant, anthropology, high-risk lifestyle behaviours prevention, automatic updating of biometric systems, and many other applications.

This thesis addresses a research aimed at proposing some reliable image-based models for the evolution trajectory of the human face from infancy to senility. Fur-

thermore, the effects of different lifestyle behaviours manifested throughout life are considered.

The fundamental objectives of this thesis are:

1. Filling the void of childhood face modeling in facial ageing studies, because the proposed models by previous literature did not take it into consideration. Most of the prior studies consider Predictive Models to estimate the face appearance in the future. For those few works that present reconstructive models, rejuvenation is considered from old ages to young adulthood.

2. Proposing a Predictive Facial Ageing Model for global and natural ageing process, irrespective of extrinsic factors, which (in addition to its independent applications) may be the foundation for any supplementary Predictive Model.

3. Presenting an approach that integrates the effects of different lifestyle behaviours into the proposed model for the natural ageing process. This approach can be a reference for modeling the effects of different behavioural factors on face in the future. The main purpose of such models is to show the young generation a realistic perspective of their future face in case of having the risky lifestyle. It can give them the opportunity to make wise and conscious decisions about their habits.

With these objectives, the thesis is commenced with raising the following three questions about the evolutionary trajectory of human face from birth to senility:

- What kind of changes occur in the face throughout the growth procedure and which components' changes are important for 2D facial growth modeling?
- What kind of changes arise in the face during ageing trajectory?
- What are the lifestyles most commonly linked with aspects of facial ageing and how do they affect the face's apparent age?

Thesis Contributions

In this thesis the below mentioned main contributions are made:

1. The Backward Facial Ageing Model (B-FAM) is proposed, aiming at digitally rejuvenating an adult person's face down to its being 3-4 years old using the corresponding adult face image as an input. This thesis proposes the first

model for adult face rejuvenation down to early childhood. In the proposed approach, different facial components and face contour are adjusted nonlinearly, based on a reliable Geometrical Model. The texture is estimated by mapping the Reconstructive Face Template, belonging to the target age group, to the estimated Geometrical Model.

2. Forward Facial Ageing Model (F-FAM) is constructed. This model approximates the face in its old ages, taking into account the natural ageing trajectory, by employing the respective young adult facial image as input. Although this model has its own applications, the principal purpose of this model is to be employed as the Primal Facial Ageing Model for any other supplementary ageing models such as the Behavioural Models. F-FAM emphasises on the facial texture transformations from input age to the target age, by employing the related Predictive Face Template, mapped to the estimated Geometrical Model. While facial geometry has minor, yet not ignorable, changes.

3. Behavioural Facial Ageing Models are presented. This is the first time that the effects of lifestyle are considered in facial ageing modeling. The main goal of these models is to show the damaging effects of the high-risk lifestyle habits on the face by estimating the young faces in their not too distant future in case of being exposed to them. For each lifestyle behaviour, an Effectiveness Factor is calculated that is the difference between the perceived age and the chronological age of the population exposed to that high-risk habit. Two Behavioural Facial Ageing Models are presented: first, Methamphetamine Addicts' Facial Ageing Model is offered to show the catastrophic effects of using this substance on the face. Further, Sun Damage Facial Ageing Model is proposed to illustrate the adverse impacts of overexposure to the sun.

4. A private database, named Facial Ageing Modeling Database (FAMD) which contains about 1600 facial images is collected. This database consists of two albums that have been used to construct the B-FAM and F-FAM models. Besides, using FAMD, 30 Face Templates are constructed in different age clusters from both life periods: 8 Reconstructive Face Templates in 4 different age clusters from the growth period, 12 Predictive Face Templates in 6 different age clusters from the ageing period, and 10 Coalesced Face Templates in 5 different age groups. These Face Templates can be used as the face prototypes for different age studies.

5. The Face Time-Machine Database (FaceTiM V1.0) which consists of 246 facial images from 120 subjects, is created essentially to test and evaluate the results. It includes two sets: “Set 1” comprises of adult face images, and “Set 2” contains childhood face images related to the individuals in set1, that can be used as the reference to evaluate the results. This database is available for facial ageing researchers.

Thesis Structure

In Chapter 1 the state of the art on facial ageing studies is presented. A literature review is done on two main topics: the human perception of the facial growth and computer vision studies on facial ageing phenomenon. Ageing studies from the standpoint of the computer vision are reviewed in two sections: studies conducted on age estimation and previous works on facial ageing modeling. The noteworthy contributions in the facial ageing modeling topic, sorted in date order, are cited along with explaining the methods of the proposed works.

Chapter 2 addresses fundamentals, containing algorithms, methods and databases used within this study. First, feature extraction is discussed. The different methods for extracting the facial feature points are presented. The AAM is selected to locate facial features, and compositional Lucas-Kanade is used for fitting AAM. Then, image warping is presented. The Moving Least Squares (MLS) using rigid transformation is explained as the main approach for image warping. After that, different existing face ageing databases are mentioned. Then, two collected databases, FAMD and FaceTiMV1.0, are introduced. Afterwards, image normalisation is discussed. Face Template construction is the last part of this chapter.

Chapter 3 presents digital facial image rejuvenation using Backward Facial Ageing Model. It starts with perusing craniofacial morphology growth in addition to defining the components’ size and distances used in geometrical measurements. For the proposed model, first, a Geometrical Model is constructed to change the facial components and the face contour. Next, the facial texture is estimated by mapping the appropriate Reconstructive Face Template to the estimated Geometrical Model. The results are evaluated using both subjective and objective criteria.

Chapter 4 introduces Forward Facial Ageing Model (F-FAM) that approximates the face in its future in the natural life conditions. This Chapter opens with a brief statement of the different structural layers of the face, comprising of skeleton, muscle, fat and skin and the effects of ageing on each layer. In this proposed model, since the input face meets its adult size, minor geometrical changes are applied. Face texture is

adapted to the target age using the corresponding Predictive Face Template. Finally, an objective performance evaluation is performed to assess the achieved results.

Chapter 5 proposes Behavioural Facial Ageing Models. First intrinsic and extrinsic influential determinants of facial ageing are discussed. Then, the general approach to construct the Behavioural Facial Ageing Models is explained. Furthermore, two Behavioural Facial Ageing Models are proposed: Methamphetamine Addicts' Facial Ageing Model and Sun Damage Facial Ageing Model. The aim of these models is to illustrate the damaging impacts of these high-risk lifestyle behaviours on the face.

The thesis is concluded in Chapter 6, with the discussion on results and envisioned perspectives.

Chapter 1

State of the Art on Facial Ageing Studies

Contents

This chapter provides the current state of the art on the facial ageing problem along with offering a historical overview pertaining to facial ageing modeling and its development.

Studies into facial ageing start with human perception of facial growth and understanding the similarities between anthropometric transformations and mathematical functions. Furthermore, facial ageing has been brought to attention by computer vision community. Computer vision works on facial ageing are either on age estimation or facial ageing modeling that can be defined as the reverse of each other.

Previous researches presented different approaches, mostly based on statistical models derived from a set of training face images to adapt the facial texture and shape to a target age. These proposed models of facial ageing often predict the face in its future based on the natural ageing process. Few works reconstruct the face in its past, mainly to show an old face in its youth. However, childhood face modeling receives no attention in the facial ageing models.

In this chapter, first, facial ageing from human perception standpoint is discussed in Section 1.1. Then in Section 1.2, computer vision studies on facial ageing phenomenon are brought up. The chapter is concluded in Section 1.3.

1.1 Facial Ageing from Human Perception Standpoint

In 1970's characterising the facial growth phenomenon started with increasing the interest to analyse the patterns of changes in characterising events [1].

By inspiration emerging from the event perception, Shaw et al. [2] defined the process of ageing as an "animate event" (versus "inanimate event") in which the ageing transformation is a symmetric operation. They detect the structural invariants of the events and the dynamic invariants of the transformations associated with the facial growth. They observed the symmetry group of ageing transformation that shows: the structural invariant specifying the species (by which different persons of the same age range can be categorized); and the more specific structural information (by which the individuality of a face is recognizable, and the same person in different age ranges can be identified). They tried to find a mathematical transformation that can help to characterise the human face from childhood to maturity. They also detected two kinds of transformations that are applied on the contour of the face in its profile view: "shearing transformation" that affects progressive change in the overall angulation of face profile, and "strain transformation" that is a kind of stretching of the face in a vertical dimension. They were aware of the fact that these two transformations did not characterise all the information by which the faces are recognised, however, they believed that by this initial success, the other proposed techniques of facial analysis would be yielded.

Pittenger and Shaw [3] proposed a theory for the face perception based on "the concepts of transformational and structural invariants". They examined the relative significance of three special patterns of growth: "strain", "shear" and "radial" growth. By inspiration of Thompson's study of morphogenesis [4], they invented two transformations that demonstrated the strain and shear components, respectively: "cardioid strain" and "affine shear". Their study indicates the radial component cannot be an appropriate model of growth by itself, as it does not produce a remodeling of facial proportions. However, "cardioidal strain" incorporates a radial component that can be an aspect of growth. In their experiments, the effect of each transformation on the perceived age was measured by recording the opinions about the relative age. Therefore, they implied a profile transformed by "strain transformation" shows more reliable rank-order age judgments than those transformed by shear. They also inferred that the small changes in "cardioidal strain" are very important and the sensed identity of a shape is maintained under the "strain transformation". They proposed "cardioidal strain transformation" as a mathematical model for morphological transformations of the human cranium as a result of growth.

Todd et al. [5] examined the association of the five different transformations with growth, namely, “cardioidal strain”, “spiral strain”, “affine shear”, “reflected shear” and “rigid rotation”. They obtained a new transformation, related with facial growth, by remodeling the head in accordance with the pressure gradient on a fluid-filled spherical object based on hydrostatics analysis. This transformation is referred to as a “revised cardioidal strain” since it is highly similar to the “cardioidal strain”. The distinction between these two transformations is that the “revised cardioidal strain” transformation affects the size of the face in a way that is more matched with the effects of the actual growth. The growth of the human head simulated by the use of the “revised cardioidal strain transformation” is shown in Figure 1.1.a.

Mark et al. [6] examined a geometrical framework for distinguishing styles of change, as an extension of Pittenger and Shaw’s [3] work. They differentiated the transformations by the pattern of change that they produce. For example, similarity transformation moves each point out along a radial line from the origin. Moreover, they indicated that every transformation maintains the unique set of properties in the transformed object. Similarity, for example, leaves angles invariant, but it changes the length of all lines without maintaining the proportions among them. Therefore, they distinguished three geometric invariants related to the facial growth that should be preserved across any transformation inducing growth-related changes: “the angular coordinate of each point” on the head, “bilateral symmetry across the vertical axis”, and “continuity of the profile contour”. They indicated that “cardioidal strain” and “spiral strain” are more similar to actual growth rather than “affine shear”, “reflected shear”, or “rotation” because the latter do not preserve one or more of the three invariants.

As regards the facial representations used in previous experiments were the two-dimensional profiles of human heads and were lacking the internal details, Mark and Todd [7] made an effort to increase the perceptual salience of human face by applying a growth model to the entire surface of the head in three-dimensions. In fact, in their experiment, the “cardioidal strain transformation” was extended to the three dimensions and applied to a 3D (three-dimensional) representation of the head in a direction that made the transformed head appear younger.

The researches on human perception of facial growth did not terminate at this level and were continued by examining the effects of different 3D aspects of the face in human perception of facial age [8][9][10].

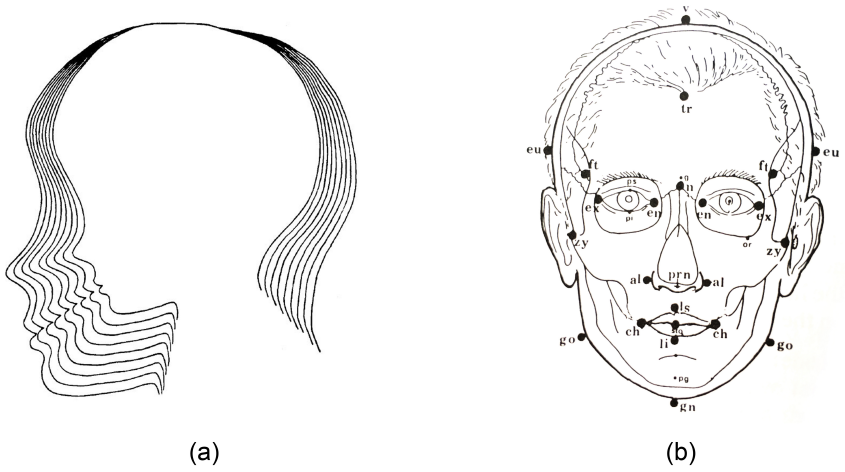

(a) (b)

Figure. 1.1 (a) The growth of the human head simulated by the use of "revised cardioidal strain transformation" from infancy (innermost profile) to adulthood (outermost profile) from [5]. (b) The schematic drawing of craniofacial landmarks of the human face in frontal aspect by Farkas [11].

1.2 Computer Vision Studies on Facial Ageing Phenom-enon

In the recent years, human faces have been taken into consideration from the computer vision standpoint in order to automatically characterise the information related to different aspects of the face including age.

The age-related studies from computer vision's perspective can be broken down to age estimation and ageing modeling that are each other's inverses. Although this research concentrates on the ageing modeling, the principles of age estimation are still relevant and some methods of automated age estimation can be used to perform the ageing simulation.

Moreover, proposed models for facial ageing trajectory can be categorised to Predictive Models which aim to age facial images, and Reconstructive Models in which the goal is facial image rejuvenation. These rejuvenation models can change an aged adult facial image to the young adults, i.e. this part is more concerned with textural modifications or can estimate an adult face appearance in its childhood, which is more challenging and requires alterations in both geometry and texture.

1.2.1 Automatic Age Estimation

Facial age estimation can be defined as estimating the age of a subject based on the biometric facial features on the basis of facial images.

One of the earliest approaches of facial age classification is using the face anthropometry to extract distances and ratios from different facial regions. Farkas [11] provided an accurate anthropometric data on the human face growth mainly for European-descent faces. He defined face anthropometry by covering measurements taken from 57 landmarks on human faces over different ages, 6 to 18 years and adults. These 57 landmarks and obtained measurements are shown in Figure 1.1.b.

The pioneers of the studies on age classification are Kwon and Lobo [12] that classified the facial images into three age groups: babies, young adults, and senior adults. Their proposed method was based on the craniofacial development theory and skin analysis. They employed six ratios of distances between facial features, as well as wrinkle analysis to estimate the age. First, babies have been distinguished from young adults and senior adults by computing the facial ratios. Then, a wrinkle geography map has been used to measure the wrinkles. The seniors are distinguished from young adults and babies by a computed wrinkle index. They employed "snakes" [13] to characterise the facial wrinkles. If wrinkles are found, and ratios indicate an adult face, the image is marked as a senior adult. An image with no wrinkles and baby-like ratios between features is marked as a baby (See Figure 1.2) . Yet, since their method for a location such as deformable templates and "snakes" was computationally expensive, the system was not fast and suitable for real-time processing.

Horng et al. [14] proposed a variance of Kwon and Lobo's work [12] for the classification of facial images into four age groups: babies, young adults, middle-aged adults, and old adults. Their presented system was composed of three phases: location, feature extraction, and age classification. Firstly, they located the facial features by finding high-intensity regions within an edge map of the face image. These features were then used to compute two distance ratios to distinguish between babies and adults. Secondly, they employed Sobel filtered images, instead of "snakes", to measure the number of the wrinkles on face images. The benefit of Sobel operator made their method simpler and faster.

Anthropometric methods for facial age estimation has been continued by many researchers. For instance, Izadpanahi and Toygar [15] presented a method based on the facial geometric features to determine the face age group. In this method, they extracted seventeen geometric feature points and ten facial measurements and classified the facial images to five age groups. They used three different classifiers for age classification, namely, "neural network classifier", "support vector classifier",and "normal densities-based linear classifier".

The anthropometry models are generally useful for face growth in young faces. However, they are not appropriate for adults. Moreover, the anthropometric models

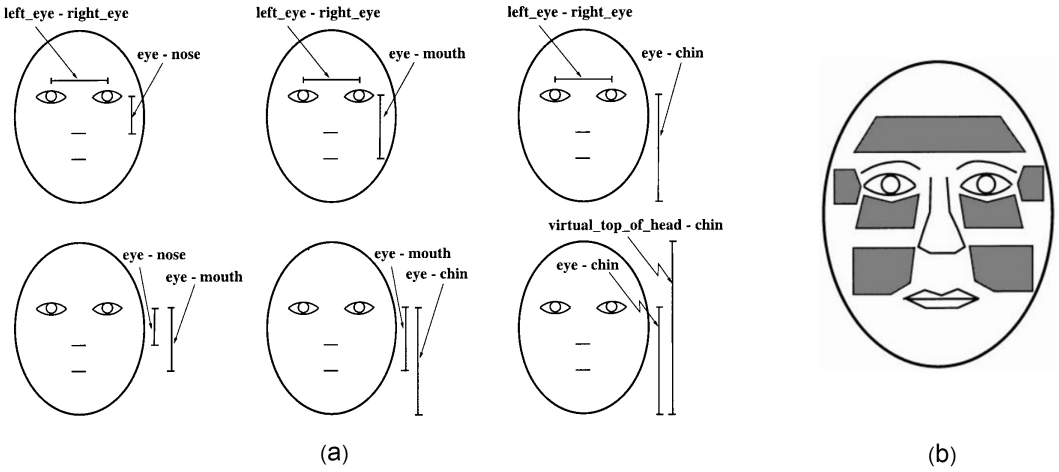

Figure. 1.2 (a) 6 ratios of distances between facial features used by Kwon and Lobo [12] to classify the facial features in different age groups. (b) The regions that are searched for facial wrinkles from [12].

only consider the facial geometry but not any texture information. These models are also sensitive to the head pose and usually frontal faces are used to measure the facial geometries [16].

Lanitis et al. [17] generated a statistical model of facial appearance, based on Active Appearance Model (AAM) [18], as the basis for obtaining a compact parametric description of facial images. They tried different classifiers for modeling the relationship between face model parameters and age, based on their age image representation, especially the quadratic ageing function.

In general, AAM based approaches can consider shape and texture rather than just facial geometry. Additionally, these methods can deal with the different age groups rather than only young ages [16]. AAM will be discussed in detail in Chapter 2.

Luu et al. [19] also used AAM to extract a combined feature vector of the facial images. They divided the classifier into two main steps. First, a binary classifier is built by Support Vector Machines (SVM) to separate youths (0-20) and adults (21-69). Then, a growth function and an adult ageing function are trained with Support Vector Regression (SVR) on youth and adult datasets respectively. For classification, first, the test image is assigned to one of the two age groups and then delivered to the corresponding age function, to estimate the exact age. Based on this work, they modified the classifier construction by adding a supervised Spectral Regression (SR) after extraction of the combined AAM feature vector [20]. SR could help to reduce the dimensionality of the feature vector. It minimises the inter-class distances while the intra-class distances are maximised. Luu et al. [21] employed the local and holistic facial features to classify a face as young or adult roughly. They combined the holistic

AAM features that are outstanding in the childhood, and the Local Ternary Patterns (LTP) features that are important for the aged faces.

Geng et al. [22], instead of dealing with each ageing face image separately, used a sequence of an individual's ageing face images all together in order to model the ageing process. To develop their method named AGES (AGing pattErn Subspace), they introduced the ageing patterns as a series of face images which are sorted in age. AGES has two steps: learning step and age estimation step. Each image is first represented by its feature vector extracted by the Appearance Model. Using Principal Component Analysis (PCA), instead of using isolated images for training, a subspace of ageing pattern is learned. If the face images from all ages are available for an individual, the corresponding ageing pattern is called a "complete ageing pattern"; otherwise, it is called an "incomplete ageing pattern". This method can synthesise the missing ages by using an iterative learning algorithm in which with each iteration a part of the missing personal ageing pattern is estimated by use of the global ageing pattern model learned so far. For age estimation, the feature vector of the image is calculated and employed to find a proper ageing pattern in the subspace by searching for the projection in the subspace achieving the smallest reconstruction error of the feature vector. Then, the test face is verified at every possible position in the ageing pattern, and the proper one is indicated by the minimal reconstruction error.

To improve their previous work, Geng et al. [23] introduced a new version of AGES, named AGES$_{lda}$. They added the Linear Discriminant Analysis (LDA) to the extracted feature vectors by the Appearance Model, to control the pose, illumination and expression variations. They built a "two-layer age estimation" system: first, test samples were classified into the three most consistent age ranges by using AGES. Then, three separately trained subspaces were used to assign the exact age. The problem of the AGES methods is that they need face images of the same person at different ages and this requirement is difficult to comply as it is not easy to collect the facial images of the same person at different ages and in the same conditions. Moreover, the AAM method only encodes the image intensity, not the texture patterns. Therefore, facial wrinkles are not included.

Instead of learning the ageing pattern for each person, the ageing pattern can be learned from many persons at different ages. The conceivable approach to learn the common ageing pattern is the age manifold [24][25][26]. For example, Fu and Huang [25] used the manifold embedding to learn the low-dimensional ageing pattern from many images at each age. In this technique, there is no necessity to present many different ages for each person. They employed various manifold learning techniques

such as Orthogonal Locality Preserving Projections (OLPP), Locality Preserving Projections (LPP), and Conformal Embedding Analysis (CEA), etc.

Geng et al. [27], to estimate the facial age proposed an algorithm named IIS-LLD to learn from the label distributions. They introduced a label paradigm to assign a label distribution to each image instead of a single label of the real age. In their method, one instance can contribute in the learning of multiple classes by extending the single label of an instance to a label distribution. This method is effective in the condition that the classes are correlated to each other and the training data for some classes is insufficient.

1.2.2 Modeling the Facial Ageing Trajectory

Facial ageing modeling is to approximate an individual's face in its past or future by employing the biometric facial features, using an input face image. Facial ageing models can be divided to:

- *Predictive Facial Ageing Models* which model the ageing trajectory and show the face in its future.
- *Reconstructive Facial Ageing Models* which rejuvenate the facial images. It can be even more precise to the rejuvenation from old adult to young adult, or from adult to the child.

Burson and Schneider [28] proposed one of the first algorithms for ageing faces. Their innovation started with the distinction of the certain characteristics which change in almost all faces to represent them as a limited number of typically aged faces such as thin men, fat men, fat women, and thin women. In their work, an image of an old face and an image of a corresponding young face were recorded. Then, the differences between old and young faces were found and recorded. Afterwards, the other recorded face images were modified and displayed with the discovered differences. (See Figure 1.3).

Burt and Perrett [29] studied relevant visual signs to age by using "facial composites" which combine shape and colour information from several faces in an age group. They considered 7 age groups for adult facial images, each spanning 5 years in the range of 20-54 years old. First, composite faces were created for each age group by computing the average face shapes and colour information for all the facial images belonging to that age group. Then, differences between the feature positions of a target face and the average of the faces in the age group were exaggerated by automated shape "caricaturing". The same algorithm was employed to caricature the age-related

Figure. 1.3 Input (left) and output (right) of the age progression method by Burson and Schneider [28].

colour information. Then after, by merging the differences between composite faces from different age groups with real face images, they marked that the perceived age of the transformed face images will increase.

Rowland and Perrett's [30] method was also based on the facial prototypes creation for different age groups to perform the predictive gender and age transformations. The database images were warped based on the locations of feature points. Average faces of the different age groups were computed and the difference warp field and the colour change were applied to the novel faces.

A research group tried to characterise a pattern of change for the ageing parameters. To find these parameters, Pitanguy et al. [31], first, defined the variation of certain face regions where the ageing process is noticeable. Then, measured the variations of 26 parameters of frontal and 17 parameters on the profile images in two different ages. By these measurements, the curves of facial ageing parameters were obtained. Then, Leta et al. [32] and Pitanguy et al. [33], manipulated facial images using these obtained ageing curves.

Tiddeman et al. [34] represented the face by 2D (two-dimensional) shape vectors as well as pixel intensities in the face images each belonging to an age group and then superimposed the difference on the primary face. To do this, they defined the shape of each face in the set with 179 points located around the facial features and face border. They used the facial prototypes just to define the differences between two sets of images.To apply the differences on a facial image: the face's new shape was calculated, subject and prototypes were warped to the new shape (Figure 1.4), and finally, colour at each pixel was transformed. Tiddeman et al. [35] carried on to achieve the more realistic texture by improving the facial texture characterization. They introduced a method based on "locally estimated probability distributions". They separated the high and low-resolution information by transforming the image into a wavelet domain. Then, calculated a mapping from the original set to the target set based on the "probability distributions" of the input and output wavelet values at each

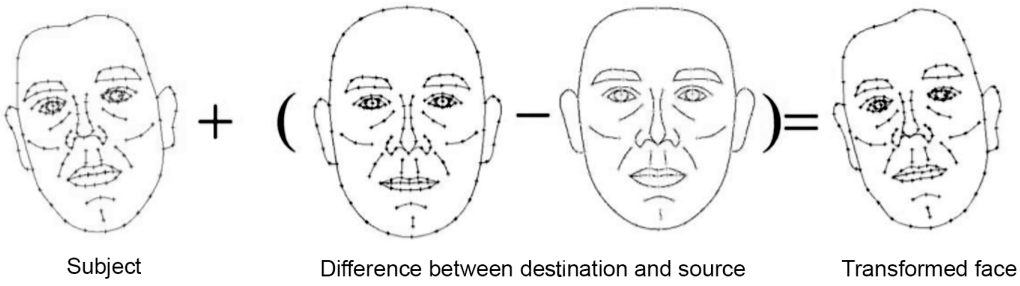

Figure. 1.4 Illustration of the shape transformation approach by [34].

point. These distributions were estimated from the example images using the Markov Random Field (MRF) assumption and were estimated by smoothing the histogram of example values.

Lanitis et al. [36] generated a statistical appearance model for face ageing. They found three formulations for ageing function: linear, quadratic, and cubic. This ageing function is proposed to explain the age variations. It estimates the relationship between the age of a person and its model parameters. In fact, they generated the in-between ages by computing the random face vectors in the region of interest, estimate their age and average face images in a group that have the same age. To simulate the facial ageing, they searched for the nearest neighbour in the database and used the ageing curve of that face.

Scandrett et al. [37] presented a semi-automatic procedure in which PCA was applied to a set of faces in order to construct shape and texture models. Two different age progression algorithms were examined to predict the effects of ageing: a linear and a "piecewise method" based on the average trends. The results of the linear model are persuasive for the huge age gaps such as 10 years. The outcomes of this model for the small ageing gaps can also be reliable for adults since their face shape do not change remarkably over the time. For the ageing of children, the "piecewise model" is more appropriate.

Ramanathan and Chellappa [38] proposed a model for the craniofacial growth of human faces during formative years (0–18). They were inspired by the "revised cardioidal strain transformation" growth by Todd et al. [5], and also considered the collected anthropometric measurements of facial landmarks by Farkas [11]. However, their proposed approach did not take into account the textural variations across age.

Then, in continuation of their work, Ramanathan and Chellappa [39], introduced a computational model to characterise the shape and texture variations in adult faces. They proposed a parametric muscle model for human face shape manipulation, by inspiration from Waters' muscle model [40]. His model identifies three types of

Figure. 1.5 An example of the appearance prediction across ages by [39]. The 1st column is the input image. The 2nd column illustrates the shape transformation results for the weight changes across ages. The 3rd, 4th, and 5th columns illustrate the textural variations induced on the shape transformed image, using image gradient transformations that stand for the "subtle", "moderate", and "strong" wrinkles.

facial muscles based on their functionalities: "Linear muscle", "Sheet muscle", and "Sphincter muscle". The texture was manipulated by "an image gradient-based texture transformation function" that characterises the facial wrinkles and other effects of ageing. They considered the shape transformation for the different types of weight change (gain/loss) across ages. In addition, three classes of wrinkle variations are considered for the texture model: "subtle", "moderate" and "strong" wrinkles. Figure 1.5 demonstrates an example of their results.

Suo et al. [41] presented a "multi- resolution dynamic model" to simulate the face ageing by using both geometrical and textural information. They adopted a "high-resolution grammatical face model" [42] to the large variations of the facial structures and completed the model with age and hair features. In this model, they integrated the global appearance changes in face shape, hair style, deformations and ageing effects of facial components, and wrinkle appearance in various facial zones. They also adopted a dynamic Markov process on their age graph. This generative model was trained based on a dataset of face images which were manually divided into different age groups and annotated into hairs and facial components. An example of their simulation results is shown in Figure 1.6

Ubaid et al. [43] used the textural variation to predict and classify the human facial ageing. In their proposed methodology, the facial regions with more age-related textural variations, more specifically "feature cheek", were concentrated for estimating the age. Feature area detection was done by applying Hough transform on the images. They extracted different properties such as contrast, correlation, homogeneity, entropy from the cheeks and tried to reduce the dimension of the data. In their proposed system the Polynomial Regression method was used for age prediction and classification by defining a polynomial from the known age and using the defined polynomial for testing.

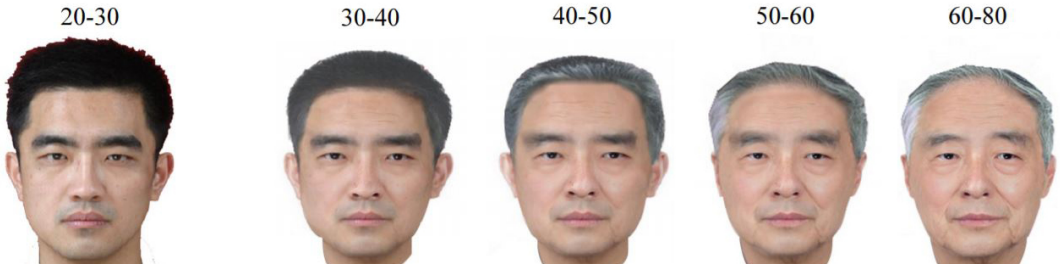

Figure. 1.6 An example of the simulation results from [41]. The leftmost image is the original image. The 2nd to 5th images are synthetic aged images at 4 consecutive age groups.

Kemelmache and Suwajanakorn [44] represented an "illumination-aware age progression" which takes a child face image as an input and creates a set of facial images at different ages as an output. Same as some previous works, they constructed their ageing model based on composite faces built from a group of the faces in the same age range, as well as anthropometric changes. To perform the age progress on a face photo, first, the pose was corrected by warping the input face to approximately frontal pose. Then, the source and target age cluster averages were relighted to match the lighting. Then after, flow age difference between two age clusters was applied. Finally, the change ratio variation in head shape was performed.

Shu et al. [45] tried to automatically render ageing faces in a personalised way on a set of age-group specific dictionaries. They believed that the ageing process should contain the personalised facial characteristics such as mole, birthmarks or permanent scar, and prototype-based age simulation methods cannot preserve them. In their method, first, the multiple "ageing dictionaries" were designed for different age groups. Moreover, the ageing layer and the personalised layer for an individual were defined in order to capture the ageing characteristics and the personalised characteristics, respectively. Then, they trained all "ageing dictionaries" on the collected short-term ageing database. For an input face, they rendered the personalised ageing face sequence from the current age to the future age step by step on the learned "ageing dictionaries".

Some few Reconstructive Models have been previously proposed. In these rejuvenation criteria, face variation is mapped from aged adults to young adults, not to childhood. For instance, Bastanfard et al. [46] offered a modeling algorithm to rejuvenate the old adult facial images to young adult with two techniques. These techniques are the facial deformation based on the "face anthropometrics theory", and remove wrinkles based on what they called "wrinkles inpainting".

Later, Guo [47] tried to make faces look younger by separating ageing details from facial structures without using any learning examples with keeping facial identities. Their proposed system contains three steps. First, an input colour face image is

decomposed into face structure, ageing detail, and colour. Second, the specular highlight in the original facial image is recovered. Third, to create an anti-ageing face image, the face structure, colour, and the recovered specular highlight are combined.

Table 1.1 lists the notable contributions in the facial ageing modeling topic, sorted in date order, and by specifying the type of the proposed model based on being predictive or reconstructive.

Table 1.1 The list of the notable contributions in the facial ageing modeling topic sorted in date order.

No	Reference	Summary of contributions	Date	Type
1	Burson and Schneider [28]	Proposed one of the first algorithms for ageing faces. They recorded the differences between the old and young faces and modified the other young face with that differences.	1981	Predictive
2	Burt and Perrett [29]	Studied relevant visual signs to age by using facial composites which combine shape and colour information from multiple faces. Their proposed method was based on creating the prototypes for different age ranges.	1995	Predictive
3	Rowland and Perrett [30]	Their proposed method was also based on prototypes. The difference warped field and the colour change were applied to the input image to change its age.	1995	Predictive
4	Pitanguy et al. [31]	Characterised the variations of parameters in frontal and profile images for two different ages and obtained the curves of facial ageing.	1996	Predictive
5	Leta et al. [32]	Manipulated facial images using the ageing curves obtained by [31].	1996	Predictive
6	Pitanguy et al.[33]	Determined a pattern of change for facial parameters during the ageing process based on the numerical fitting of measures from the samples.	1998	Predictive
7	Tiddeman et al. [34]	Demonstrated the face by 2D shape vectors and pixel intensities in the face images and then superimposed the difference on the primary face.	2001	Predictive
8	Lanitis et al. [36]	Generated a statistical appearance model to simulate the facial ageing by searching for the nearest neighbour in the database and used the ageing curve of that face.	2002	Predictive
9	Bastanfard et al. [46]	Offered a modeling algorithm by facial deformation based on the “face anthropometrics theory” and removing wrinkles.	2004	Reconstructive (aged adult to young adult)

10	Tiddeman et al. [35]	Proposed a method based on locally estimated probability distributions for improving the realism and influentiality of facial transformation.	2005	Predictive
11	Scandrett et al. [37]	Presented a PCA-based semi-automatic procedure to construct the shape and texture models. They examined a “linear” and a “piecewise” age progression algorithms.	2006	Predictive
12	Ramanathan and Chellappa [38]	Employed anthropometric parameters to define the deformation of the face during child growth.	2006	Predictive
13	Suo et al. [41]	Introduced a “multi-resolution dynamic model” by using the both geometrical and textural information.	2007	Predictive
14	Ramanathan and Chellappa [39]	Proposed a model which comprises the shape variation model and the texture variations model in adult faces.	2008	Predictive
15	Guo [47]	Made faces look younger by detaching ageing details from facial structures without using any learning examples.	2011	Reconstructive (aged adult to young adult)
16	Ubaid et al. [43]	Used the textural variation to predict and classify the human facial ageing by concentrating on the facial regions with more age-related textural variations.	2013	Predictive
17	Kemelmache and Suwajanakorn [44]	Represented an approach that takes a single photograph of a child as input and automatically produces a series of age-progressed outputs between 1 and 80 years of age.	2014	Predictive
18	Shu et al. [45]	Tried to automatically render ageing faces in a personalised way on a set of age-group specific dictionaries.	2015	Predictive

1.3 Conclusion

In this chapter previous works in the field of facial ageing have been reviewed. It is inferred that the early works have used non-statistical methods which employ the similarities between the anthropometric changes of head and mathematical functions. Most of the recent works have used the statistical methods to present a model using a set of facial images as the training data. Then, the shape and texture variations have been applied to the input image based on the achieved statistical models.

From the literature review, it is deduced that almost all of the formerly proposed models for face ageing are predictive models and few works have been done in facial image rejuvenation. While there is no work that can approximate the childhood face appearance based on an adult facial image. Moreover, all of these models are based on the natural ageing process, and the effect of the lifestyle behaviour on face apparent age has been neglected.

In the course of this work, some desirable methods and algorithms have been used to integrate into the face ageing models, most of which have been employed by studies cited in this chapter. However, the employment of them may be different from the former works. For instance, AAM and its fitting methods, image warping, and face prototypes. These observed methods and algorithms will be explained in the next chapter.

Chapter 2

Fundamentals for Model Construction

Contents

This chapter presents appropriate and essential methods and algorithms, as well as other essentials for creating a model from facial ageing process. For instance, feature extraction method, image warping algorithm, and the proper database of facial images. Most of these methods and algorithms have been employed by previous works as mentioned in Chapter 1.

It is worth mentioning that the purpose of this chapter is not to introduce the new algorithms for pattern recognition or image processing, rather the aim is the timely and effective use of existent techniques in order to integrate an efficient model. Each of these methods is an extensive topic by itself, but this chapter is confined to the brief discussion of them.

Chapter is organised as follows: First, facial feature point extraction is discussed in Section 2.1. Image warping is explained in Section 2.2. In Section 2.3 facial ageing image databases and image normalisation are presented. Then, face template construction is described in Section 2.4. Chapter is concluded in Section 2.5.

2.1 Facial Feature Points Extraction

In order to attain a better insight of human face, its prominent characteristics must be extracted. One common method to extract the facial characteristics is locating the feature points on the face images. Therefore, Facial Feature Points Detection (FFPD) is an important matter in physiognomy and face related studies. FFPD has variety of applications including facial modeling, face normalisation, face tracking, facial swapping [48] and etc.

Many face characteristics lie on geometry, shape and distribution of facial components such as eyes, nose, and mouth. The facial feature points are mainly around the facial components and can describe the shape, scale and distribution of them, so that they can be named geometrical features, as in this study. The aim of the FFPD is to localise the shape of an input facial image based on the facial appearance. Facial feature detection is commonly a very difficult problem since the faces are differ in thousands ways. Moreover, the human face's shape is affected by different expressions and facial appearance is highly affected by lighting conditions, occlusions such as facial hair, glasses, hats and etc.

In the literature, various algorithms are employed to extract the facial features [18] [49][50][51]. According to Wang et al. [52] the methods for the shape variation or the appearance variation of facial feature extraction can be placed into four categories: Constrained Local Model (CLM)-based methods [49][53][54][55][56][57][58][59], Active Appearance Models (AAM)-based methods [18][60][61][62][63], regression-based methods [51][64][65] and other methods.

CLM-based methods fit a shape model to a target image through a high-dimension optimisation on an objective function [66]. In most of the CLM-based methods, fitting process has two steps: first, a response map for each landmark is obtained by an "exhaustive local search" [59]. Then, optimisation is applied on the achieved response maps [59][66]. In the training phase, a shape model is learned from the facial shapes and is taken as prior correction of facial feature points' configuration. In fact, in this offline step, a shape model and the local experts are learned from the training shapes using a set of facial images. Each local expert is trained using the facial appearance around the corresponding feature point and then is employed to compute the response map which evaluates the detection accuracy. In the online phase, the output shape can be obtained from a given image by optimisation of the objective function. For the fitting of CLM-based methods two steps should be iterated until reaching the satisfactory convergence: predicting the local transposition of the shape model points, and constraining the configuration of all points to hold the shape model [52].

In AAM-based methods, first, a model is constructed from the appearance variation of the entire context. In the training phase, shape and appearance variations are made from shapes and set of images. Then, in testing phase, the constructed statistical models of the shape and appearance are matched to a new image [18][67].

Regression-based methods directly learn a regression function from image appearance to the target output which is the shape. It means that the shape is directly estimated from the appearance without learning any shape model or appearance model.

There are other methods which do not belong to the aforementioned categories of methods, so they can be assigned to the following subcategories [52].

Graphical model-based methods which use graphical model to describe the relation between facial feature points [68][69]. Graphical models can be defined as an association of "graph theory" and "probability theory" [69]. These models are a group of probability distributions defined regarding a directed or undirected graph. These methods usually refer to "tree-structure-based methods" in which each facial feature point is taken as a node and all points as a tree, and Markov Random Field (MRF)-based methods that model the location of all points with loops.

Joint Face Alignment Methods simultaneously align a set of facial images that have a variety of geometric and appearance variations.

In Independent Facial Feature Point Detectors the locations of all facial feature points or a group of points are predicted together [52].

Deep Learning-Based Methods, such as Luo et al. [70] proposed a hierarchical face parsing method, based on deep learning, that first detects faces at both the parts and component levels and then computes the "pixel-wise label maps". The feature can then be easily obtained from the boundary of the label maps.

Covering all of the facial feature extraction methods and their extensions is out of the scope of this study; therefore, since in this study AAM is used for feature extraction, and these models are an extension of the Active Shape Models (ASM), in the following sections, these two methods are briefly discussed.

2.1.1 Active Shape Models (ASM)

Active Shape Models are the shape-based models belonging to the CLM-based methods category that are among the earliest and most well-known approaches for feature extraction in which shape variability is learned through observation [49].

These models represent the objects as sets of labelled points and introduce the Point Distribution Models (PDM) by obtaining a model of shape and its variation using a set of landmark points.

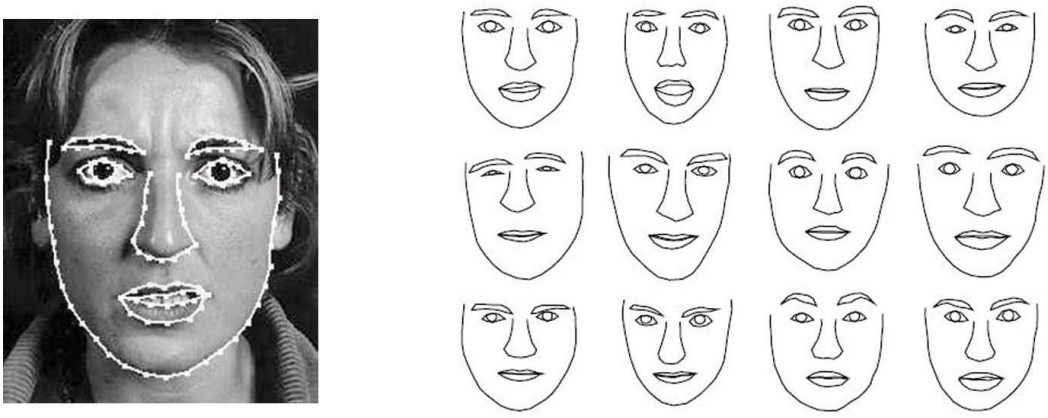

(a) (b)

Figure. 2.1 (a) An example of face image annotated with landmarks in the training phase by Cootes [72]. (b) The example face shapes from training set of shapes where each image is annotated with 133 landmarks [72].

In this method, each model defines a way that the shapes in the training set tend to vary from the mean [71]. In fact, ASM is a statistical model of the object shape where an iterative procedure deforms the example of the object to find the best fit to the new image. By applying limits to the parameters, it can be guaranteed that the shape of the instance remains close to the original training examples' shape.

Similar to the most of the facial feature point detection methods, ASM consists of training phase in which the model is trained with annotated landmarks across all training face images to build a profile model for the landmarks.

In the training phase, it should be decided how many points are desired to be trained to the system and the position of the landmarks should be defined. According to the different applications, different numbers of points that should cover the frequently used areas can be extracted; these are the areas which have the most important information on the face. Figure 2.1.a shows an example of annotated face image with 133 landmarks by Cootes [72] and Figure 2.1.b is a set of shapes from a training set of their labelled faces.

Then, ASM uses Principal Component Analysis (PCA) to reduce the dimensionality of the data and make it more manageable. PCA computes the main axes of variation in a training set of labelled examples.

Matching the shape model to a new image involves local searches of the vicinity of each landmark for the best match. It means, the model locates each landmark independently, then it will correct the locations by observing the location of the

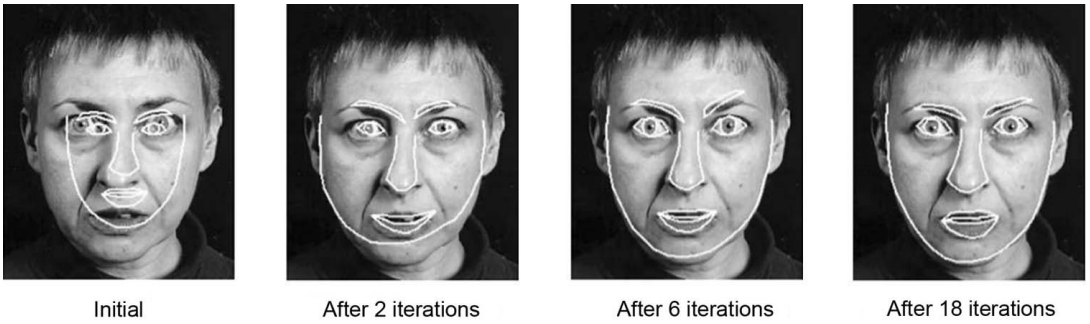

Figure. 2.2 Searching using Active Shape Model of a face from Cootes [72].

landmarks with respect to each other. Figure 2.2 shows ASM searching from Cootes [72].

2.1.2 Active Appearance Models (AAM)

AAM [73] is a generative, non-linear, and parametric model which is a direct extension and a generalisation of the ASM approach. However, it combines a shape variation model with an appearance variation model in a "shape-normalised frame". Generally, AAM has three main phases:

1. Statistical linear shape model
2. Linear texture model
3. Combining the shape and texture for appearance model [18][73]

The shape model construction is similar to ASM model. It is constructed from a set of annotated facial images. The shape is represented by n concatenated points' vector;

$$s = (x_1, \ldots, x_n, y_1, \ldots, y_n)^T \tag{2.1}$$

where (x_i, y_i) is the location of the i^{th} points and, n is the number of points.

This shape representation does not contain any explicit information about the connectivity. The shapes are normalised using Procrustes analysis [74] and then projected onto the shape subspace created by PCA. So, shape model is defined as;

$$s = \bar{s} + p_s b_s \tag{2.2}$$

where s is the shape vector, $\bar{s}$ is the mean shape, p_s is the set of "orthogonal modes" of shape variation and b_s is set of shape parameters.

Next, a vector is chosen, as the mathematical representation of texture;

$$g = (g_1, \ldots, g_m)^T \tag{2.3}$$

where m is the number of pixel samples over the face surface.

To construct the texture model, all training faces should be warped to the mean-shape frame to collect the texture information between the landmarks. The result is the shape-free textures;

$$g = \bar{g} + p_g b_g \tag{2.4}$$

where $\bar{g}$ is the mean texture, p_g is the orthogonal mode of variation that is derived from training set and b_g includes the texture parameters in the texture subspace.

Finally, a combination of the shape and texture is analysed using 3^{th} PCA on the data as follows and the appearance subspace is created.

$$b = \begin{pmatrix} W_s b_s \\ b_g \end{pmatrix} = \begin{pmatrix} W_s P_s^T (s - \bar{s}) \\ P_g^T (g - \bar{g}) \end{pmatrix} \tag{2.5}$$

where W_s is a diagonal matrix that a suitable weighting between pixel distances and pixel intensities is obtained through it [67]. After performing the PCA;

$$b = Qc \tag{2.6}$$

where Q is the eigenvector that its rank will never exceed the number of the examples in the training set, c is the vector of appearance parameters that controls both the shape and texture of the model.

The 3^{th} PCA can remove the correlation between shape and texture model parameters and represents the more compressed model in which the shape and texture are expressed directly as functions of c;

$$s = \bar{s} + P_s W_s Q_s c \tag{2.7}$$

$$g = \bar{g} + P_g Q_g c \tag{2.8}$$

where

$$Q = \begin{pmatrix} Q_s \\ Q_g \end{pmatrix} \tag{2.9}$$

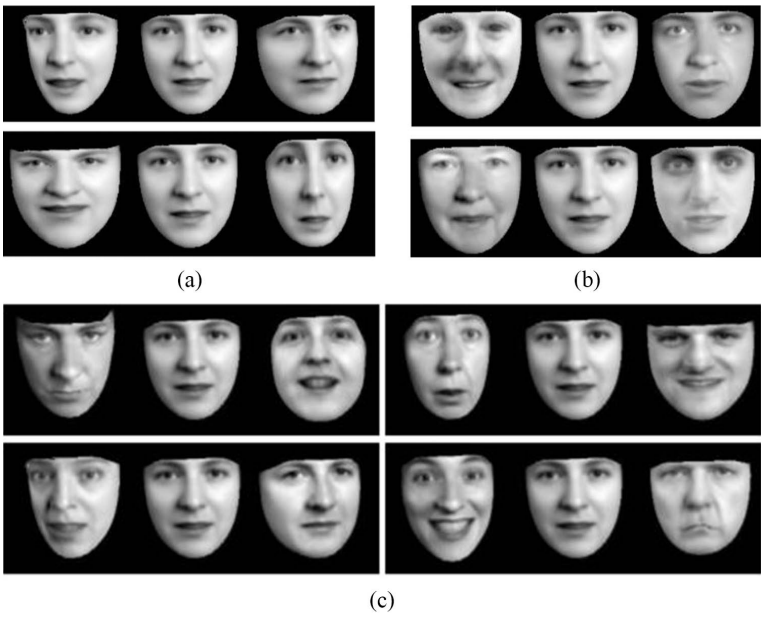

Figure. 2.3 An example of shape, texture and appearance variations from Cootes et al. [18] (a) The first two modes of shape variation. (b) The first two modes of grey-level variation. (c) The first four modes of appearance variation.

An example of shape, texture and appearance variations from Cootes et al. [18] are shown in the Figure 2.3

In general, AAM is relatively fast, but it has pose variation limitation. It also is sensitive to the lighting conditions and occlusions. However in this study, as the selected facial images for the database are all with almost the same pose (frontal), nearly the same appropriate lighting conditions, and they are also with the minimum of facial expressions, therefore, AAM can be an appropriate choice.

2.1.2.1 Active Appearance Model Fitting

After training the model, it should be able to be fitted on the input face images. This is the most critical phase in AAMs. Fitting in AAM is an iterative procedure; at each iteration it estimates a set of changes in the pose and the model parameters, which then leads to a better fitting of the image. In fact, it can be treated as an optimisation problem in which the difference between a new image and synthesised image delivered by AAM, should be minimised [67].

Typically, the update of the current model is a function of the error between the image and the model. There are two main approaches for modeling this function [62]:

The first is to learn the function via regression, such as original AAM in which a linear relation between the error in the image and the error in the parameters updates

is considered [73][75]. These approaches are usually fast but approximate. In the original AAM, a difference vector is defined as the difference between the rendered AAM, with the concatenated shape and colour parameters $p = \{\alpha, \beta\}$, and the face image,

$$\delta I(x) = I\left(AAM(x; p)\right) - T(x) \tag{2.10}$$

where δI is difference vector, x is a two-dimensional sample point, $T(x)$ is the sample intensity at position x on the target face image, and $I(AAM(x;\ p))$ is the rendered appearance model with parameters p in the sample point x. Hence, to find the best match between the image and the model, the magnitude of difference vector, $\Delta = \|\delta I\|^2$ should be minimised by varying the model parameters, p.

The second is fitting AAMs through non-linear least-squares, such as Lucas and Kanade method, in which by having the current estimates of the shape parameters, the input image is warped onto the model coordinate frame and then an error image is computed between the current model sample and the image that the AAM is being fitted to [76].

2.1.2.2 Lucas–Kanade Algorithm

The Lucas–Kanade (LK) is one of the most popular techniques in computer vision. LK was initially proposed to image alignment and then was extended to be used in AAM fitting. The primary aim of LK, which is a Gauss-Newton gradient descent non-linear optimisation algorithm, is to "minimise the sum of the squared errors between two images" [77]. The usual approach to image alignment is gradient descent. There are numerous derivations of this algorithm. These derivations differ in terms of use an additive or compositional approach for updating. Another difference is in the approximation algorithm performed in each gradient decent step (Gauss-Newton, a Newton, a steepest-descent, or a Levenberg-Marquardt). Finally, an important difference that have a large impact on the algorithm efficiency, is that which image is fitted to another, the rendered image to the target image, or vice-versa. The detailed review of these algorithms are given by Baker and Matthews [77]. It can be said that the algorithms can be categorised as either additive or compositional, and as forwards or inverse.

In this study, two algorithms are targeted in order to face fitting: the forward additive algorithm and the inverse compositional algorithm [78, p. 46]. These algorithms were extended for fitting appearance models by Matthews and Baker [79].

The main purpose of the LK algorithm is minimisation of the sum of the squared differences in pixel intensity between the target image (T), and a warped input image (I), by differing the parameters of the warp and define an image warp $W(x;p)$, with parameters p [77].

The sum of the squared errors is:

$$\sum_{x} [I(W(x;p) - T(x))]^2 \tag{2.11}$$

This equation can be solved in an iterative process in which the parameters are updated via an additive manner.

To optimise the equation 2.11, it is assumed that a current estimate of p is known and then LK algorithm iteratively solves the equation to gain the parameters Δp. Therefore the expression is minimised as:

$$\sum_{x} [I(W(x;p+\Delta p) - T(x))]^2 \tag{2.12}$$

and then the warp parameters are updated:

$$p \leftarrow p + \Delta p \tag{2.13}$$

These two steps are repeated until the estimates of the parameters p are fulfilled. By applying a first order of the Taylor expansion on $I\ (W(x;\ p\ +\ \Delta p))$ the equation 2.12 is linearised as:

$$\sum_{x} [I\left(W(x;p)) + \nabla I \frac{\partial W}{\partial \mathrm{p}} \Delta p - T(x)\right]^2 \tag{2.14}$$

where $\nabla I = \left(\frac{\partial I}{\partial \mathrm{x}}, \frac{\partial I}{\partial \mathrm{y}}\right)$ is the gradient of the image I evaluated at $W(x;p)$. In other words, ∇I is calculated in the I coordinate and then warped back to the T coordinate using the current estimate of the warp $W(x;p)$. The term $\frac{\partial W}{\partial \mathrm{p}}$ is the Jacobian of the warp;

$$\frac{\partial W}{\partial \mathrm{p}} = \left(\frac{\partial W}{\partial p_1}, \frac{\partial W}{\partial p_2}, \ldots, \frac{\partial W}{\partial p_n}\right) \tag{2.15}$$

By minimising the equation 2.14

$$2\sum_{x} \left[\nabla I \frac{\partial W}{\partial \mathrm{p}}\right]^T [I\left(W(x;p)) + \nabla I \frac{\partial W}{\partial \mathrm{p}} \Delta p - T(x)\right] \tag{2.16}$$

where $\nabla I \frac{\partial W}{\partial \mathrm{p}}$ is referred to as the steepest descent images. By putting this equation equal zero and solving:

$$\Delta p = H^{-1} \sum_{x} \left[\nabla I \frac{\partial W}{\partial \mathrm{p}} \right]^{T} [T(x) - I(W(x;p))] \tag{2.17}$$

where H is the $n \times n$ Hessian matrix. This equation shows the Δp are the "steepest descent parameter updates" multiplied by the inverse of the Hessian matrix where Hessian matrix defined as [77]:

$$H = \sum_{x} \left[\nabla I \frac{\partial W}{\partial \mathrm{p}} \right]^{T} \left[\nabla I \frac{\partial W}{\partial \mathrm{p}} \right] \tag{2.18}$$

Therefore, the parameter warp, p, are found by iteratively applying the equations 2.17 and 2.13.

The only requirement on the warps $W(x;p)$ is that they are differentiable with respect to the warp parameters p. Therefore, this algorithm can easily be used for AAMs.

2.1.2.3 The Inverse Lucas–Kanade Algorithms

The re-evaluating of the Hessian in every iteration of LK algorithm has a long computation time. The Hessian could be precomputed and then re-used, if it was constant, but the Hessian is a function of p in both formulations. There are different solutions to approximate the Hessian, but it is difficult to evaluate these approximations. Therefore, it is better to solve the problem in a similar way with a constant Hessian. The key is switching the role of rendered image and the target image [80]. This can be done by using the inverse algorithms. The inverse compositional algorithm switches the role of the image and the template, and updates the parameters by applying the image warping. Therefore, the derivatives are always evaluated at $W(x;0)$ and, thus are constant [77].

The result in the inverse compositional algorithm minimises:

$$\sum_{x} [(T(W(x;\Delta p)) - I(W(x;p))]^{2} \tag{2.19}$$

Here, in the error function, the roles of the input image and the target image are reversed. With the respect to p and then updating the warp:

$$W(x;p) \leftarrow W(x;p) \circ W(x;\Delta p)^{-1} \tag{2.20}$$

as with the LK algorithm, equation 2.19 is minimised using a first order of the Taylor expansion:

$$\sum_{x}[\left(T\left(W\left(x;0\right)\right)+\ \nabla T\ \frac{\partial W}{\partial \mathrm{p}}\ \Delta p-I\left(W\left(x;p\right)\right)\right]^{2} \tag{2.21}$$

Again the solution to the least squares problem is:

$$\Delta p=H^{-1}\ \sum_{x}\left[\nabla T\ \frac{\partial W}{\partial \mathrm{p}}\ \right]^{T}\left[I\left(W\left(x;p\right)\right)-T\left(x\right)\right] \tag{2.22}$$

where H is the Hessian matrix in which I is replaced by T:

$$H=\sum_{x}\left[\nabla T\ \frac{\partial W}{\partial \mathrm{p}}\ \right]^{T}\left[\nabla T\ \frac{\partial W}{\partial \mathrm{p}}\right] \tag{2.23}$$

and Jacobian $\frac{\partial W}{\partial \mathrm{p}}$ is evaluated at $p=0$.

Hence, Hessian does not require updating between iterations and needs only to be applied once as a pre-computation.

2.1.2.4 Fitting Inverse Compositional Lucas –Kanade to an Image

Matthews and Baker [79] improved the Inverse Compositional Lucas–Kanade algorithm to fitting AAMs [78, pp. 45-50]. The LK algorithm and AAM [18] share some similarities in their fitting methods. The LK minimises the l^2-norm of image difference between the target image and the rendered image using a gradient descent method. To improve the inverse compositional LK algorithm to fitting AAMs, the project-out method of Hager and Belhumeur [80] is used, which separates texture changes from shape changes in the model. The error function is defined as bellow:

$$\|\bar{g}\ \left(W\left(x;\Delta\alpha\right)\right)+\sum_{i}\beta_{i}g_{i}(W\left(x,\Delta\alpha\right)-I\left(W\left(x;\alpha\right)\right)\ \|^{2} \tag{2.24}$$

where $\bar{g}$ is the average texture from the AAM, g_i are the eigenvectors that describe the colour variations. α and β are respectively the shape and colour parameters of the AAM. The equation is solved simultaneously with respect to α, β and p.

If we designate that the linear subspace extended by a collection of vectors g_i by span(g_i) and its orthogonal complement by $span(g_i\ )^{\perp}$, the error function can be rewritten as :

$$\|\bar{g}(x)+\sum_{i}\beta_{i}g_{i}(x)-I(W(x;\alpha))\|^{2}_{span(g_i)^{\perp}}+\|\bar{g}(x)+\sum_{i}\beta_{i}g_{i}(x)-I(W(x;\alpha))\|^{2}_{span(g_i)} \tag{2.25}$$

where $\|.\|_L^2$ is the L^2-norm of the vector projected on the linear subspace L. The first term can be immediately simplified. Any component in $span(g_i)$ can be ignored, as the norm only considers the components of vectors in the orthogonal complement of $span(g_i)$. Thus, the first term does not depend on β_i. Therefore it is minimised:

$$\|\bar{g}(x)+I(W(x;\alpha))\|^2_{span(g_i)^\perp}+\|\bar{g}(x)+\sum_i \beta_i g_i(x)-I(W(x;\alpha))\|^2_{span(g_i)} \tag{2.26}$$

For any α or p, the minimum of the second term is always evaluated to zero. These two terms can separately be minimised. The first term can be minimised with respect to α and p, and then by finding β_i, using that optimal values α and p as constant, the second term can be minimised. As g_i are orthogonal from the PCA the second minimisation has a simple linear solution;

$$\beta_i = \sum_x g_i.[I(W(x;\alpha,p))-\bar{g}] \tag{2.27}$$

the dot product is obtained after the first minimisation.

Now, it is time to projecting the steepest decent images into $span(g_i)^\perp$span:

$$J_i = \nabla\bar{g}\frac{\partial w}{\partial \alpha}-\sum_i[\sum_x g_i.\nabla\bar{g}(x)\frac{\partial W}{\partial \alpha}]g_i(x) \tag{2.28}$$

The first term of equation 2.26 is computed using the Taylor series expansion;

$$\sum_x[I(W(x;\alpha))-\bar{g}(W(x;0))+\nabla\bar{g}\frac{\partial W}{\partial \alpha}\Delta\alpha] \tag{2.29}$$

Assuming that $W(x;0)=x$, it can be solved as a least squares problem;

$$\Delta\alpha = H^{-1}\sum_x J^T[I(W(x;a))-\bar{g}] \tag{2.30}$$

where $H=J^TJ$ is the Hessian and J is the projection-out derivatives of α. The efficiency of this algorithm is no longer dependent on α, rather it is due to the Jacobian.

By composing the current shape warp, $W(x;p)\leftarrow W(x;\alpha)\circ W(x;\Delta\alpha)^{-1}$, the shape parameters can be updated. Within this method it is assumed that the colour components g_i do not change with any of the parameters, but changes in lighting can change the colour of the face model and the distribution of the intensities [78].

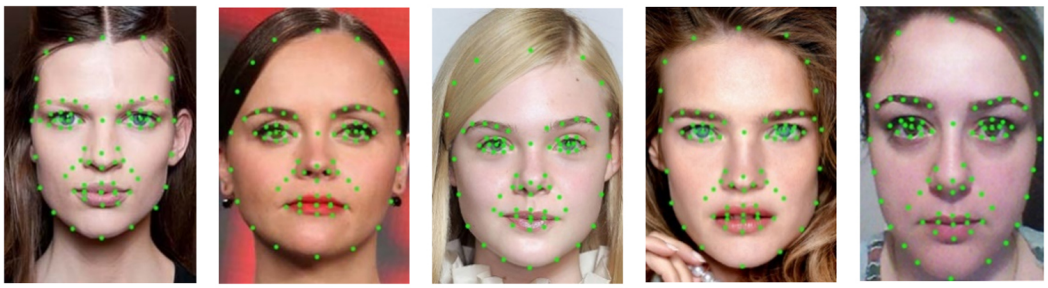

Figure. 2.4 Illustration of the face images with 79 extracted feature points. These face images are mostly chosen from celebrities' portraits found on the internet.

2.1.3 Geometrical Feature Extraction

In this work the training set of 500 facial images is used, each labelled with 79 points around facial components and face contour.

According to the steps mentioned above, first, the shape model is constructed by designating landmark points at face key positions to outline the main features within a training set. Procrustes analysis and PCA are applied for the shape normalisation and shape subspace creation as mentioned before. Then, the texture model is defined within the shape free frame. As the shape model, the texture is also generated using a linear combination of basis variation vectors. In order to collect the texture information between the landmarks, an image warping function is applied. All training faces are warped to the mean-shape to have the shape-free texture. Then after, to learn the appearance model, the shape variation is removed from the texture. This is achieved by first, warping each facial image to the reference frame defined by the mean shape, then, applying the PCA on the shape-free textures, to obtain the appearance model. Finally, AAM is fitted to an input image using aforementioned Inverse Compositional Lucas –Kanade method.

Once the geometrical feature extraction is terminated, face images are labelled with 79 landmark points related to the face components and the contour (see Figure 2.4).

2.2 Image Warping

Warping is an important phase in many image processing applications. It has been used during the last decades in computer vision, computer graphics and medical images. Almost any application of digital image processing needs at least an occasional change of the location, scale, or orientation of the image.

In general, a digital image warping is a geometrical transformation of a digital image. There is a wide variety of warping algorithms. The critical aspects of the image warping algorithms are speed, accuracy, and complexity. Choosing the appropriate algorithm depends on the application.

In this section two-dimensional warping is described, and then the chosen algorithm for this study is discussed.

2.2.1 Texture Mapping

Texture mapping was developed by Catmull [81] as a way of improving the realism without increasing the geometric complexity of a scene. In fact, it is a shading technique for image processing in which a texture image is mapped onto a surface in a three-dimensional scene. The advantage of texture mapping is that it can add the details to the scene with only a modest increase in rendering time.

There are different techniques for mapping an image. The two classic ones are forward mapping and inverse mapping. Forward mapping is a many-to-one mapping in which several points in the source image map to the same point in the destination image. An inverse mapping or one-to-many mapping is where several points in the destination image map to the same point in the source image. The characteristic of inverse mapping is that a value in all the pictures in the destination image is assured, while in forward mapping it's possible to leave out some unevaluated destination points. [82, pp. 4-6] .

In addition to this, they indicate different implementation techniques. A warp described by a forward mapping is performed by scanning the source image, pixel by pixel, calculating the corresponding location in the destination image by evaluating the mapping function and painting that location in the destination image with the colour of the source pixel. On the other hand, a warp described by an inverse mapping is applied by pixel by pixel scanning of the destination image, calculating the corresponding location in the source image by evaluating the mapping function, and painting the destination pixel with the colour of the calculated source location [82, p. 4].

If (u,v) represents the image coordinate in an original image, and (x,y) in a warped image:

$$\text{Forward mapping:} \begin{cases} x = x(u,v) \\ y = y(u,v) \end{cases} \tag{2.31}$$

$$\text{Inverse mapping:} \begin{cases} u = u(x,y) \\ v = v(x,y) \end{cases} \tag{2.32}$$

The fundamental transformations involved in image warping are:

$$\text{Translation:} \begin{cases} x = u + t_x \\ y = v + t_y \end{cases} \tag{2.33}$$

where t is the translation factor.

$$\text{Scaling:} \begin{cases} x = s_x u \\ y = s_y v \end{cases} \tag{2.34}$$

where s is the scale factor.

$$\text{Rotation:} \begin{cases} x = u\cos(\theta) - v\sin(\theta) \\ y = u\sin(\theta) + v\cos(\theta) \end{cases} \tag{2.35}$$

where θ is the rotation angle.

Shearing in one or both axis:

$$\text{X - Axis:} \begin{cases} x = u + h.v \\ y = h.v \end{cases} \tag{2.36}$$

$$\text{Y - Axis:} \begin{cases} x = h.u \\ y = v + h.u \end{cases} \tag{2.37}$$

where h is the shear factor.

2.2.1.1 Two-Dimensional Mappings

There are many possible kinds of 2D mapping. Here, only some of the most important and practical classes of 2D mapping are discussed [82, pp. 6-7][83][84, pp. 14-21].

Affine Mapping: Affine mapping is an important class of linear 2D geometric transformations which maps variables in an input image by applying a linear combination of translation, rotation, scaling, and shearing. Affine mappings preserve parallel lines, allowing to avoid compacted axes when performing 2D projections. Furthermore, equispaced points are preserved. The mapping between two arbitrary triangles can be obtain by an affine mapping or it can map a source triangle into a destination parallelogram. However, more general distortions are impossible. For example, to warp a rectangle into a quadrilateral, a bilinear, projective of some other complex mappings are needed. Affine transformation is closed under composition and inverse. For any affine mapping;

$$\begin{cases} x = au + bv + c \\ y = du + ev + f \end{cases} \tag{2.38}$$

Bilinear Mapping: A bilinear mapping, or bilinear transformation, handles the four-corner mapping problem for non-planar quadrilaterals. It is mostly used in the forward mapping where rectangles are mapped onto non-planar quadrilaterals. Bilinear mappings preserve the horizontal or vertical lines in the source image. The points along horizontal and vertical lines in the source image remain equispaced. However, diagonal lines map onto quadratic curves at the output. For any bilinear transformation:

$$\begin{cases} x = auv + bu + cv + d \\ y = euv + fu + gv + h \end{cases} \tag{2.39}$$

Perspective Mapping: A perspective mapping or the projective mapping has eight parameters and like bilinear mapping, it can be used to map any quadrilateral in the source image onto another quadrilateral in the destination image. Lines in all directions are preserved in perspective transformations, however, it does not preserve the distance relationships. Like the affine transformations, the perspective transformations are closed under composition and inverse.

$$\begin{cases} x = \frac{au+bv+c}{gu+hv+i} \\ y = \frac{du+ev+f}{gu+hv+i} \end{cases} \tag{2.40}$$

Polynomial Mappings: A polynomial image transformation is the one where the source image coordinates are defined as bivariate polynomials in the destination image coordinates. It is also possible to define the destination image coordinates as polynomials in the source image coordinates, leading to a class of transformations different from the above. The polynomial coefficients are often derived from known positions of a few points in the image using least-squares methods.

$$u = \sum_{i=0}^{N} \sum_{j=0}^{N-i} a_{ij} x^i y^i \quad , \quad v = \sum_{i=0}^{N} \sum_{j=0}^{N-i} b_{ij} x^i y^i \tag{2.41}$$

2.2.2 Image Warping Using Moving Least Squares (MLS)

The term “image warping” refers to the mapping of intensity values from one spatial distribution into another spatial distribution.

For each image warping, some set of handles should be employed to control the deformation. There are variety of algorithms available for image warping based on using different types of the handles. These handles may have the form of points, lines or polygon grids.

Grid-based techniques generally require aligning grid lines related to the control points of the spline with features of the image, which becomes difficult for the user. Free-form deformations are along these algorithms [85][86][87]. Specifying the information using set of lines is an improvement of the grid-based techniques which have been proposed by Beier and Neely [88] and it creates smooth deformation. However, they can produce complicated warps and sometimes generate unsought folding in the deformation. A point can be the simplest deformation handle. For instance, Bookstein [89] proposed an approach of deformations specified by finitely many points-correspondence in an irregular spacing.

Moreover, the class of the transformation have been used to deform the image can differ from one algorithm to another.

In this study, image deformation using Moving Least Squares proposed by Scott Schaefer et al. [90] is used. They have provided a method to create the smooth and realistic deformations of images based on linear Moving List Squares (MLS) [91].

This work consists of three types of class transformation to fulfil image warping: affine transformation, similarity transformation, and rigid transformation. It also allows a choice of the deformation, using either set of points or line segment sets to specify the warp. By using MLS, in fact, the need to triangulate the input image is eliminated and smooth deformations are created [92]. They have also derived “closed–form formulas” for both similarity and rigid MLS deformation in order to make them simple and easy to implement [90].

As it is illustrated, the results of the warping with MLS using sets of points to control the deformation are sufficient for performing the deformations on the face. As a result, the method which employs the set of points as a handle, can be appropriate for image warping in this work. Because there are 79 formerly extracted feature points on the face image that can control the desired deformations.

Besides, it is indicated that the deformation results of the affine warping are not very desirable and realistic, for both points and lines handles, due to the stretching made in the deformed images. These artifacts are created since affine transformations include deformations such as non-uniform scaling and shear. To remove these unsought deformations, the similarity and rigid-body transformations can be used instead of fully linear transformation.

Similarity transformations are a special subset of affine transformations that only include translation, rotation and uniform scaling. The results of this transformation are better than affine MLS by preserving angels, as expected. However, this deformation scales some part of the deformed images. To remove the uniform scaling, the deformation using rigid transformation can be applied.

According to the all above-mentioned, in this study, MLS using set of points and the rigid transformation is chosen to perform the image warping on the faces.

To find the best transformation function (f) that maps a set of controlled handles (p) to the deformed positions of the controlled handles (q) the MLS deformation is employed. Therefore, to generate the deformed image, the function f is applied to each point v in the undeformed image. The function f needs to satisfy three conditions to be useful for the deformation:

1. "Interpolation: The handles p should map directly to q under deformation. $(f(p_i) = q_i)$."
2. "Smoothness: f should generate smooth deformations."
3. "Identity: If the deformed handles q are the same as the p, then f should be the identity function $(q_i = p_i \Rightarrow f(v) = v)$" [90].

Having a point v in the image, the following equation should be solved for the best transformation $l_v(x)$ that minimises;

$$\sum_i w_i |l_v(p_i) - q_i|^2 \tag{2.42}$$

where p_i and q_i are row vectors and the weight w_i is

$$w_i = \frac{1}{|p_i - v|^{2\alpha}} \tag{2.43}$$

Since in the least square problem w_i are depending on the point of evaluation, this method can be named a Moving Least Square minimisation. Hence, for each v a different transformation $l_v(x)$ is obtained. Now, the deformation function f is defined to be $f(v) = l_v(v)$ by satisfying the three above-mentioned properties. $l_v(x)$ consists of: a linear transformation matrix M and a translation T.

$$l_v(x) = xM + T \tag{2.44}$$

Equation 2.42 is quadratic in T. It can be directly solved for T in terms of the matrix M that yield:

$$T = q_* - p_* M \tag{2.45}$$

where p_* and q_* are weighted centroids.

$$p_* = \frac{\sum_i w_i p_i}{\sum_i w_i} \quad , \quad q_* = \frac{\sum_i w_i q_i}{\sum_i w_i} \tag{2.46}$$

Accordingly, T can be substitute in the equation 2.44 and $l_v(x)$ can be rewritten only in terms of the linear matrix M as;

$$l_v(x) = (x - p_*)M + q_* \tag{2.47}$$

Therefore, the least square problem of the equation 2.42 can be rewritten as:

$$\sum_i w_i |\hat{p}_i M - \hat{q}_i|^2 \tag{2.48}$$

where $\hat{p}_i = p_i - p_*$ and $\hat{q}_i = q_i - q_*$. This framework helps to explore different classes of transformation matrices M. In particular, in this work a rigid transformation has been chosen for M.

In order to have the realistic results, deformations should be as rigid as possible; that is to say, the space of deformations should not even include uniform scaling [92]. Due to non-linear constraint that $M^T M = I$, this problem, generally, seems very difficult to approach. However, the closed-form solutions from the Iterative Closest Point (ICP) community are well-known to solve this problem [93]. Thus, the closed-form solution for rigid-body transformations results in the transformation matrix:

$$M = \frac{1}{\mu_r} \sum_i w_i \begin{pmatrix} \hat{p}_i \\ -\hat{p}_i^{\perp} \end{pmatrix} (\hat{q}_i^T - \hat{q}_i^{\perp T}) \tag{2.49}$$

where μ_r is the scaling constant;

$$\mu_r = \sqrt{(\sum_i w_i \hat{q}_i \hat{p}_i^T)^2 + (\sum_i w_i \hat{q}_i \hat{p}_i^{\perp T})^2} \tag{2.50}$$

so that $M^T M = I$. This deformation is non-linear, but it can still be simply computed.

Figure. 2.5 The results of applying the image warping. Original facial image (left). The deformed face using the rigid MLS method (right).

Vector $\overrightarrow{f_r}(v)$ is a rotated and scaled version of the vector $v - p_*$. To compute $f_r(v)$, we normalised $\overrightarrow{f_r}(v)$, scale by the length of $v - p_*$ and translated by q_*.

$$f_r(v) = |v - p_*| \frac{\overrightarrow{f_r}(v)}{|\overrightarrow{f_r}(v)|} + q_* \tag{2.51}$$

For this deformation that uses points as control handles, the rotated vector is:

$$\overrightarrow{f_r}(v) = \sum_i \hat{q}_i A_i \tag{2.52}$$

where A_i is:

$$A_i = w_i \begin{pmatrix} \hat{p}_i \\ -\hat{p}_i^{\perp} \end{pmatrix} \begin{pmatrix} v - p_* \\ -(v - p_*)^{\perp} \end{pmatrix}^T \tag{2.53}$$

In this study, there are 79 facial feature points that can be employed as control handles. The results of warping applied on the facial images to change the size of the face and its different components are shown in Figure 2.5

Note that, in order to attain the desirable smoothness, the creation of nested spaces made by feature points around each component, should be avoided.

2.3 Facial Ageing Image Databases and Image Normalisation

In order to propose an accurate model of the facial ageing, appropriate dataset for training and testing the model is the primary requirement. Yet, data collection for the purpose of the facial ageing modeling is a very crucial and challenging task as

collecting the chronometric facial images from an individual is really problematic. Few facial databases have been provided for facial ageing studies in comparison to the databases for the other face-related research fields such as face recognition, facial expression, etc. Some benchmark ageing databases that have been collected to help the study of the age-related problems are as below:

- FG-NET (Face and gesture recognition network) ageing databas [94] was released in 2004 to support the research activities related to the ageing. This database comprises of 1,002 colour or grey-scale face images of 82 subjects in the age range 0-69 years, with large variation of lighting, pose, and expression. This database is the only available database that provides age separated face images of the individuals in the age range 0-18 years. However, age distribution for different subjects is not uniform.

- MORPH database [95][96] contains face images of adults in different ages. This database organised into two 'albums'. MORPH Album 1 comprises 1,690 facial images from 515 individuals, men and women, of different ancestry groups. The age range is from 15 to 78 years. MORPH Album 2 contains around 14,000 digital images. However, this database provides only adult face images and does not contain the childhood face images.

- FERET (Facial Recognition Technology) [97] program ran from 1993 through 1997 with the primary aim to develop automatic face recognition that could be used in security and law enforcement. Then, the FERET image database was collected to support government monitored testing and evaluation of face recognition algorithms. This database consists of a total number of 14,126 grayscale facial images, with different pose range from frontal to left and right profiles. FERET comprises a few galleries of age separated face images of subjects such as Duplicate I Probe-set (722 images), Duplicate II Probe-set (234 images) and Gallery-set (1,196 images).

- YGA (Yamaha Gender and Age) [25] database contains 8,000 outdoor colour images of 1,600 Asian subjects, from 0 to 93 years of age. Each subject has about five frontal images, at the same age, labelled of the approximate age. The photos contain large variations in illumination, facial expression, and makeup.

- WIT-DB (Waseda human-computer Interaction Technology-Database) [98] provides about 5,500 different Japanese subjects face images (about 2,500 females and 3,000 males), with 1 to14 face images for each subject labelled by actual

age, from 3 to 85 years. The faces are frontal, without any occlusion, normal facial expressions except for smiles in some of the images, and wide variety of lighting conditions. Facial images are divided into 11 age categories.

- HOIP (The Human and Object Interaction Processing) [99] face database includes 300 subjects in various from 20 to 60, half females and half males. The images are categorised and labelled in 10 age groups from 15 to 64 with five years interval. The face images are with neutral expression and in an illumination controlled environment.

- IFDB (Iranian Face Database) [100] is the first image database in Middle East and contains around 3,600 colour facial images of 616 Iranian subjects. This database includes images of different people at specific unique ages, between 2 and 85 years old. However, for a given person, no face images corresponding to different ages are provided.

- PAL database (Park Ageing Mind Laboratory) [101] was created at the University of Michigan in 2004, strictly for the academic research purposes. They describe a database of 575 individual faces ranging from 18 to 93 years of age, containing 216 faces of adults age 18-29, 76 adults age 30-49, 123 adults age 50-69, and 158 adults age 70 and older. This database was developed to represent different age groups, with emphasis on identifying the older adults.

There are more available ageing databases such as AI&R Asian Face Database [102], LHI face database [103], Burt's Caucasian face database [29], Gallagher's Web-Collected Database [104], Ni's Web-Collected Database [105], IMDB-WIKI [106], and CHICAGO face database [107]. Figure 2.6. shows sample photos of some of these databases. While they provide the facial images for different age ranges, still most of these databases do not supply the facial images of the same individual in different ages. Therefore, they are generally employed for age estimation and age-invariant face recognition purposes. From all above-mentioned databases, only three contain multiple images of the same individual at different ages; FG-NET, MORPH and the FERET. There are no predefined protocols for such databases, the age distribution for the subjects is not the same and the images do not span a range of years for each individual. Still, these databases are used in few Predictive Facial Ageing Modeling and age progression studies.

As there are limitations in using some common databases, which are not suited to develop a robust and reliable model for many reasons, highlighted through the five points below, we have created our database.

1. Database Structure: Some of the databases, such as FG-NET, contain images from the same subject at different ages; however, the age categories are not defined as required by our model. In addition, the images are not uniformly distributed among ages [108]. Moreover, in some cases, database contains adult faces within different age ranges. For example, in MORPH database the images are from 16 to 70 years old, so, we do not have any references from the individual's childhood which are needed for B-FAM evaluation purpose, will be explained in Chapter 3.

2. Image Quality and Image Resolution: The main target of our work is to propose and to validate a reliable face ageing model. Since we consider that texture and geometry information are important to match the human being's visual perception, high-resolution and high-quality images are required. This can be achieved by considering a selective environment, through a specific protocol. Unfortunately, in some available databases (e.g. FG-NET, MORPH), images are of low quality and/or low resolution. In addition, they are captured in an uncontrolled environment.

3. Capture Conditions: To ensure a reliable model, only frontal images are considered. Therefore, images highlighting poses, lighting, and occlusion, etc. should be discarded.

4. Facial Expressions and Emotions: Facial images with the following expressions: disgust, anger, fear, sadness, happiness, surprise, and contempt cannot be used to produce a model and should be discarded.

5. Image Type: Since the visual perception is an important factor in our study, the proposed model is sensitive to the colour information. However, some mentioned databases contain mixed versions of images in colour and in grayscale which is not suited for our model.

The created database, named Facial Ageing Modeling Database (FAMD) comprises around 1,600 facial images that have been gathered using the web. This database contains two albums:

- Backward Facial Ageing Collection (BFAC), contains around 700 face images corresponding to various ages from 3 to 18, for constructing the Backward Facial Ageing Model (B-FAM), which will be discussed in Chapter 3.

Figure. 2.6 Sample photos of some existing databases. (a) FG-NET database [94]. (b) MORPH database [95][96]. (c) IFDB database [100]. (d) CHICAGO face database [107].

- Forward Facial Ageing Collection (FFAC), consists of around 900 face images corresponding to various ages from 20 to 80, to develop the Forward Facial Ageing Model (F-FAM), which will be discussed in Chapter 4.

To reduce the impact of the face pose on the final results, only frontal face images with minor pose variations, facial expressions, and without occlusion are included. Then, all the collected images in each album have been classified into:

- 4 different age groups, named Cluster 3-4, Cluster 7-8, Cluster 12-13 years old and the Cluster Adult, separated by gender, for BFAC album.
- 6 different age groups, named Cluster 21-30, Cluster 31-40, Cluster 41-50, Cluster 51-60, Cluster 61-70 and Cluster 71-80 for FFAC album, separated by gender.

As a consequence of diversity in the resolution and also face tilt, normalisation is required. After the normalisation, all images have fixed eyes position, same eyes size, zero angle tilt and constant image size. This database is used to create the model, extract the geometrical measures and Face Template construction in both childhood and adulthood.

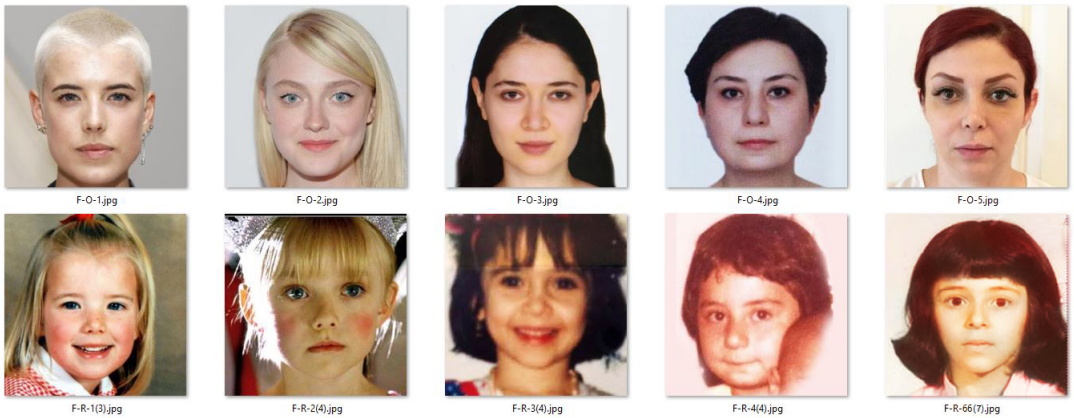

Figure. 2.7 The illustration of the sample images from FaceTiM V1.0. First row shows the adult face images from Set 1, the second row shows the childhood face images belonging to the first row subjects from Set 2.

Further, Face Time-Machine Database (FaceTiM V1.0) is created mainly to test and evaluate the results of the B-FAM. This database consists of the facial images from 120 subjects (246 images) in two sets. The 'Set 1' contains adult face images selected or acquired from 120 individuals, including public movie stars and volunteers' face images. The 'Set 2' contains at least one childhood face image that belongs to the individuals in 'Set 1' that can be used as the reference to compare the simulated results. All the images are labelled with the age in the defined age clusters range. FaceTiM has been published and can be a benchmark for the researchers working on digital face ageing or rejuvenation to evaluate the algorithms aiming to predict human faces in the future, or to make the face look younger. Figure 2.7. illustrates some sample images from both sets of the FaceTiM database. This database is collected by biometrics research group at the Laboratoire Images, Signaux et Systèmes Intelligents (LiSSi) laboratory and is available on [109].

It is worth to mention the legal restrictions in using facial images, especially for children. By considering the existing databases, it can be figured out that specific acquisition protocols to capture the children face images can rarely be found. Therefore, we have mostly used celebrities' facial images that are more accessible.

2.3.1 Image Normalisation

Since the collected databases are containing the facial images captured in the unconstrained environments, the image normalisation has been applied to equilibrate the size, resolution, tilt, etc.

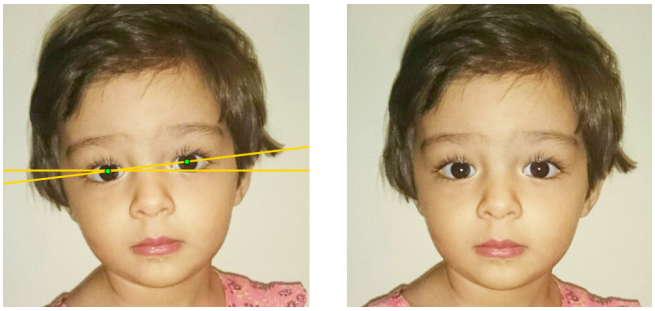

Figure. 2.8 Face tilt normalisation; the center of the eyes are brought in a straight line.

To normalise the collected databases, images of the whole database have to share a common origin $O_{x,y}$. The point at mid-distance between eyes $E_{x,y}$ needs to be at the same position. A translation should be applied to the images by Δ_x and Δ_y, which are equal to the difference between the point in the middle of the image and the actual point between the eyes.

$$\Delta_x = O_x - E_x \quad , \quad \Delta_y = O_y - E_y \tag{2.54}$$

Since in this study, it's aimed that we keep the actual face scales, therefore the face size gets scaled up/down by the size of the eyes, with its associated distance for each age cluster (see Figure 3.2). For the Cluster 3-4, Cluster 7-8, Cluster 12-13 years old and the Cluster Adult, the eye length is respectively 26.7mm, 27.5mm, 29.8mm, and 30.7mm [110, pp. 130-133], considering the fact that beyond the age of 16, the geometrical growth reaches almost its maximum and the eyes stop changing [110][111]. Of course in order to achieve this goal some feature points for the eyes should be extracted which is previously explained.

Once this process is done, since many algorithms are dependent on the careful positioning of face images into the same canonical pose, the procedure is followed by aligning all face images based on their eye locations (eye-based alignment) [112].

The line segment can be formed using two eye center points, and the angle θ between this line and the horizontal line can be obtained. The image is then rotated by that angle (see Figure 2.8).

$$\theta = atan \frac{LeftEye_y - RightEye_y}{LeftEye_x - RightEye_x} \tag{2.55}$$

Eventually, a database with images having a resolution of 500×500 pixels and 200 dpi is obtained.

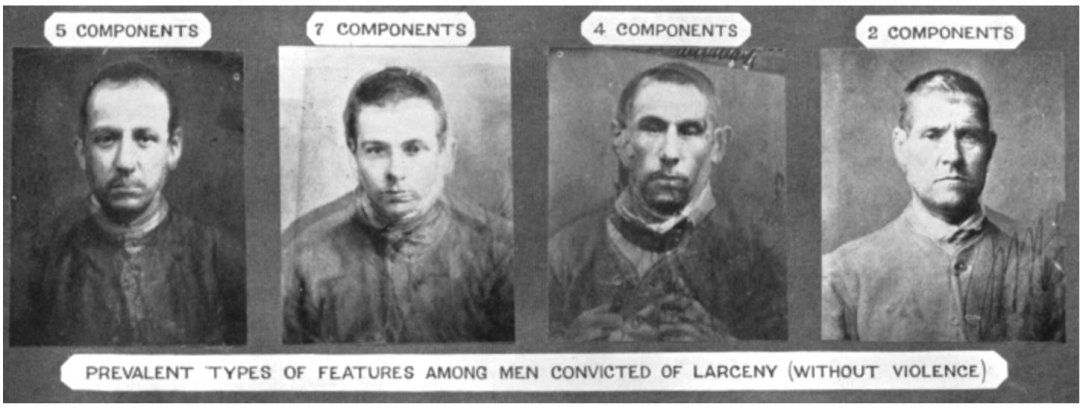

Figure. 2.9 Illustration of Galton's composite portraitures [113].

2.4 Face Template Construction

For the first time, Sir Francis Galton created 'Composite Portraiture' in the 1800s. To produce a single blended image, Galton combined photographs of different subjects through repeated limited exposure (see Figure 2.9). He was interested to test if there is a recognisable criminal type revealed by the composite portraits, but his experiments in this direction proved no such type revealed [113].

After that, average face have been considered to find the common characteristics of the constituent faces, as in this study.

Perrett et al., then, tested the Averageness Hypothesis to observe if averageness is the determinant of the attractiveness in the faces [114].

In this work, average face is employed for: Face Template construction in which the whole images in one age cluster are averaged, and fuse two images as one of the methods of fusion, in order to texture adaption (this will be explained in the chapters ahead).

To average the faces, first, constituent images should be aligned, as Galton aligned the constituent images using the distance between the pupils. To begin, this task is done using 5 points for which, a couple of images are extracted from the database. For each image, the center of each eye, the tip of the nose, the center of the mouth and the bottom of the chin have been selected as landmark data points. Then, the distances between these landmarks are minimised using translation, rotation, and scaling. Eventually, the average of the images is calculated. The results appear somewhat fuzzy (Figure 2.10.a).

Therefore, for alignment, all the 79 extracted feature points are employed. First, features are extracted from all images. Then, the average of each feature point is calculated. Afterwards, all the faces are warped to the calculated mean coordinates.

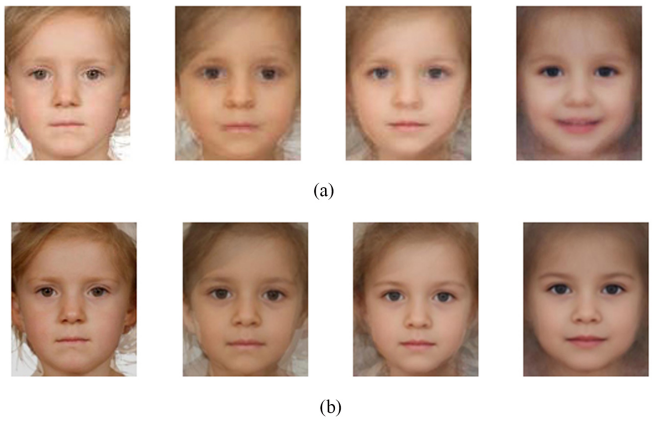

Figure. 2.10 Illustration of some face averages, from left to right using 2, 5, 10 and 50 facial images from the 3-4 years old female age cluster. (a) Using 5 alignment points. (b) Using 79 extracted facial feature points.

Next, the final average is calculated by:

$$\mu = \frac{1}{n}\sum_{i=1}^{n} x_i \tag{2.56}$$

where n is number of faces and x is a single face vector.

Figure 2.10 demonstrates the difference between calculated average faces with 5 and 79 alignment points, using 2, 5, 10, and 50 facial images from the 3-4 years old female age cluster. From these achieved faces it can be comprehended that the average face computed from some face images does not look like the constituent faces; yet it contains the similarities between the faces. Moreover, the more images are used the closer the face to a real one becomes.

2.5 Conclusion

In the chapter left behind, the required algorithms and methods for the model construction have been discussed.

First, different methods of facial feature extraction have been cited. Since the facial images in our created database are almost frontal, with the minimum facial expression, and nearly the appropriate lighting conditions AAM is an appropriate method for feature extraction. For training, 500 facial images each annotated with 79 landmarks have been used. From the examined derivations of the Lucas and Kanade method for fitting AAM to the images, the inverse compositional algorithm has been

selected. This algorithm improves the efficiency since most computationally expensive calculations are applied in the pre-computation phase.

For image warping, image deformation using MLS have been employed. To do this, after comparing the results of different control handles and transformations, extracted facial feature points are selected as handles to control the desired deformations in face components. The rigid transformation is chosen as the transformation function since it gives the best smooth results according to the current application, without stretching and uniform scaling.

Further, some existing face ageing databases are discussed, and the proofs for creating a new database have been mentioned. Since the existing databases do not meet our model requirements such as structure, image quality and resolution, capture conditions, expressions, emotions and etc., two databases are created and introduced: Facial Ageing Modeling Database (FAMD) for models construction, and FaceTiM V1.0 for evaluation purposes.

In the last section of the chapter, Face Template construction, with different number of points to alignment, is described. It is inferred that the more the number of engaged points, the better the Face Template.

Now that the algorithms, methods, and other requirements are discussed, they can be integrated in different facial ageing models discussed in this theses. In the three next chapters, we will describe how these methods are applied in constructing different ageing models to rejuvenate or age the facial images.

Chapter 3

Digital Facial Image Rejuvenation Using Backward Facial Ageing Model (B-FAM)

Contents

Although the facial ageing modeling has been an active research topic and many efforts have been made in this field, face image rejuvenation, particularly, adult to child rejuvenation has not received competent attention. The main focus of the existing literatures in this topic has been the prediction of the face in its older ages. Yet, the facial ageing modeling is not only to predict the face in its old ages, but also to estimate the face in the different age groups.

Thus, the Backward Facial Ageing Model, propounded in this chapter, can fill the void of childhood face modeling in the facial ageing studies. It will show that it is possible to digitally rejuvenate an adult face appearance back to its 3-4 years age [115][116]. In this model the face shape and components are non-linearly adjusted to the target age using a reliable Geometrical Model. Then, face texture is adapted using a relative Reconstructive Face Template.

This chapter is organised as follows; first, facial growth trajectory is discussed in the Section 3.1. Then, age groups and subgroups are defined in the Section 3.2. Facial feature assortment and geometrical measurements are raised in Section 3.3. After, Section 3.4 presents the rejuvenation model development. Some experimental results and evaluation techniques are discussed in Section 3.5. The chapter is concluded in the Section 3.6.

3.1 Facial Growth Trajectory

Child face in not a miniature model of the adult face. The process of its evolution is truly complex. To study the craniofacial growth process, variety aspects of the face should be considered. In this procedure, changes in the hard tissue structure and soft tissue take place at different times, in different directions and with different rates [117]. To model the face growth process or, as in this chapter, to rejuvenate the face image down to childhood, it is important to peruse craniofacial morphology and be knowledgeable of the several aspects of the growth.

First, let us define "facial growth". Growth is the increase in size and change in facial proportions over the time as Wilton M. Krogman defined. Therefore, it is the quantitative and the measurable sight of the biologic life. Growth might be the change in proportions, size, texture, and complexity and in general, change in quantity. Development, however, includes all the changes from a single cell till death. It can be said, growth is an "anatomic phenomenon" whereas development is a "physiological and behavioural phenomenon". According to this, the focus in this study is nearly facial growth [118, pp. 46-47] .

Facial geometry growth is affiliated with adaptability of soft tissue with hard tissue growth. Moreover, when dealing with facial growth, there are usually two important matters to consider; intensity and direction of the growth. In the following, both direction and intensity of growth-related changes, in hard and soft tissues, for different facial landmarks are briefly discussed.

Eyes: The eye is a complex organ, although it is small. A newborn's eye has approximately 70 percent of the size of an adult's eye [119, p. 24]. That is why eyes seem larger in proportion to the head. Over the first three years of life, the eyes grow rapidly and continue to grow through the childhood until they reach almost their adulthood length by age of 13; however, the changes are dedicated and insensible. The eye socket grows as the eyeball grows and gives the appropriate space to the eye to grow in different directions [120, ch. 1]. The visible part of the eyeball has only 1/6 of the eye's total surface area, and the rest are hidden behind the eyelids. In this study, eye size is the visible part of the eye that is the palpebral fissure length, which is the distance from the endocanthion to the exocanthion landmarks (see Figure 3.1).

Nasal: A young child has a small rounded nose which is vertically short and shallow, with a small protrusion. In childhood, the nasal bridge is quite low and the nasal profile is concave. The human nose continues to grow in downward and forward

directions until early adulthood. The length of the nose, in average, increases about 1–1.5mm per year. The vertical dimension of the nose has more share of growth than the anteroposterior projection. Increase in width of the nose is about 0.5 mm per year. The inclination of the nose remains constant. The nose profile changes is due to increments in nasal length [121][117].

Lips: Lips growth follows the general body growth procedure with soft tissue and muscles growth. The lips grow at the gradual rate till 15 years old. It was observed that the maxillary (upper) and mandibular (lower) lips increase in both dimensions under the influence of growth. The upper lip grows away from the palate and the lower one grows away from the chin. The upper and lower lips have their most share of the increment from age 6 to 12. In general, the lower lip grows more than the upper lip and upper lip grows slightly with age. From childhood to adolescence, increase in the thickness of the upper and lower lisps is obvious [117][118, pp. 153-154].

Face: Face continues its growth downward and forward until the adult face shape and size is reached. Skull growth is complex and inhomogeneous. Different parts of the skull are differently matured in terms of size, direction, and rate. In childhood the head is big, so it seems that it does not have a considerable growth until adulthood. The fact is that, during the growth process, the size of the body will increase three times but this ratio is two for the head. Bellow, different parts of cranium affecting frontal face shape and size will be discussed.

Forehead: The brainpan has much greater extent than facial complex in childhood. It grows earlier and faster so that cranial cavity reaches 90% of its size by 5 years of age [117]. The forehead in young children is bulged and seems very large and high as the frontal lobe of the brain is huge in size, and also because the face beneath it is still comparably small.

The large head- small face is noticeable up to ages 7 and 8. In the process of growth, the face enlargement is much more than forehead so that the proportionate size of the forehead becomes reduced [122][123].

Anterior Facial Height: anterior facial height is the sum of upper and lower facial height which from now on in this study is called facial height (see Figure 3.1.a). Vertical growth of the child face occurs due to the both respiratory needs and tooth eruption [117]. These growth spurts take place during the third and fourth year, from

the seventh to eleventh year, and again between the sixteenth and the nineteenth year [124].

Face Width: child face is wide and less in height. Facial width growth is associated with mandibular, maxillary and zygomatic growth. Facial growth arises mostly in the vertical direction compared to the horizontal one. However, studies show that the ratio facial height/facial width increased from childhood to adulthood [125][126, Ch. 1].

3.2 Age Groups and Subgroups Definition

Globally, one can consider four main age groups in the periods of human life: infancy (1 month to 2 years old), childhood, adulthood and old ages. The general features of a person's face in the infancy is quite different from the same individual's grown face and is governed almost purely by genetic factors. Moreover, the general structure of the face has not yet formed and there are only minimal variations in facial structure of their faces. Relatively large-appearing eyes, a tiny nose, a small mouth, puffy cheeks, a high forehead, a low nasal bridge and overall wide and short proportions. As a result, the face in less than 3–year-olds cannot be very useful for identification and subsequently for many applications that can be imagined for this work. Therefore, childhood (3 to 16), adulthood (16 to 30) and old ages (after 30: With the appearance of wrinkles) are arbitrarily considered as the main age groups.

We also consider four age subgroups: 3-4, 7-8, 12-13 and 16 years old for adulthood, since these are the formative years in which most of the changes in the process of growth occur [110]. Considering the difficulty of predicting very close ages, sub-age groups are defined in a way that their age differences are more distinguishable. For example, distinction between a 4-year-old and a 5-year-old child is very difficult but differences between a 4-year-old child and a 7-year-old one are entirely visible and noticeable. In fact, subgroups have been set up in a way that transformations are clearly visible especially in the face's geometry. Therefore, age clusters for digital face rejuvenation are; Cluster 3-4, Cluster 7-8, Cluster 12-13 and Cluster Adult for 16 years old and later (until when that person can be considered as young adult).

3.3 Facial Features Assortment and Geometrical Measurements

Human face is a complex combination of many information which represents identity, gender, emotional state, and age. Many kinds of useful features can be extracted from a face image. By categorising these features, a better perception of the face is achieved and faces can be assorted based on age, gender, ethnics, and expressions. Furthermore, a model can be obtained according to the different features corresponding to the different assortments.

When dealing with face changes over the time, numerous aspects should be taken into account. For instance, in some age ranges, one can notice important face variations in both its shape and its skin texture. Therefore, facial changes can be divided as geometrical (anthropometric) and textural. In the growth process (childhood), most of the changes are geometrical, however, texture undergoes subtle changes. In the ageing trajectory (adulthood) is inverse. Based on these, facial features can be divided into two different categories:

Geometrical Features which are concerned with changes in craniofacial morphology and anthropometry of an individual. These changes can occur in the bony portions of the head and soft tissues of the face [126]. It can be said that the geometrical features have two subdivisions:

1. The information which is connected to the facial components' (eyes, nose and lips) size and their distribution.

2. The information about the face shape (the contour), consisting of the upper face, its mandible size and its maturation process.

Textural Features that are concerned with the skin changes. These changes consist of the thickness and the colour of the skin, elasticity of the facial muscles and the appearance of the wrinkles.

3.3.1 Geometrical Measurements

Changing the facial age geometrically requires the transformation of the facial components' size, distances between them, face shape, and its size. Choosing the practical scales and distances has commenced with the study of the craniofacial morphology and data collection dealing with craniofacial growth. One part of the data was about

development and understanding how organs change during the ageing process. The result was just useful to have a better perception of the facial growth so the focus was shifted to the changes in the magnitude of facial landmarks. After collecting all the craniofacial measurements, they were filtered: First, to those which were useful for 2D facial modeling. Therefore, information such as the head length and width are eliminated.

Second, to those which can present a component or its location in the face. For example from inner Canthal distance, outer Canthal distance and interpapillary distance of the two eyes, only the first one was retained as a measure for eyes distribution in the face since the other two are redundant for this study. Some of the measurements such as skull height or forehead height are included in the face shape and size.

To apply the geometrical face transformation, craniofacial measurements in different ages are needed. First, the required components' size and distances should be defined. In the following, you can find their definition by using the 79 previously extracted landmark points related to the face components and the contour.

Eye Size: Distance between the inner and outer canthus of one eye. The head should be held erect with the eyes open and facing forward.

Inner Canthal Distance: The distance between the innermost corners of one eye to the outermost corner of the other eye, in a straight line.

Nasal Height: The distance from the deepest depression at the root of the nose to the deepest concavity at the base of the nose, in a vertical axis.

Nasal Width: Distance between the most lateral aspects of the alae nasi.

Distance between Nose and Lips: Distance between the base of the nose and the border of the upper lip, in the midline.

Mouth Width: Measure from one corner of the mouth to the other. The head should be held erect with the eyes facing forward and the mouth held close and in a neutral position.

Face Shape: 20 facial feature points are the face contour indicator as cited in the previous chapter and nasal bridge is considered as the origin of the face. Accordingly, the face shape and its scale are defined using these points (Figure 3.1).

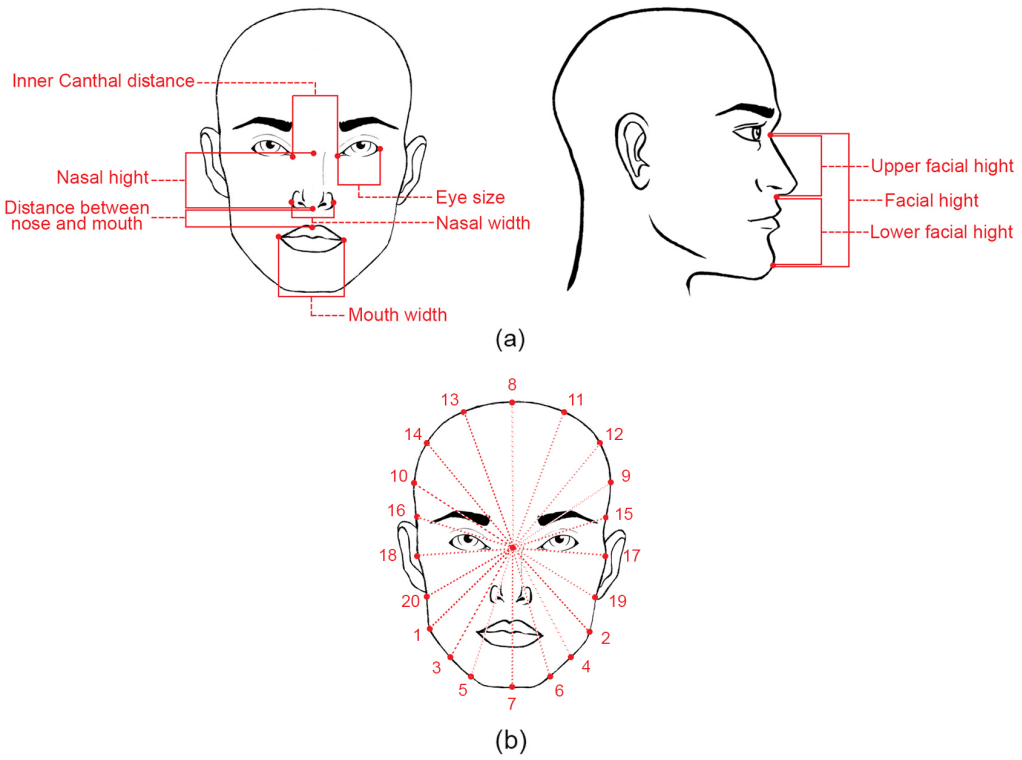

Figure. 3.1 (a) Illustration of the vertical and horizontal facial measures' definition. (b) Illustration of the 20 radiuses with their given numbers, which define the face shape and scale.

These measurements have already been done by Judith G. Hall from the birth to 16 years old [110] . Among these numbers, those corresponding to formative years (3-4, 7-8, 12-13 and 16) are considered in this study (Figure 3.2.a).

In addition to that, having the calculated average size and distance of all face images in each age cluster in our database, the same chart has been extracted (Figure 3.2.b).

As it can be seen, these two charts are very close, so, using these results, the percentage of the scale and the distance changes has been extracted. Final percentages and orders are obtained by comparing these two charts. Figure 3.3.a shows the percentage number of all components' size in different age clusters compared to the adult components' size. Reference measures are the measures of the early years of adulthood. Note that an adult, in terms of geometry, means a person with more than 16 years of age because the geometrical growth of the face winds up at this age.

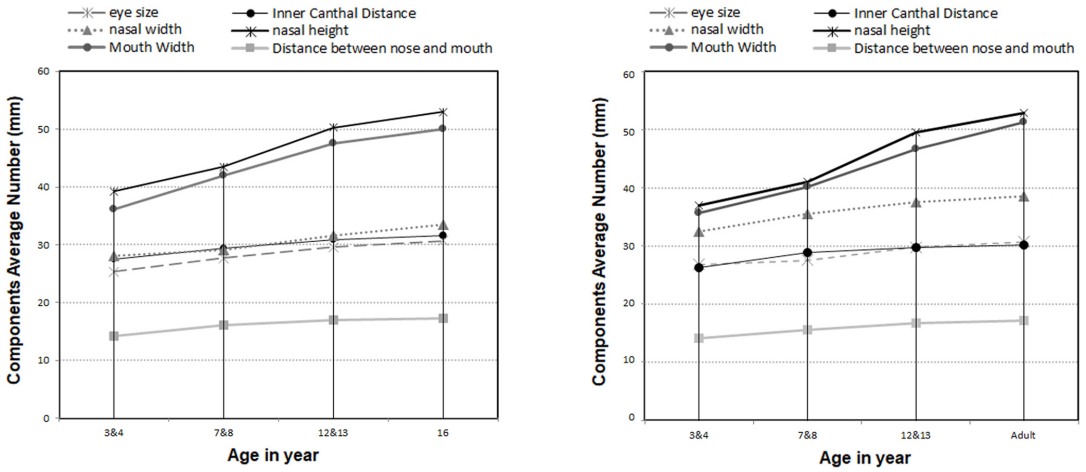

Figure. 3.2 (a) Facial components' size and distances - both genders, four age clusters – extracted by Judith G. Hall [110]. (b) Facial components' size and distances - both genders, four age clusters – extracted from calculated average size and distance of all face images in each age cluster.

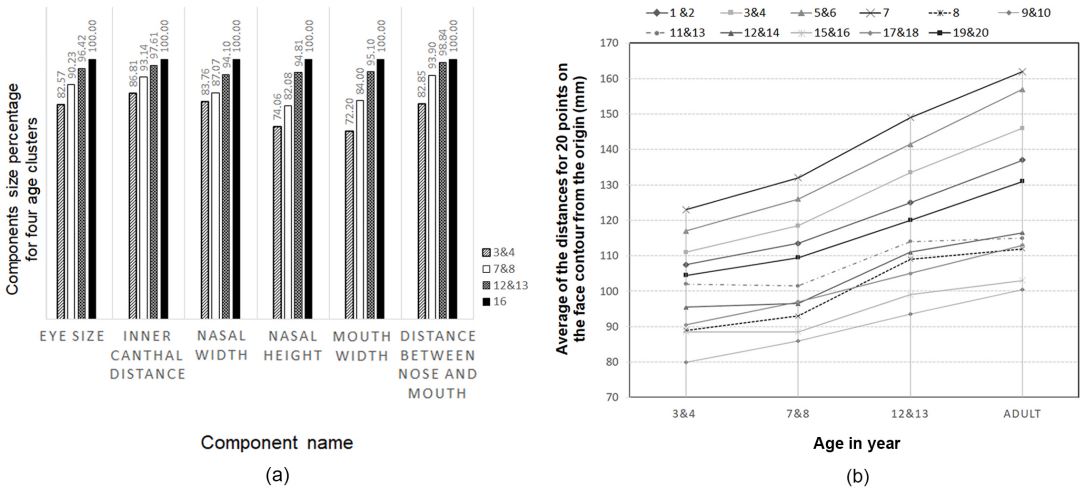

Figure. 3.3 (a) Percentage of the components' size in different age clusters compared to the adult components' size - both sexes, four age clusters. (b) Average distance of each point on the face contour from the origin - both genders, four age clusters – extracted from calculated average radiuses of all face images in each age cluster.

3.4 Rejuvenation Model Development

Information from research resources [110] [11] show that there are two periods in facial ageing:

1. From birth to adulthood, that can be named formative years, in which most of the changes related to the geometry appear. There are minor changes in the skin colour, facial hair colour, and the density. It can be said that the textural variations tend to be subtle during this period.

2. Adulthood which is the end of growth until old ages. The majority of changes in this period are related to the skin texture. The skin becomes thinner and darker with less elasticity; this is the time for wrinkles to appear. Some small craniofacial changes such as the shape change of the face and eyes also occur.

B-FAM is dealing with the childhood face alterations, so the geometrical variations have more important roles.

In this work, the procedure is separated into two parts: geometrical and textural. At the end, the final result is visualised through merging these two sections.

3.4.1 Geometrical Model

Since the geometrical features have been divided into two parts, the facial transformation will be applied in two steps:
1) Components' Scale and Their Distribution, which are defined by some modifications such as eye size, inner Canthal distance, nasal height, nasal width, the distance between nose and lips, and mouth width, all previously measured. Each face component is considered as a discrete object.

For mathematical description of the component's shape, a finite number of points along the boundary are located in the feature extraction phase and concatenated to a shape vector. Face components are each modified according to a special scale factor that is the percent of the component's size in an age cluster. Besides, their distances are modified, if required, according to a translation vector.

$$S_i = \alpha S_j + d \qquad (i < j \ , \ 0 < \alpha < 1 \ ) \tag{3.1}$$

where S_i is the target component's size, α is the scale factor, S_j is the current component's size, and d is the translation vector. j is the input age, i is the target age, and for backward modeling $i < j$. For adult to child rejuvenation, α is always between

zero and one since all the face components' sizes in childhood are smaller than their sizes in the adulthood. Note that, the order of the changes is important. It means that at first the size changes, and then translation is applied to modify the distances and decomposition of the facial component distribution.

2) Face Contour: the nasal bridge is considered as the origin of the face and 20 points for the contour get extracted in the feature extraction phase. The face shape can be defined by these points and its scale is defined by 20 radiuses obtained from those and the origin point. Studies show that in the process of facial growth, these radiuses do not change similarly; the upper face and the mandible mature unevenly. For each radius, one different coefficient is obtained. For example, the forehead has larger share of the face in childhood compared with adulthood. Yet as the face is symmetric, some of them can share the same coefficient (see Figure 3.1.b and 3.3.b). Since holding the same angles in the radius proportion is important, in order to apply the changes the following method is used. Where $O(O_x, O_y)$ is the origin of the face, $C_j(C_{xj}(n), C_{yj}(n))$ is the facial contour point in the input age j, and $D_j(n)$ is the distance between them for n equals 1 to 20,

$$D_j(n) = \sqrt{(C_{yj}(n) - O_y)^2 + (C_{xj}(n) - O_x)^2} \tag{3.2}$$

For calculating the angle $\theta(n)$:

$$\tan\theta(n) = \frac{C_{yj}(n) - O_y}{C_{xj}(n) - O_x} \tag{3.3}$$

$$D_i(n) = \frac{D_j(n)}{\beta} \qquad \beta > 0 \tag{3.4}$$

$C_i(C_{xi}(n), C_{yi}(n))$ is the point of interest which is the point corresponding to the target age face contour, $D_i(n)$ is the new radius. β is the coefficient which differs from one age cluster to another and there are 11 different β to change a face in age j to the face in age i (see Figure 3.4.a).

$$C_{xi}(n) = C_{xj}(n) + D_i(n) * \cos\theta(n) \tag{3.5}$$

and

$$C_{yi}(n) = C_{yj}(n) + D_i(n) * \sin\theta(n) \tag{3.6}$$

The final result of geometrical changes is shown in Figure 3.4.b.

As the mathematical aspect is done, the result should be visualised. To visualise the geometrical correction, image warping should be applied. As completely explained

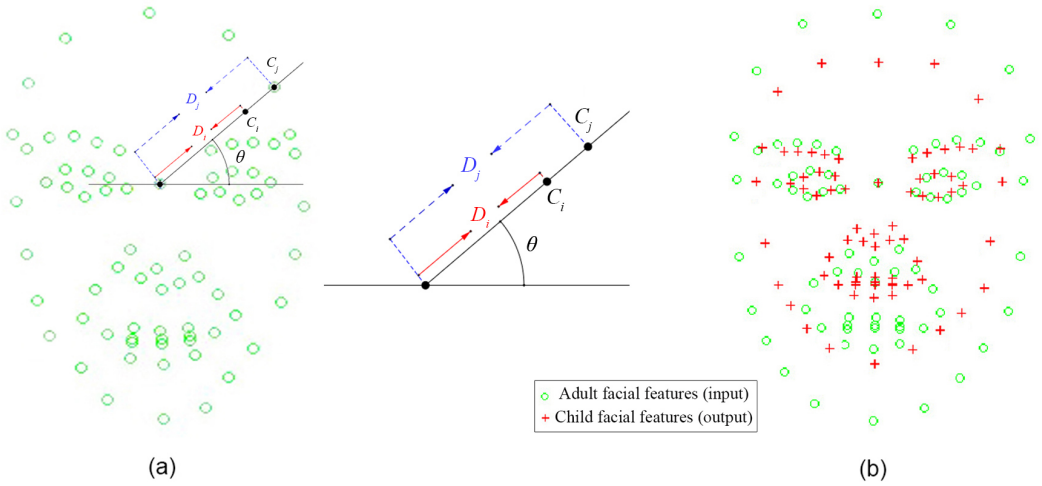

Figure. 3.4 (a) How adult facial contour radiuses are changed - C_j is changed to the C_i by having the β coefficient and keeping the angle θ constant. (b) Result of geometrical changes for both components and facial contour from adult (green circles) to 3-4 years old child (red crosses).

in Chapter 2, image warping changes the input into an output image according to a mapping between the input and output space. For this reason, the points in the image, yet not deformed, should be mapped to the deformed image. For example, in Figure 3.4.b the facial points for the adult face image (green circles) should be mapped to the points for the 3-4-year-old facial points (red crosses).

3.4.2 Reconstructive Face Templates

Since growth process depends on the genetic and the complex environmental interactions, growth related effects on the face are different from one person to another. However, the facial growth pattern similarities among the people in the same age cluster cannot be disregarded.

To study these common characteristics in an age range, an average face is calculated (explained in Chapter 2). In fact, the average of the facial images in the same age cluster can demonstrate; first, the sum of the important and distinctive similar information for that specific age; that is why it has been named *Face Template*. Second, the typical differences between two age clusters. Of course the more these two ages are far from each other the better the differences are distinctive.

Initially, the Face Templates are constructed using 5 points for which all images in an age cluster are selected and the average was calculated based on steps mentioned in Section 2.4. The results in the first row in Figure 3.5 show the Face Templates resulted from this method, which are not satisfying because of the blurriness in some

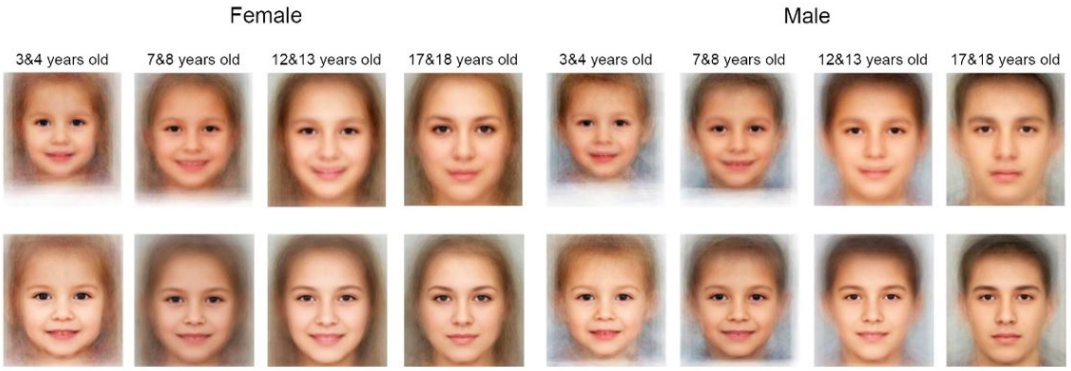

Figure. 3.5 Illustration of the failures in creating the Reconstructive Face Templates - both sexes – four age clusters. The first row includes the Face Templates constructed by using only 5 points. The second row includes the Face Templates constructed using all the extracted facial feature points that are mostly with a smile which should be eliminated.

parts of the face, such as facial components boundaries and especially the face contour. Moreover, extracting the facial features and the information of the texture is not easy.

Therefore, this time Face Templates are constructed using all of the extracted feature points according to the different phases, fully described in Chapter 2, by employing feature extraction, image warping and averaging among all the faces in each age cluster.

It can be said, for each facial image $f(k,\rho)$, k describes the value of a pixel position ρ. $T(\lambda,\rho)$ is the Face Template for one age cluster, described by the Face Template colour λ , which is the average of the pixel values for the same pixel position ρ from all facial images in an age cluster. In fact, this is a fusion method to fuse multiple images in order to combine their related information.

$$T(\lambda,p) = \frac{1}{n}[\sum_{i=1}^{n} f_i(k,\rho)] \tag{3.7}$$

n is the number of facial images in the age cluster.

These results are sharper; the face contour and facial components' borders are vivid. The features and the textures are also clearer as it can be seen in the second row of the Figure 3.5.

However, this time, the weakness of the calculated Face Templates is that the Face Templates are with smile. The reason is, in the collected database most of the face images are faces with a smile on them. This affects the quality of the results because of the changes made in the size of the mouth and the existence of laugh lines on the two sides of the lips as it can be seen in Figure 3.10.b and c. To have the better Face Templates and solving these issues in the final results, the database is revised and the

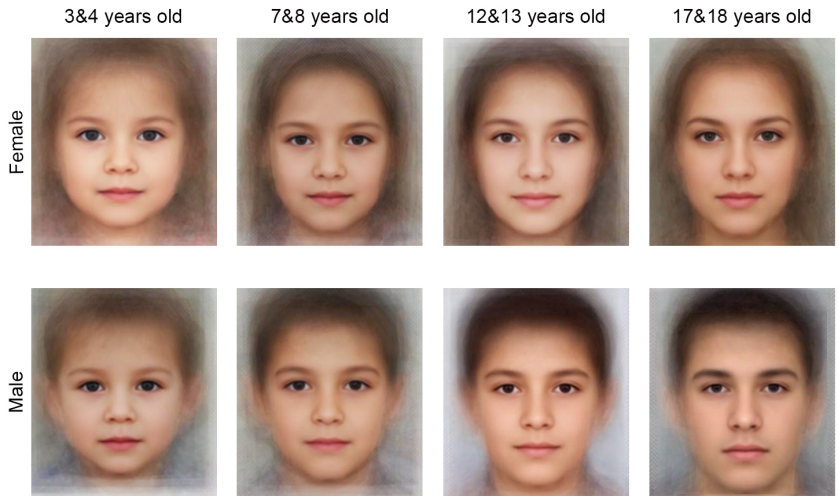

Figure. 3.6 Illustration of the final Reconstructive Face Templates, both sexes – four age clusters.

faces with big smiles are pretermitted and replaced. As it can be seen in the Figure 3.6, the final *Reconstructive Face Templates* are in a better condition and the obtained results using them are more satisfying.

3.4.3 Textural Model

Although the geometrical results have geometrical characteristics related to the associated age groups, they are not visually sufficiently realistic and convincing. Therefore, in order to have a better textural aspect, they should be fused with the Reconstructive Face Templates belonging to the same age cluster.

To apply the fusion, the geometrically changed face is fused with the associated Reconstructive Face Template, by engaging the 79 facial feature points and the image warping. In fact, first, the average of the coordinates of these two face images is calculated. Then, the facial feature points in the Face Template and the geometrically changed face image are warped to the calculated average coordinates. At the end, these two face images are fused by using the texture averaging.

In applying the Textural Model, there are some intricacies that significantly change the quality of the results:

Keeping the Original Eye Shape: As mentioned before, to apply the texture variation, both face images (Reconstructive Face Template and the geometrically changed face image) should be warped to the calculated mean coordinates of each feature point. By paying more attention to the primary results and taking into consideration that in many cases, people are recognised by their eyes, the original shape of the eyes

is preserved. For this reason, when the averages of coordinates are calculated, the feature points corresponding to the eyes will not be considered. Instead, the eyes in the Face Template image will be warped to the eyes coordinated in the geometrical result. Otherwise, the eyes area in the result will be blurred.

Weighted Average Calculation: In order for the result to have a texture most proximate to its related age group, the main face image and the Reconstructive Face Template should undergo an average calculation procedure. The given weight to each input is very crucial. It means that it can be decided which face image has more share in the result; the main one (Geometrically changed) or the Face Template. Of course, the more shares the main face image has, more similarity in the result is obtained. Most often, a percentage between 50 and 70 for the weight of the main face image, gives an acceptable result.

These results also contain all the expected geometrical characteristics defined for a face in the target age. In the meantime, their texture is adapted under the influence of the Reconstructive Face Template. Thus, these results are visually realistic and acceptable (Figure 3.10). For weighted average:

$$\mu_w(\lambda,\rho) = \sum_{i=1}^{n} w_i f_i(k,\rho) \tag{3.8}$$

μ_w is the weighted average of two face images and w is the weight given to each face image. As a matter of fact, in this case, we have only two images so $n = 2$. Hence, it can be said, Face Template construction for instance is a special case of the weighted average where all the face images have equal weights.

To achieve the percentage range between 50 and 70, a survey has been made on the results of 34 adult input images. For each input image, the percentages from 10 to 90 were given to the main face to achieve a range of results. Note that, 0% for the main face means that only the Reconstructive Face Template is used and 100% means that the effect of the Face Template is neglected, so these two conditions are passed up. Then, we asked 100 people to choose the percentage that gives the most likely result to a reference image from the input face's childhood. Figure 3.7. shows the average of the responses for all 34 sets of results. As it can be seen most of the chosen percentages are between 50 and 70. The input images are selected from Set 1 and childhood face images used as reference are from Set 2 of FaceTiM database.

Mask Creation to Keep the Natural Eye Colour: With a closer examination of the obtained results, it is undeniable that in order to have better results in the images

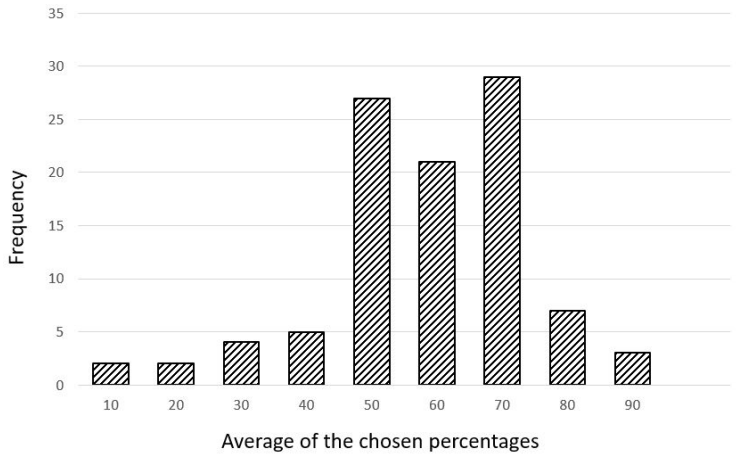

Figure. 3.7 The histogram of the chosen percentages for the share of geometrically changed faces based on the highest similarity to the childhood reference images.

of people who have coloured eyes, some pre-processing should be done before the average calculation. To this purpose, iris should not be considered in calculating the average (see Figure 3.8).

To do this, a binary mask is overlaid onto the eyes area in the Face Template, to prevent the masked area from getting included in the calculation. The area is selected by using double thresholding with pixel values and morphology-based opening and closing, which are derived from the operations of erosion and dilation [127][128].

In fact, we use opening to preserve the region that have the similar shape to the structuring element or can completely contain structuring element while eliminating all other regions of foreground pixels. If I is the eye region from the facial image and H is the structure element that arbitrary defined, opening is:

$$I \circ H = (I \ominus H) \oplus H \tag{3.9}$$

which is the morphological operation of "an erosion followed by a dilation". Opening removes the isolated foreground structures that are smaller than the H structure element, and keeps the larger structures. Closing is:

$$I \bullet H = (I \oplus H) \ominus H \tag{3.10}$$

which is the morphological operation of "a dilation followed by an erosion". Closing fills the holes in the foreground that are smaller than the H structure element [127, p. 209]. If the selection is not perfect then a manual selection can be created.

It is worth mentioning, in calculating the average in this section, eyes are weighted separately.

Figure. 3.8 Mask creation for keeping the original eyes colour. From left to right, created eye mask, geometrical result and rejuvenated face image.

Figure 3.9 shows the general overview and the different steps of the modeling approach. This diagram shows that the work is composed of 3 main sections: Data collection and pre-processing (which consists of normalisation and feature extraction), Face Template construction that have already been stated, and B-FAM that consists of different parts of the model.

3.4.4 Backward Facial Ageing Model (B-FAM)

Based on the steps mentioned above, B-FAM is proposed for digital facial image rejuvenation. In this model each rejuvenated face, in one of the formative years, is the sum of the Reconstructive Face Template correspond to that specific age and its special geometrical characteristics, facial differences and details:

$$F(i) = w_1 T_r(i) + w_2 \varphi(f(j)) \quad , \quad \begin{cases} i < j \\ 0.5 < w_2 < 0.7 \\ w_1 + w_2 = 1 \end{cases} \tag{3.11}$$

where $F(i)$ is the input face image in the age i, $T_r(i)$ is the Reconstructive Face Template in the same age, and $\varphi(f(j))$ is the transformation function applied on the face f in age j to adapt the geometrical aspect of the face to the target age i, by keeping the entire differences and details related to the input face. j is the input age, i is the output age and $i < j$.

This sum is the weighted sum in which w_1 and w_2 are weights given respectively to the Reconstructive Face Template and result of the geometrical transformation function. $0.5 < w_2 < 0.7$ that can be confirmation for the fact that most of the alterations during formative years are geometrical and texture undergoes slight changes.

This ageing model can even be carried out for different ethics or genders. For example, a Mongolian face in the age i can be presented with the sum of a typical Mongolian face in that specific age and its particular details and differences. Of course, the more face images used in the database in creating the Face Template, the more exquisite the results are.

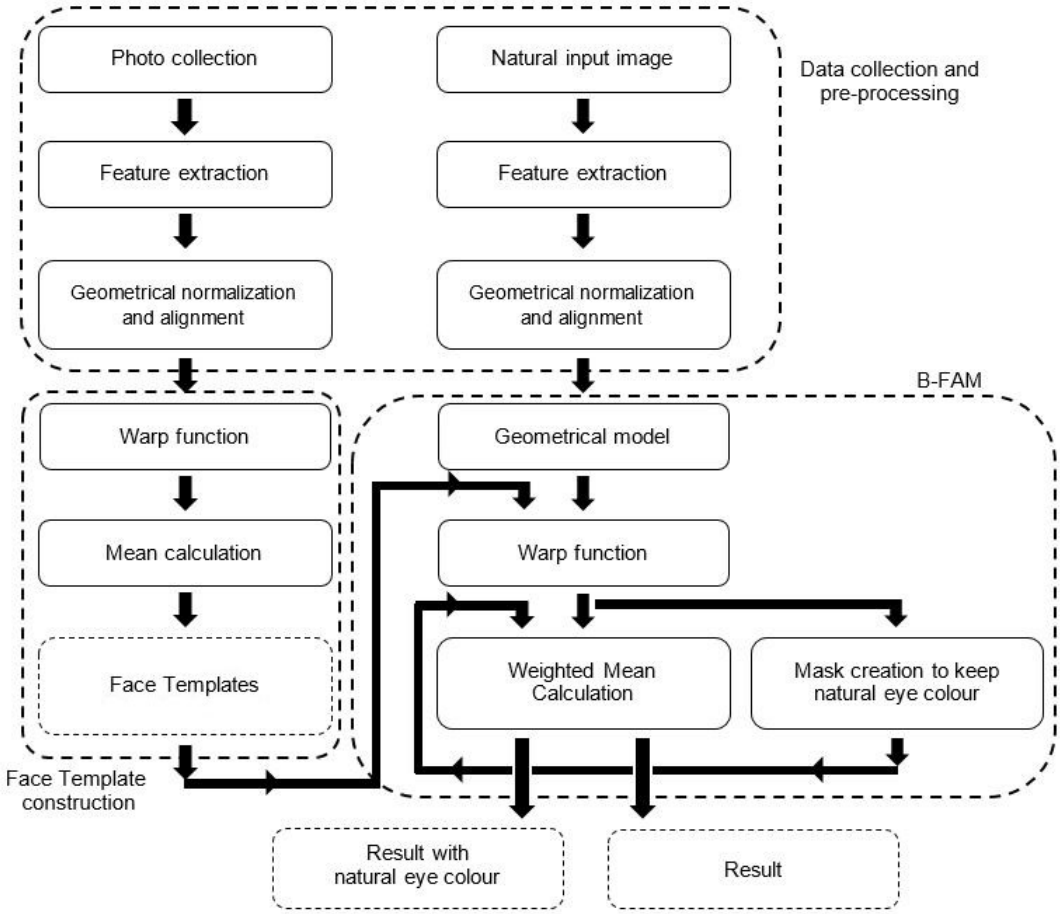

Figure. 3.9 General organization of the work.

3.5 Experimental Results and Evaluation

3.5.1 Database and the Final Results

In order to study the facial changes during the growth ages and construct the model, Backward Facial Ageing Collection (BFAC) album from the Facial Ageing Modeling Database (FAMD), explained in Chapter 2, is used. This album contains almost 700 facial images in 4 different age clusters, Cluster 3-4, Cluster 7-8, Cluster 12-13 years old and the Cluster Adult, separated by gender.

For testing the model, 112 adult face images from Face Time-Machine Database (FaceTiM V1.0), Set 1, are used, which are frontal and almost without any facial expressions. Besides, 112 face images from Set 2, that contains childhood face images belongs to the individuals in Set1, are employed as the reference to compare the simulated results.

According to the presented model, the input is an adult face image and the result is how it might have looked in one of the defined age clusters. The reference face images have been employed to compare the results and to evaluate them. Some of the results are shown in Figure 3.10. In this figure the size difference between age clusters is preserved to better representation of the growth process.

The model can generate faces in different specified age clusters (Cluster 3-4, Cluster 7-8, Cluster 12-13 and Cluster Adult). However, we have changed the faces only to some age clusters that we actually have references for them, in order to be able to evaluate the results.

Figure 3.11 illustrates the rejuvenation results on one subject facial image in different age clusters.

To evaluate the results, two criteria are used: An objective comparison using a face recognition system and a subjective comparison based on the human perception of the accuracy of the results.

3.5.2 Objective Performance Evaluation

Objective evaluation shows how much the results and the references are distinguished as the same person by a face recognition system. The reference face images were used in the enrolment phase and the results as the probe image. Then, an assessment on the outcomes of the system is needed.

When dealing with biometric systems, two factors are taken under consideration: FAR (False Acceptance Rate, the proportion of impostors that are accepted by the

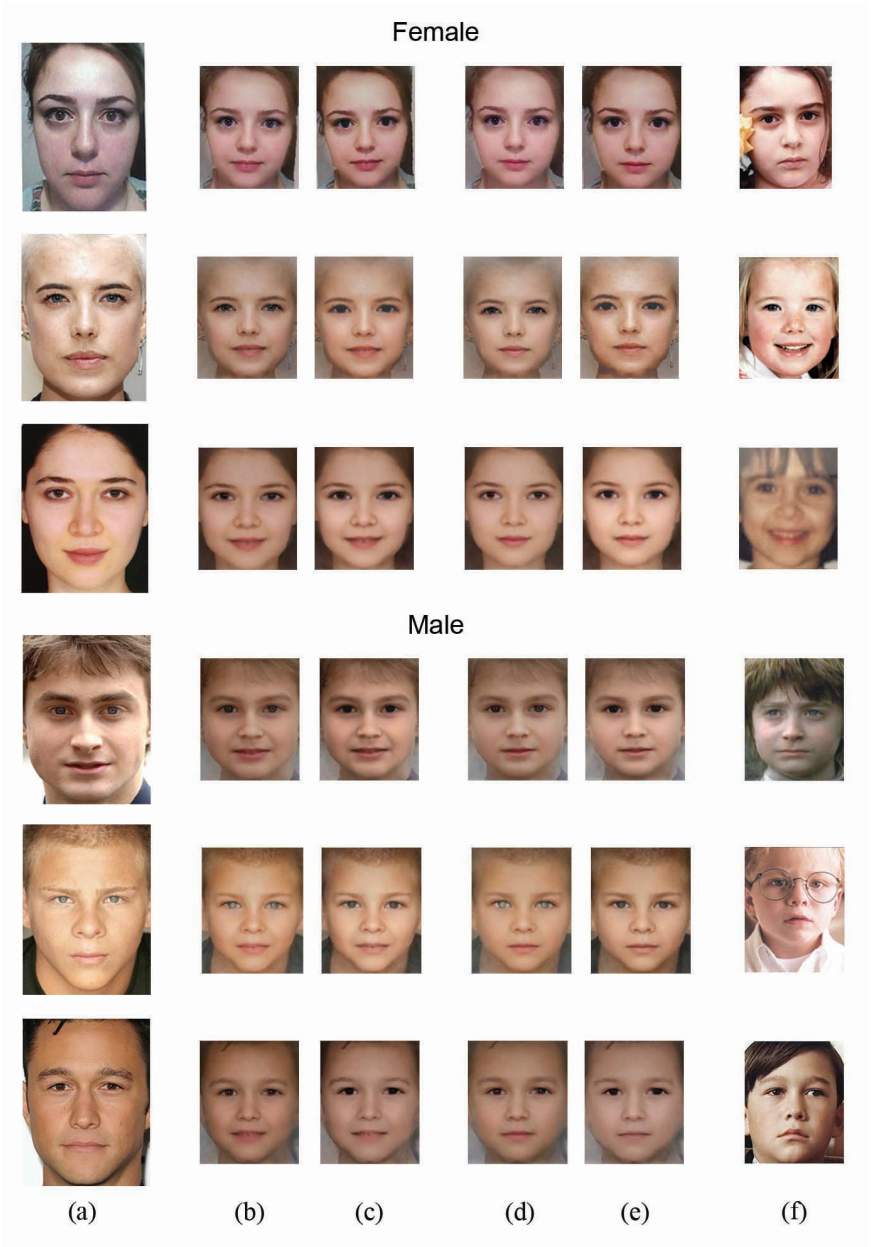

Figure. 3.10 Results of applying B-FAM. (a) Original image - young adult. (b) Result using Face Templates with smile and natural eye colour. (c) Result using Face Templates with smile and calculated average eyes. (d) Result using Reconstructive Face Templates without smile and with natural eye colour. (e) Result using Reconstructive Face Templates without smile and with calculated average eyes. (f) Reference image in approximately the same age as the result, for further comparison.

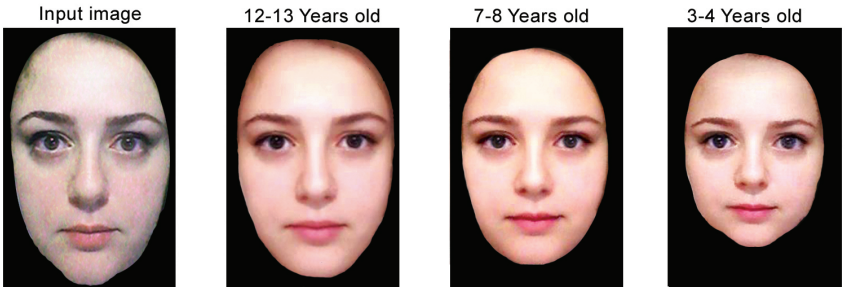

Figure. 3.11 Illustration of the rejuvenation results in different age clusters.

biometric system) and FRR (False Rejection Rate, the proportion of authentic users that are falsely denied) [129][130]. While the system threshold can be adjusted to any arbitrary value, there is no objective method to assess the efficiency of the produced FAR and FRR values. As an alternative, the Equal Error Rate (EER) of a system can be used, to give a threshold independent performance evaluation [131]. In fact, EER is the cross point of FAR and FRR, where the rate of false acceptances and the rate of false rejections are equal. The lower the EER is, the better the system performs.

Figure 3.12 shows Receiver Operating Characteristic (ROC) and Detection Error Trade-off (DET) curves for our proposed model, tested with the face recognition system. As it can be seen, the equal error rate (EER) is about 21.5% for 112 subjects. Indeed, by extending the number of the images in the database, a more accurate number for the EER of the system will be achieved. In addition to the database issues mentioned above, the quality of the reference face images influences the evaluation results. That is because most of the references do not have the same pose, light condition or the same facial expression as the final result. Moreover, it is obvious that the face recognition system's performance can affect the evaluation result and of course by changing the approach the performance can also be slightly changed.

Since, the goal of this study is not to propose a face recognition system, for the objective evaluation a stable commercial face recognition system is used as a black box to show the high similarity between simulated faces and their references. Of course, by changing the approach, the performance can be changed slightly.

This system implements image indexing and provides the API (Application Program Interface) which extracts a template from the faces and match them. A template extracted from a face is stored in a database and then is used to match the faces. Thus, for each 2 given faces, the system matches 2 faces at the given FAR and FRR and gives us a similarity value. This face recognition system is tested on the FRGC database and has the successful identification of 93% if acceptable false positive is 0.1%. The ROC diagram of the system is shown in Figure 3.13.

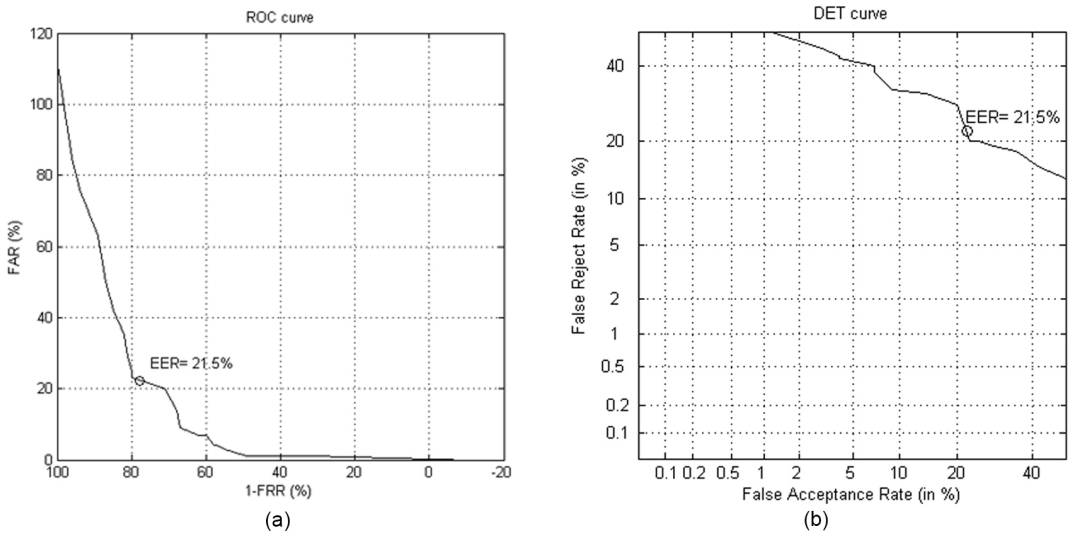

Figure. 3.12 Evaluation curves. (a) EER of the B-FAM in ROC curve. (b) The detection error trade-off (DET) graphs for B-FAM.

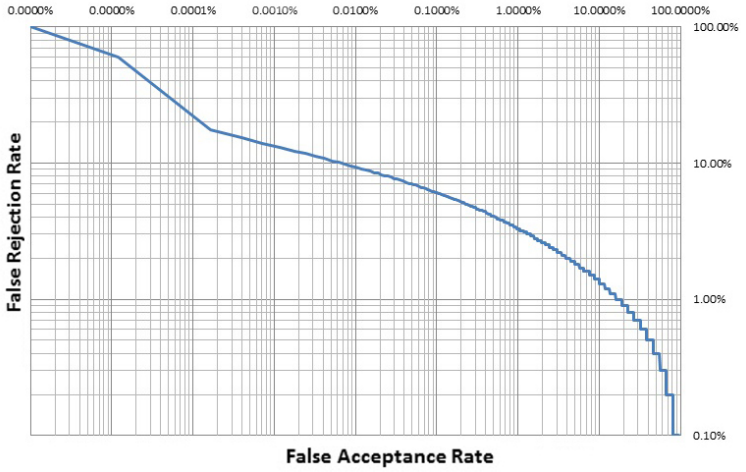

Figure. 3.13 ROC diagram of the face recognition system used to evaluate results objectively.

Figure. 3.14 A sample of face images that were shown to the subjects for rating the similarity in the faces.

3.5.3 Subjective Performance Evaluation

Subjective evaluation tells how much the results and the references look alike by performing the user study. More specifically, we have asked people to evaluate the results. Two protocols have been proposed:

- The first one is to compare our results to the references at the same age. Each person was shown the results at the age *i*, and a reference in the same age. They had rated the similarity between the two faces. All images were cropped only to the region of interest. A sample of face comparison is shown in the Figure 3.14. The total number of comparisons used is 100. The calculated average and the standard deviation for each result are shown in Table.2.

By studying the averages, it can be realised that most of the results are relatively satisfactory. Figure 3.15 is the histogram of the similarity rates given to the results by the respondents. As it can be seen most of the given rates demonstrate about 70% similarity between simulated face image and reference image. In other words, 78.57% of responses indicate more that 65% similarity.

In order to show the effect of alterations made on the face, photos of celebrities are used which have mostly undergone surgery, have makeup on or had taken any other actions affecting the natural procedure of their face growth. It is worth noting that, these kinds of alterations made on the face are a big challenge, specifically for the age reduction modeling. Even with the input faces having undergone surgery or makeup on, the model is still capable of making the input face images younger and the results are quite comparable with the reference images. It is noticeable that the more natural the input face is, the more realistic the result will be.

It can be seen that the measured standard deviations are nearly high and that a large amount of variation exists in the grades given to each result, by the participants of the survey. This means that the results are remarkably comparable from the point of view

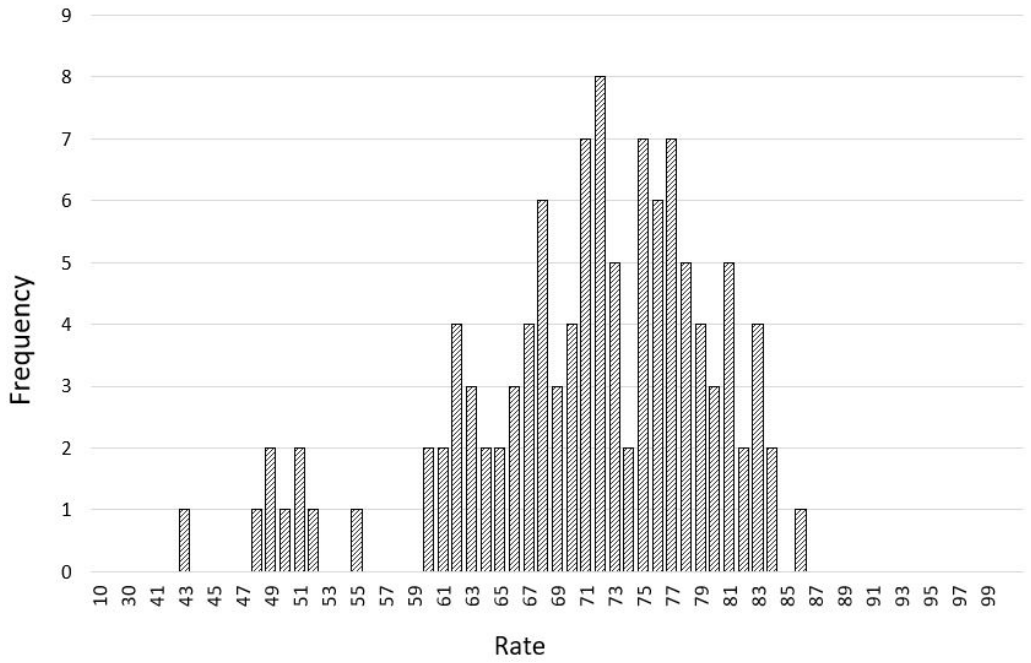

Figure. 3.15 The histogram of the similarity rates given to the results by all the respondents.

of some of the respondents, but that is not the same for all. Some very low ratings may come from the inability to understand the work's concept efficiently.

- The second one is to match the adult face image with an image from its childhood. The results are assorted first into male and female categories, then they are placed into sets, categorised by hair and eye colour (see Figure 3.16). In each matching set, we have two rows of face images, one for adults and another for their childhood. People should compare these two rows and match them by pair, according to the probability of being the same person at different ages.

The total number of submissions received is 107. The calculated average of the correct answers for each set is shown in Table 3. As it can be seen, the percentages of the correct matchings for each set are satisfyingly good. The average number of the correct answers is 93.56%. It means that from the respondent's view, while the results have the characteristics of a typical child's face, they also have their present special characteristics, differences and details of the original adult face images, which makes the matching decision easy.

This result can lead us to questioning the proficiency of the human performance on this task, or to doubt that should we better always rely more on having a face recognition system on the side, in order to evaluate the results of facial ageing modeling.

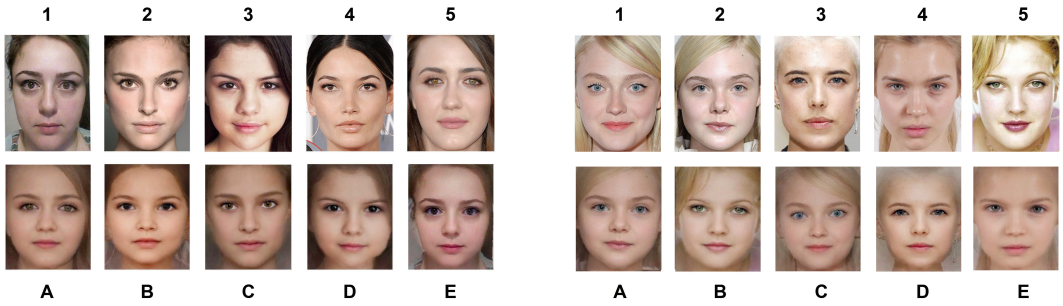

Figure. 3.16 A sample of the matching faces that were shown to the subjects. (a) An example of a dark hair and eyes-female set. (b) An example of a blond hair and coloured eyes-female set.

Table 3.1 Table of the calculated average and standard deviation of given similarity in percentage for 112 separate results.

Result No.	Average ± SD	Result No.	Average ± SD	Result No.	Average ± SD
1	78.1±18	38	69.8±17.1	75	73.3±20.8
2	63.7±22.7	39	42.2±24.9	76	49.3±24.8
3	59.8±22.8	40	66.6±17.9	77	82.2±16.4
4	68.1±20	41	70.7±23.1	78	76.2±21.2
5	75.3±16	42	71.9±17.7	79	77.9±15.0
6	71.6±18.3	43	60.2±20.9	80	74.2±22.0
7	50.8±21.3	44	72.5±19.4	81	78.2±14.9
8	65.5±20.5	45	67.7±19.8	82	80.8±13.8
9	48.6±25.4	46	71.5±21.2	83	71.9±20.2
10	74.3±14.5	47	76.5±20.0	84	62.9±21.8
11	67.8±18.3	48	69.7±19.7	85	77.8±17.8
12	67.4±19.2	49	74.1±21.1	86	80.5±16.8
13	61.3±19.4	50	75.1±16.0	87	74.7±19.0
14	61.6±18.5	51	78.8±19.4	88	67.0±19.4
15	50.3±19.2	52	80.1±15.9	89	71.7±19.9
16	49±28.2	53	76.2±17.3	90	85.2±13.0
17	70.6±19.9	54	70.7±24.3	91	79.4±19.4
18	70±19.2	55	82.1±16.7	92	76.6±20.6
19	62.5±24.2	56	75.3±19.5	93	54.6±23.8
20	67±20.3	57	71.2±23.5	94	72.9±22.4
21	77.3±15.4	58	83.4±15.9	95	67.5±24.1
22	70.6±18	59	76.3±17.8	96	68.4±21.8
23	64.6±17.8	60	73.7±18.5	97	79.4±14.9
24	61.4±21.3	61	78.4±17.4	98	72.6±17.7
25	71.6±18.1	62	65.3±22.0	99	64.6±24.1
26	47.2±26.7	63	59.1±22.7	100	51.6±26.0
27	65.5±20	64	75.5±19.4	101	76.9±14.8

28	81.3±15.4	65	81.0±15.5	102	67.4±18.3
29	67.8±20.4	66	72.9±23.9	103	75.5±14.0
30	70.7±19.9	67	69.3±23.0	104	82.3±18.8
31	63±18.9	68	75.5±18.6	105	81.6±12.9
32	60.6±22.2	69	82.4±16.9	106	74.4±25.1
33	63.3±23.1	70	74.4±18.1	107	80.0±14.8
34	62±17.9	71	77.9±18.3	108	70.2±15.6
35	73.0±16.5	72	71.8±23.7	109	66.5±22.7
36	68.1±15.7	73	71.0±20.2	110	80.1±17.7
37	74.1±18.0	74	76.4±18.2	111	77.6±19.3
112	83.6±14.8				

Table 3.2 Calculated average of the correct answers for each set of face image matching.

Gender	**Dark hair & eyes**	**Dark hair & coloured eyes**	**Blond hair & coloured eyes**
Female	95.09	93.49	92.95
Male	89.94	-	94.34

3.6 Conclusion

In this chapter, the Backward Face Ageing Model (B-FAM) for the digital face image rejuvenation has been presented. This model, for the first time, digitally rejuvenates an adult face appearance down to its early childhood.

First, the Geometrical Model has been applied on the face; the face components and face contour have been non-linearly changed using a robust Geometrical Model. In order to adjust the texture to the target age, the weighted sum calculation has been applied on the geometrical results and the related Reconstructive Face Template. As to improve the quality of the results, some techniques have been used to maintain the eyes' original shape and colour.

The EER of the objective evaluation performed on the results, is about 21.5% for 112 subjects. Indubitably, by increasing the number of the subjects the more accurate number will be achieved. The quality of the reference face images used in the enrolment phase, influence the evaluation result. Thus, by replacing the better images as the reference, the EER number can be decrease. Of course the impact of the face recognition system's performance cannot be ignored.

For a more precise evaluation of the model, subjective performance evaluation is also performed. For the first protocol of subjective performance evaluation, which is to compare our results to the references at the same age, 78.57% of respondents observe more than 65% similarity. For the second protocol, which is to match the adult face image with the simulated image for its childhood, 93.56% respondents gave the correct matching answer.

It means our results are notably accepted by respondents as a child face image, and the resemblances between the modeled results and adult input images are also evident for participants.

In general, from the results and the outcomes of the performance evaluations it can be inferred that while simulated faces have the geometrical and textural characteristics of a typical child's face in the target age, the personal identity characteristics and details of the original input face are preserved. It indicates the presence of an accurate rejuvenation model.

In this proposed approach the effects of the non-facial factors that can influence the perception of an individual's age, such as hair style, facial hair, and makeup are not counted. These factors can be considered in the future improvements of the model.

It can be said, all the actions affecting the natural process of the facial growth such as heavy makeup and cosmetic surgeries are challenges for reconstructing a child face image from an adult face image. Hence, their effects can influence the accuracy of the model.

In the next chapter Forward Facial Ageing Model (F-FAM) will be presented. This model predicts an adult face appearance in its future by considering the natural ageing procedure. Unlike the B-FAM, in F-FAM most of the alterations are related to the face texture.

Chapter 4

Forward Facial Ageing Model (F-FAM)

Contents

In this chapter Forward Facial Ageing Model (F-FAM) is presented in order to predict the facial appearance of a young adult in its future. This model is based on the effects of the generic factors that are involved in natural ageing process.

The purpose of this chapter is not only presenting a model to predict the facial ageing in adult image faces, but to build a model as a foundation for the novel and practical forthcoming models. As a matter of fact, in this chapter the influence of the natural ageing trajectory on the different aspects of the face is modeled, and in the next chapter the effects of the different external factors on this process will be integrated into this base model.

Unlike B-FAM in which the focus is essentially on geometrical aspects of the face, in F-FAM the geometrical variations are subtle and alterations are mostly in facial texture. Texture adaptation to the target age is performed using the relative Predictive Face Templates.

The chapter organization is as follows: First, structural layers of facial ageing are discussed in Section 4.1. Model development is stated in Section 4.2. In Section 4.3 some results are illustrated and evolution method is discussed. Section 4.4 is the conclusion.

4.1 Structural Layers of the Facial Ageing

Proposing a reliable model for facial ageing requires an understanding of both youthful and elder face anatomy and ageing stigmata on the face. It is substantial to know which parts of the face are affected by ageing and how these changes will appear on the face.

The outcomes of the morphological studies indicate the face does not age homogeneously, rather, its ageing is associated with many dynamic components. It can be said that the facial ageing is associated with changes in all structural layers of the face, namely, skeleton, muscle, fat, and skin [132]. In the following, there is a short statement of the ageing effects on each mentioned layer.

4.1.1 Facial Skeleton Alterations with Ageing

Facial skeleton foundation undergoes changes through life. This alterations are either differential growth, which accrues during the childhood to adulthood and enables the infant skull to assume its adult form, or resorption of the certain areas of facial skeleton, that arise with ageing [133].

Facial skeleton resorption by ageing is heterogeneous. All different bones are not affected in the same level. Therefore, for a better understanding of the skeleton resorption impact on the face age, first the facial skeleton is divided to some sub-regions, then the receding level and the orientation in each area is studied. Figure 4.1 shows these different sub-regions of facial skeleton.

Periorbital Area: The periorbital area consists of the forehead, the eye socket and rims, the eyelids and surrounding areas, including the eyebrows. This area seems to be the first area to show the signs of ageing.

Studies indicate that the orbital aperture undergo resorption by ageing. However, changes occur at different rates, are site specific and uneven. Many studies have been done on the effects of ageing on this region. Here some of the outcomes are cited; there is no significant changes in orbit angle in ageing [134]. Orbital aperture width and area has significant increase with increasing the age [135]. Superior and inferior orbital rim recede with the age [136] (see Figure 4.2.a). One of the causes of increasing vertical eyelid length, lower eyelid curve distortion and hollow eyes is the lake of the rim support.

Midface: The midface skeleton consists of the maxilla bone and left / right zygomatic bone [137] (see Figure 4.1). The grade of bone resorption in the midface is also not

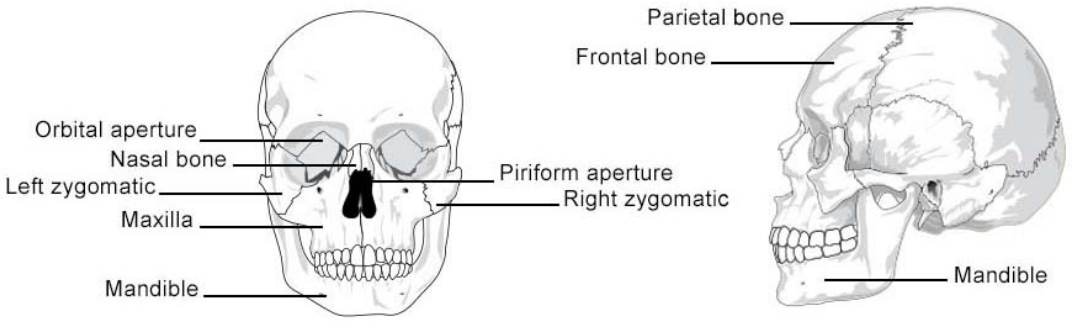

Figure. 4.1 Illustration of the primary bones of the face.

uniform. The maxilla is more susceptible to have age-related alterations than the zygomatic bone. Studies show maxillary angle decreased about 10° in old individuals (>60 years) comparing to young people (<20 years) [133]. This maxillary retrusion might cause the prominence of the nasolabial fold [138].

Nasal Area: Similar to the situation of the orbital aperture, as the edges of the nasal bones recede with age, piriform aperture enlarges with manifestation of ageing. The posterior displacement of the bone rim at the lower piriform aperture is greatest. This area is very important for supporting the lateral crura (Figure 4.2.b) and tip of the nose. Therefore, one of the characteristics of the aged face is the long and dropped nose [133][139]. Moreover, studies indicate special bone loss in the lower part of the piriform aperture with ageing which contributes to deepening of the nasolabial fold with age [140].

Lower Face and Mandible: There is no significant age-related changes in the mandible and ramus width. Mandibular body height and length and ramus height have significant decrease with age. Also, Mandibular angle increase with increasing the age. These alterations can be the cause of the appearance change in the lower third of the aged individuals'face, such as sagging chin and jowl. Missing teeth can escalate ageing signs in this region.

4.1.2 Facial Muscles Transformation through Ageing

Facial muscles' size and architecture are transformed in ageing process. Most of these alterations emerge from the loss of skeletal muscle mass and strength that happen as a result of ageing [141, Ch. 1].

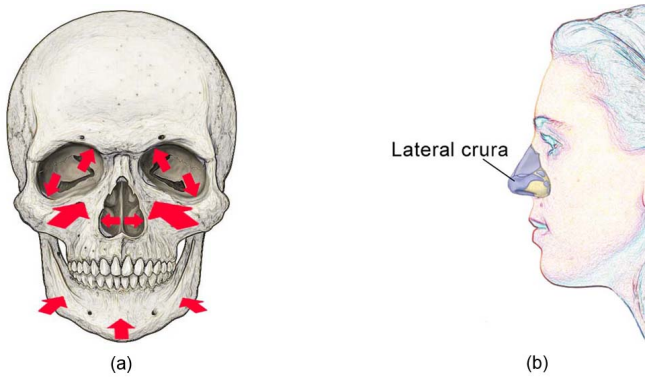

Figure. 4.2 (a) Indicating the areas of the facial skeleton susceptible to resorption with ageing. The magnitude of the arrows represents the amount of the resorption. (Figure is adapted from [133, Fig. 5]). (b) Displaying the lateral crura on the nose which descends in the result of ageing.

Numerous studies prove the role of superficial muscular aponeurotic system (SMAS), in facial ageing. SMAS is a mid-level muscular layer of the face that separates the deep facial fat from the superficial facial fat [122][142]. Analyses of MRI (Magnetic Resonance Imaging) images from individuals in different ages indicate that the ageing muscles in the midface shorten and straighten, as they seem in spasm [140]. It can be said that the attenuation in these muscles can cause the sagging appearance to the face. Changes in these muscles can also affect the nasolabial lines known as laugh lines.

Moreover, orbicularis oculi muscles lose their strength by ageing. It causes descent and deflation of the upper eyelids, as well as laxity in the lower ones [143]. It makes the brows, particularly the outer corners, descend over time.

Changes in the muscle encircles the mouth including lisps (Orbicularis Oris muscle) can cause wrinkles around the lips and dropping mouth corners. Figure 4.3.a shows the facial muscles.

4.1.3 Facial Fat Compartment and Its Changes with Ageing

Pattern of the fat deposition on the face undergoes specific alterations due to the ageing process. For instance, fat loss, deformation, and descending are the facial ageing signs.

Facial fat is composed of different parts such as nasolabial, jowl, malar, forehead, lateral temporal-cheek, periorbital fat and etc. [144]. Different fat compartments in the face are altered at different rates. Facial fat redistribution, accumulation and atrophy by ageing is even different from one person to another. Some of these facial fat disposition changes that affect the facial ageing are cited below:

Figure. 4.3 (a) Illustration of the facial muscles. (b) Facial fat distribution on the face (Figure is adapted from [144]).

Forehead fat loss can cause deep wrinkles in forehead and drooping of the eyebrows downward.

Orbital fat expansion occurs with age and displace the soft tissue of the lower eyelid and it causes double convexity deformity and under-eye bags [142].

Malar and jowl fat descend that can lead to nasolabial lines, square facial contour and double chin [122] [145]. Figure 4.3.b illustrates the fat distribution on the face.

4.1.4 Facial Skin Ageing

Skin is the most superficial and complex structural layer of the face that its appearance is the primary indicator of the age. To better express, facial ageing processes has strong connection with phenotypic changes in cutaneous cells [146].

Skin consists of three layers: 'epidermis', 'dermis' and 'subcutaneous tissue' [147] (see Figure 4.4). The epidermis is the most-outer layer of the skin that represents the appearance of texture and colour. It consists of keratinocytes and melanocytes. The dermis is the deeper layer, forming the main volume of the skin. It is made up of fibres, cells and substances and is responsible to support the blood vessels and nerves that are included in it. The fibres available in the dermal layer are mostly collagen and elastin. About 80% of adult skin dry weight consists of collagen [146]. Collagen fibres give a high tensile strength to the skin and protect it against overstretching. Elastin constitutes about 5% of the dermis. It gives elasticity and resilience to the skin. As the skin quality deteriorates with age, the dermis also undergoes morphological, physical and chemical changes with ageing.

Overall, many of the skin's functions decline with age; epidermal turnover, sebum function, immune function, wound healing, vascular reactivity, sweat production, and vitamin D production and etc. [146]. The skin changes in function and structure and

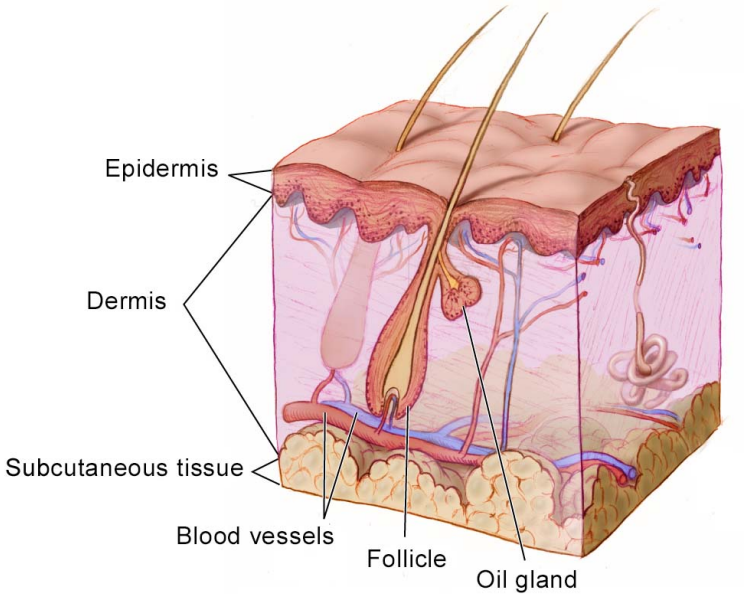

Figure. 4.4 Anatomy of the skin and its different layers consist of "Epidermis", "Dermis", and "subcutaneous tissue".

becomes thinner with age [148]. Collagen atrophy is a main factor in skin ageing which leads to increase in laxity and wrinkles.

Similar to the collagen, elastin is a fibre-forming functional protein. Elastin fibres and collagen fibrils are closely linked together, so they are prevented from overstretching and can rebound after a short-term stretching. Degenerative changes in dermal elastic fibres can also be speeded up with ageing. 'Transepidermal water' content of the skin decrease with age due to the skin barriers function alterations [149] [150]. It can lead the skin to dryness and deep facial creases and wrinkles.

In addition to all of the above, some pigmentary changes occur on the face with ageing. The number of melanocytes, a mature melanin-forming cell in the skin, decreases by ageing. The development of new melanocytes also declines. As a result, the skin of the elderly is more marked by pallor. Hence, an aged face skin is wrinkled, saggy, and pale.

To brief, changes in the balance of all above mentioned facial layers cause the hallmark of ageing, based on which a Predictive Facial Ageing Model is built without considering each layer separately. These signs are summed up as follows [151] (note that, 't' is for texture-related changes and 'g' is for geometrical changes):

- Forehead wrinkles (t)
- Lateral Canthal lines or crow's feet wrinkles (t)
- Glabellar frown lines which are the vertical lines in between brows (t)

- Brow droop (g)
- Full bags (Under eye bags) (t)
- Increase in vertical lower-eyelid length (g)
- Wrinkles beneath eye (t)
- Nasolabial folds (t)
- Nose elongation and tip movement (g)
- Marionette lines that run from the corner of each side of the mouth to the corner of the chin (t)
- Upper lip wrinkles (t)
- Ptosis of lower face and sagging chin (g)
- Jowl refers to the small focal accumulation of fat in the lower cheek overlying the jaw bone (g)
- Paler and turned grey or yellow skin (t)

Figure 4.5 demonstrates these symptoms in the different parts of the skin and on the whole face.

4.2 Ageing Model Development

Same as for the facial growth, age-related facial changes can be assorted as geometrical and textural. However, inverse of the growth process, in ageing trajectory, geometry undergoes tiny changes and most of the transformations are textural. To proof, from above-mentioned face ageing hallmarks, assorted to the geometrical (marked with ‘g’) or textural (marked with ‘t’), most of them are texture-related changes. Therefore, face transformation from one age to another is performed in two geometry and texture parts.

4.2.1 Geometrical Model

4.2.1.1 Geometrical Measurements

To apply the geometrical face changes, even delicate, craniofacial measurements in different age groups are required. To choose the scales and distances associated with

(a)

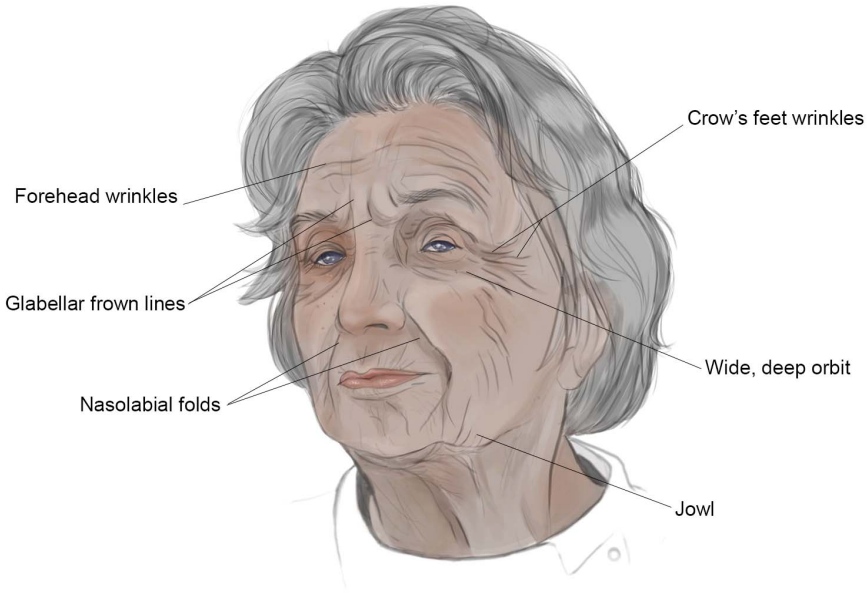

(b)

Figure. 4.5 Signs of facial ageing. (a) The highest grade of the ageing manifestation in different parts of the Caucasian face from [151] (b) Illustration of the ageing marks in whole face.

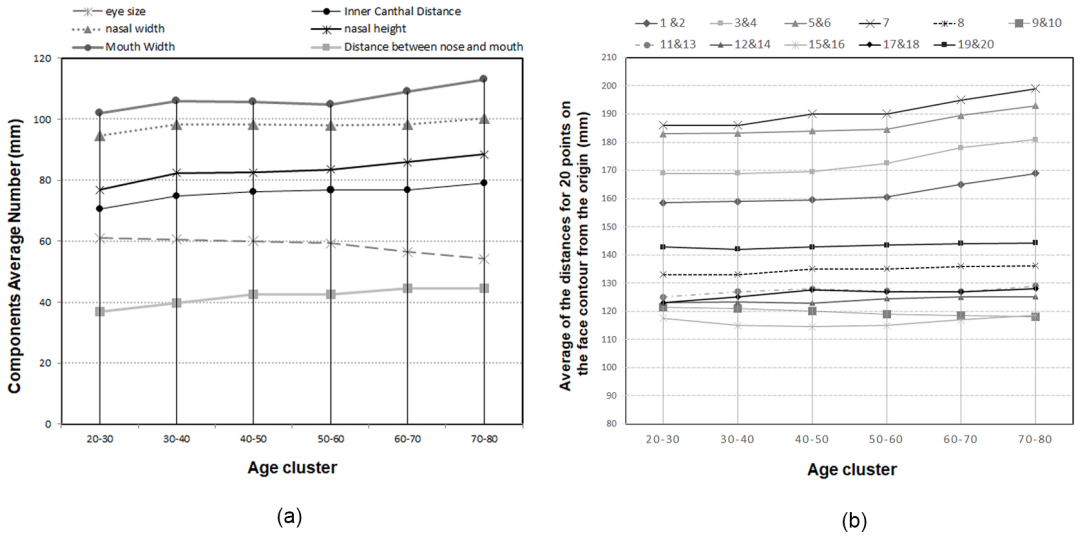

Figure. 4.6 (a) Facial components size and distances - both genders, six age clusters – extracted by calculated average of size and distances from all facial images in each age cluster. (b) Average distance of each point on the face contour from the origin - both genders, six age clusters – extracted from calculated average of radiuses of all facial images in each age cluster.

ageing process, and definition of the components' size and their distribution, the determined standards in 3.2.1 are used. To remind, these measures include: eye size, inner Canthal distance, nasal height, nasal width, distance between nose and lips, and mouth width. Face shape is also defined by 20 facial feature points and nasal bridge.

Since the face has reached its adult shape and the maximum size by entering to the adulthood, there is no detailed accomplished geometrical measurements for the adulthood, as have been done for the childhood. To extract these measures in different age groups, the facial images from the FFAC album of the FAMD dataset are used. To remind, there are 6 afferent sub-age groups in adulthood named Cluster 21-30, Cluster 31-40, Cluster 41-50, Cluster 51-60, Cluster 61-70, and Cluster 71-80, arbitrarily defined for this study. The age clusters are defined in a way that the ageing differences between two continuous clusters are distinctive.

All the mentioned measures are achieved by calculating the average number of size and distances obtained from all the face images in the 6 age clusters. Note that, to this purpose genders are not separated. Figure 4.6.a illustrates the changing process of components' size and distribution from 20's to 80's. Moreover, the size of the 20 facial radiuses in different age clusters from 20's to 80's, extracted by calculating the average of facial radiuses in each of 6 age clusters, are shown in Figure 4.6.b.

It can be seen that differences between the two age clusters are very tiny, however even these minor alterations can make the face look older and these tiny variations' impact could not be denied.

4.2.1.2 Geometrical Transformations

As in B-FAM, the geometrical transformation is applied in two parts by employing the facial feature points:

1) Component's Size and Their Distribution: as the facial components have the maximum of their scale and find their right location on the face, some slight modifications such as distance between eyebrows and eyes, nasal height and lips size should be applied as previously explained as the signs of an aged face. These modifications are each performed according to the scale factor which is defined between two input and output age clusters illustrated in Figure 4.6.a. For these changes based on equation 3.1:

$$S_i = \gamma S_j + d \qquad (i > j \quad , \quad 0 < \gamma \ ) \tag{4.1}$$

where S_i is the target component's size, γ is the scale factor, S_j is the input component's size, and d is the translation vector. However for forward face age modeling, the input age is less than the output age $(i > j)$.

2) Face Contour: as before, the nasal bridge is considered as the origin of the face and facial shape and its scale are defined by position of 20 points on the face contour and their distance from the origin.

Studies indicate in the process of the facial ageing, face size does not have a significant change especially in 2D frontal view. Thus, the probable changes may be related to the face shape, distinctively in its lower third part. Because one of the age variation effects associated with shape is the jowl alteration that can happen as a result of fat loss and muscle reduction.

To modify the frontal facial shape, some facial feature points on the chin are employed along with the origin. Recurrently, holding the angle to apply the changes is important. The same equations 3.2 to 3.6 from Chapter 3 can be employed to model the facial shape. However, for forward model, $i > j$ and β can be less, more or equal one.

The result of shape alterations is shown in the right side of Figure 4.7. It can be seen that even with these minor changes the perceived age of the face can be different.

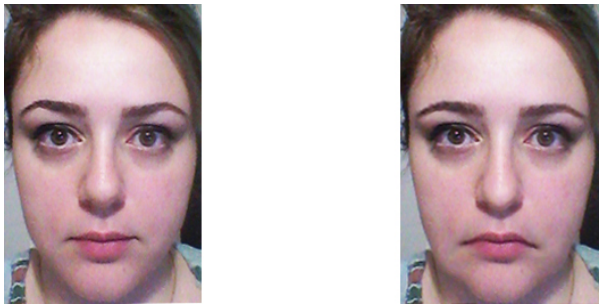

Figure. 4.7 Illustration of geometrical change in nose, eyebrows, lips and jowl; it can be noticed that even with these minor alterations the age of the face is changed. The image in the left is input adult face image and the image on the right is geometrically changed face image.

To depict these alterations, geometrical transformation should be operated on the image domain. In fact, these alterations can be performed by moving the content from the coordinates in the image not yet changed to the dislocated coordinates. It is the image warping that has already been elaborated in Chapter 2.

4.2.2 Textural Model

As previously mentioned, most of the alterations in the ageing trajectory, are textural variations that come from either skin's direct change. Or they are alterations associated with facial skeleton, muscles, and fat in ageing process that can affect facial geometry, but are reflected on the texture. For instance, as the result of some bone resorption there is a concavity and darkness under eyes that can affect the face profile view, but in 2D frontal view it should be visualised by textural modifications. Therefore, Textural Model has an important role in the forward ageing model.

4.2.2.1 Predictive Face Templates Construction

Since the ageing process is under the influence of different factors like genetic, health and lifestyle, age-related effects and ageing rate is different from one person to another. Nevertheless, the common age-related aspects of the faces in one specific age range cannot be ignored. As an example to prove, a person in their 60's, in the best conditions of genetic, lifestyle, health and intensive skin cares never can look like as their 20's. This is the attribute of facial ageing that is employed to propose an ageing model. However, it can sometimes happen in reverse, that is to say, a 20 years old person can look like an individual in their 30's or 40's in the special conditions of health and lifestyle that will be fully discussed in the next chapter.

As cited before, mathematical average of the faces categorised in an age cluster and same gender can show all the common characteristics in the facial features that

they all share. Moreover, a Face Template illustrates the common differences between age cluster's members. The more these two age clusters are far from each other, the better these distinctions are determined.

To build the Face Templates for F-FAM, the second album of the FAMD database consists of 900 adult facial images in 6 different adult age clusters (Cluster 21-30, Cluster 31-40, Cluster 41-50, Cluster 51-60, Cluster 61-70, and Cluster 71-80) and two genders have been used.

Once more, similar to what had been done for growth process and what was fully explained in Chapter 2 for Face Template construction, the average of facial images for each age cluster is calculated, using the extracted feature points, image warping, and equation 3.7.

After having a deeper look at the calculated Face Templates (Figure 4.8.a), especially for the older age groups, it is clear that the effects of the high-frequencies, creases and wrinkles, which are representative of the ageing marks in facial images, have been diminished. It is obvious for everyone that texture average calculation, from a set of images, defaces the high frequencies and details. It gives a smooth texture result since it eliminates very high and very low frequencies. Therefore, for a better representation of the facial deep wrinkles and high-frequencies on the Face Templates, their influence should be amplified. To amplify the high-frequencies and emphasise the fine details, the high-pass filter has been applied on all the face images in an age cluster before averaging.

$F_{Sharpened}$ is an enhanced facial image by increasing the contrast of the given facial image F around the thresholds, considering that the added noise in the identical sections of the facial image shouldn't be a lot [152, pp. 60-62] [153, pp. 133-136].

$$F_{Sharpened} = F + A[F - F * H] \quad , \quad A > 0 \tag{4.2}$$

where A is an ascending factor, H is the kernel applied to enhance the facial image and $F * H$ is the smooth version of the facial image F.

According to the definition of 2D convolution the smooth version of F, F_S, is:

$$F_s = F(x,y) * H(x,y) = \int_{\tau_1=-\infty}^{+\infty} \int_{\tau_2=-\infty}^{+\infty} F(\tau_1,\tau_2).H(x-\tau_1, y-\tau_2) d_{\tau_1} d_{\tau_2} \tag{4.3}$$

Therefore;

$$F_{Sharpened} = F + A[F - F_s] \quad , \quad A > 0 \tag{4.4}$$

Now, again, the average of all the facial images in the age cluster should be calculated, as regards in the equation 3.7, $f = F_{Sharpened}$.

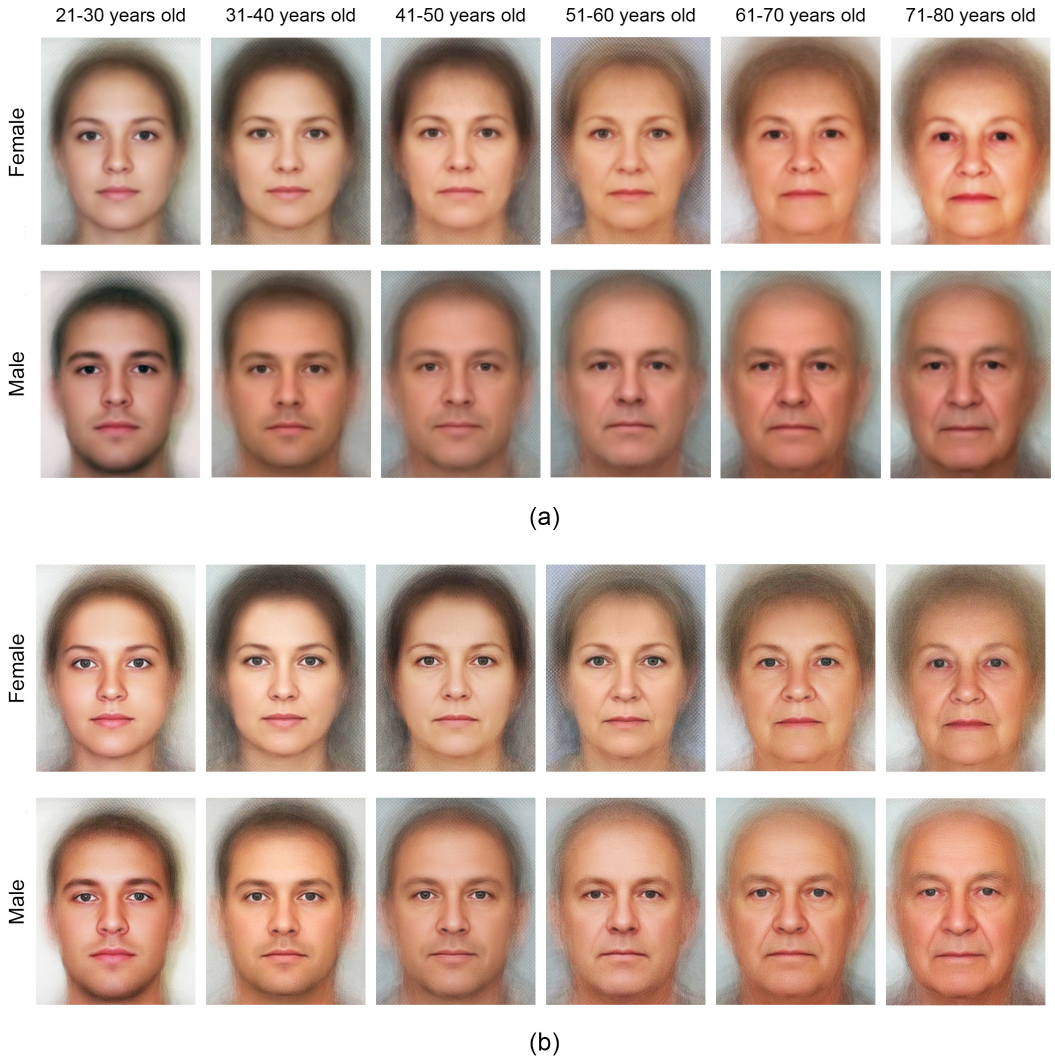

Figure. 4.8 (a) Illustration of the failure in creating the Predictive Face Templates, before filtering. (b) Predictive Face Templates, built after high pass filtering, for both genders and 6 different age clusters.

As a result of sharpening, some parts of the face such as nasolabial folds, lower eyelids and the lines at the corner of mouth are more recognizable in the new version of the Face Templates. These Face Templates are named *Predictive Face Templates*.

Predictive Face Templates related to the different age clusters are shown in Figure 4.8.b. As it can be seen, ageing progression in different decades, from 20's to 80's, is thoroughly displayed by these Face Templates. Indeed, changes in the size and form of the face components and muscle reduction are completely noticeable.

The more accurate the database classification is, the more distinctive analogies are. As a result, the higher quality Face Templates are achieved. To explain, if the database is classified according to different ethnics, each ethnicity will have its dedicated Face

Template that illustrate the precise and subtle differences and characteristics special to that specific ethnicity. Consequently, the results of studies on the age-related facial characteristics will be more reliable, and the simulated faces will also be more realistic. Different ethnicities differ in the facial components size and form, face shape, and texture ageing process in both time of ageing signs appearance and the face regions that signs emerge (ethnic related factors that affect the ageing will be discussed in the next chapter).

4.2.2.2 Application of the Textural Model

As the most tangible changes with ageing are related to the texture, the output result of the Geometrical Model is not really close to the target age and should be manipulated by the Textural Model. To do this, geometrically modified facial image should be combined with the Predictive Face Template belonging to the desired age cluster. For this objective, the two images should be fused, using the weighted sum, and image warping as explained in Chapter 3.

The facial shape does not generally changed during adulthood, except in the conditions that the shape of the face or its components transformed due to a special disease or gain/lose weight. Therefore, to apply the fusion, instead of warping the geometrically changed face image and associated Predictive Face Template to the average coordinates, the Predictive Face Template is warped to the geometrically changed face coordinates. Eventually, these two face images are fused.

Making decision for share of each face image in the final result is very important. Since, texture has the more share of variations in ageing process, assigning the higher percentage to the Face Template, should normally deliver the result look more closely to the target age. Most often, a percentage between 60 and 70 for the Face Template, give relatively acceptable result. For the weighted sum equation 3.8 is used. To achieve the percentage range between 60 and 70, a survey, similar to what was done in B-FAM, is performed. We asked people to choose whichever percentage that has the closer associated result to the target age. Obviously, to the extent that the person's face characteristics does not change completely and is identifiable. Figure 4.9. demonstrates the average of the 100 responses for 20 sets of results.

Moreover, for applying the Textural Model, some details should be considered to have the better results, as they have been applied for B-FAM. For instance, the original eye colour should be preserved, as it is very important for identification and having the natural and realistic results. To do this, as it has been done in Chapter 3, a binary mask covers the surface of the eyes area in the Predictive Face Template to prevent the masked area from being included in the average calculation. The eyes region is

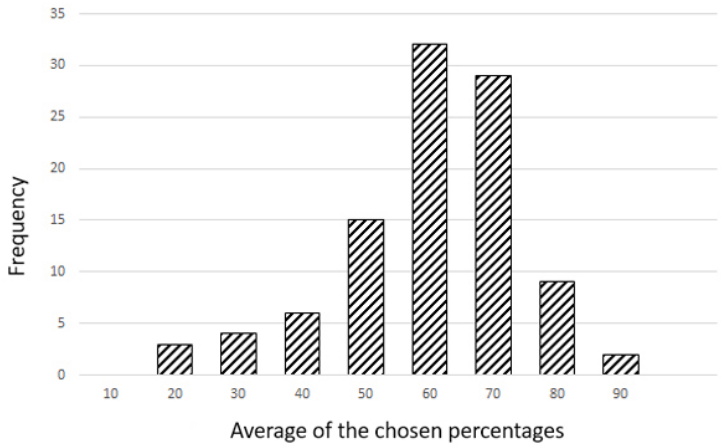

Figure. 4.9 Histogram of the chosen percentages for the share of the geometrically changed faces that give the best associated results to the target age.

selected using double thresholding with pixel values and morphology-based opening and closing.

4.2.3 Forward Facial Ageing Model (F-FAM)

Based on the above-mentioned phases, the F-FAM is proposed for the natural face ageing trajectory:

$$F(i) = w_1 T_p(i) + w_2 \psi(f(j)) \quad , \quad \begin{cases} i > j \\ i - j = 10k \ , \ k \in \mathbb{N} \\ 0.6 < w_2 < 0.7 \\ w_1 + w_2 = 1 \end{cases} \tag{4.5}$$

where, $f(j)$ is the input face in age j. $F(i)$ is the simulated face in the age of i, $T_p(i)$ is the Predictive Face Template in the same age range, and ψ is the transformation linear function applied on the face $f(j)$ consists of all geometrical alterations by keeping the details related to the input facial image $f(j)$ intact. i is the target age and j is the input face age. In F-FAM $i > j$ and $i - j = 10k$, $k \in \mathbb{N}$ since the age clusters are spanning 10 years between 20 and 80. The bigger $i - j$ the more differences become visible between input and simulated face. w_1 and w_2 are the weights given to the Predictive Face Template and the transformed input faces.

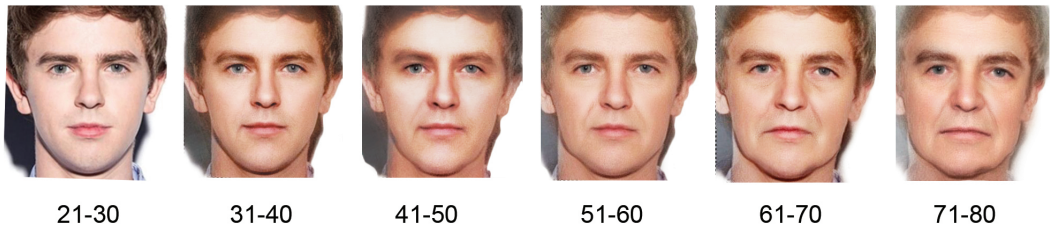

Figure. 4.10 Illustration of the ageing results on one subject in different age clusters.

4.3 Experimental Results and Evaluation

4.3.1 Tested Database and the Final Results

In order to test the model , the F-FAM is applied on 20 young adult face images form PAL database [101], which are frontal and almost without any facial expressions.

According to the presented model, the input is a normal adult (20 to 30 years old) face image (Figure 4.11.a) and the result is how it might look in the future, more specifically in the 41-50 age range. To show the results of the F-FAM, we intentionally use young adult faces, around 20 years. Since young adult faces have the minimum signs of ageing, thus, the distinguishing of the simulated ageing signs on the output facial images compared to the input is easier.

For the results, the target age 41-50 is chosen with the purpose to add the effects of different lifestyle factors in the future. Note that, if the simulated faces are in the range of 60's or 70's, adding the effects of the different external factors will be very difficult. In these age ranges, face have already highest grade of the ageing marks, so the distinguishing between the ageing signs caused by the natural ageing and behavioural ageing is very difficult. Some of the results are shown in Figure 4.11.b.

However, F-FAM can generate faces in all specified age clusters (Cluster 21-30, Cluster 31-40, Cluster 41-50, Cluster 51-60, Cluster 61-70, and Cluster 71-80). Figure 4.10 illustrates the results of the ageing progress simulation on one young adult face image.

4.3.2 Performance Evaluation

To evaluate the results, subjective performance evaluation is used. We asked people to rate the resulted facial images. Each person had been shown the results at the range age of 41-50 and is asked to estimate the age of the face image. All images were cropped only to the region of interest.

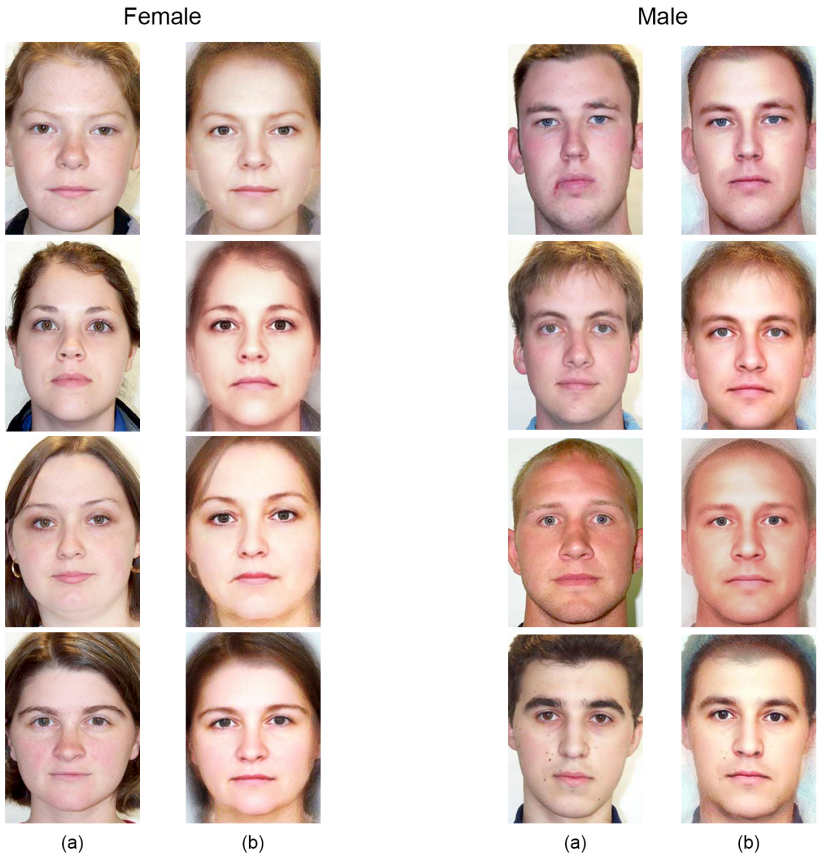

Figure. 4.11 Illustration of the results of applying F-FAM. (a) Input images (b) Outputs of applying the model. The output age cluster is 41-50.

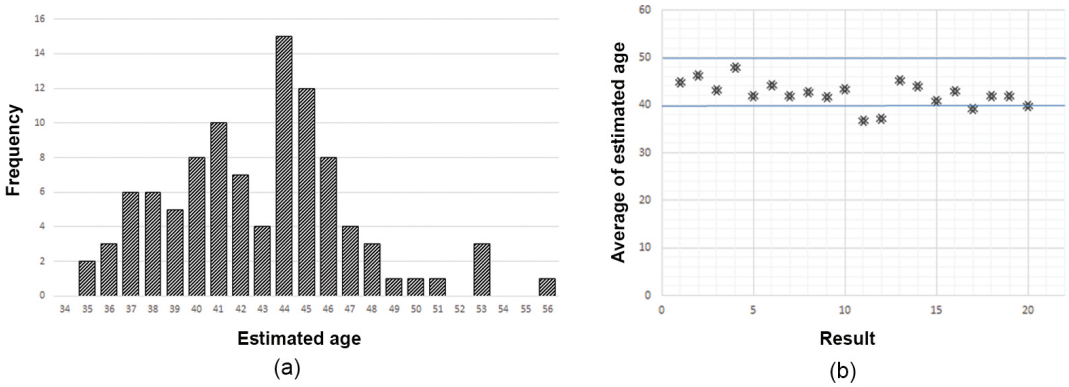

Figure. 4.12 (a) Histogram of the estimated ages by the respendants for the result of F-FAM. (b) Scatter diagram for average of all estimations for each result.

The total number of the estimation used is 100. The calculated average and the standard deviation for the results are shown in Table 4.1. The table shows that the results are in the desired age range from the participants' point of view.

Table 4.1 Average of the estimated age and standard deviation for 20 simulated face by F-FAM in the age range of 41-50 – separated by gender of the participants and face images gender.

Respondents' gender	**Number of respondents**	**Estimated age of female simulated faces**	**Estimated age of male simulated faces**	**Total estimated age**
Female	44	44.3±4	42.5±4.2	43.4±3.7
Male	56	43.4±5.3	39.8±4.9	41.6±4.4
Both male and female	100	43.8±4.8	41.±4.7	42.4±4.2

For more clear display, Figure 4.12.a illustrates the histogram of estimated ages by participants for all the results. This diagram demonstrates that by most of the participants the results of the model are estimated in the expected age range, between 40 and 50, or very close to this range. In fact 65% of the responses are in this age range. Beside, Figure 4.12.b shows the average of all estimations for each result, which is again in the age range 40 to 50 for most of them. Therefore, it can be inferred that the proposed model is remarkably accurate.

4.4 Conclusion

In this chapter, the method for constructing the Forward Facial Ageing Model (F-FAM) is described. This model is presented to predict an adult face appearance in its old ages based on the natural facial ageing trajectory. In this proposed model, although the geometrical variations are delicate and most of the changes are associated with texture, their impact is not denied. Hence, the geometrical aspects of the face are adjusted to the target age by applying a Geometrical Model. Then, Predictive Face Templates have been employed to adapt the face to the target age using the weighted sum and image warping.

A subjective performance evaluation is performed to evaluate the results. 65% of the responses are in the target age range. It means that from the participants' point of view the results of the model are notably acceptable; because the face image is not only older than the input face image but also is in the desired age range. So it can be said that the model is prosperous and accurate.

Note that, in this proposed model the effects of fine wrinkles are not integrated, nevertheless, the results seem in the target age cluster. It is proving that the manifestation of ageing is not only related to the wrinkles, rather it depends on the changes in different layers of the face.

This Predictive Facial Ageing Model, in addition to covering the need of a model for the natural ageing process, can be a foundation for the more specialised face ageing models such as Behavioural Facial Ageing Model which will be discussed in the next chapter.

Chapter 5

Behavioural Facial Ageing Models

Contents

Although, the facial similarities between the people from the same age group are irrefutable, yet ageing pattern in each person is unique and associated with the various intrinsic and extrinsic determinants [154][155][156] .

Setting the effects of lifestyle habits up to a facial ageing model can lead to more realistic results. The main aim of the Behavioural Face Ageing Models is to give the perspective of the face in the future in case of having risky lifestyles and help people to consciously decide about their lifestyle habits. In this chapter, for each lifestyle behaviour one Effectiveness Factor (Δ) is calculated which is the difference between the apparent age and the actual age. Then, based on F-FAM and Δ, an ageing model is constructed for each lifestyle behaviour.

This chapter is organised as below: Frist, facial ageing influential determinants are discussed in Section 5.1. Primal Facial Ageing Model is explained in Section 5.2. In section 5.3 Effectiveness Factor on apparent age is defined. Then, Behavioural Facial Ageing Model is proposed in Section 5.4. Coalesced Face Templates are defined in Section 5.5. Methamphetamine Addicts' Facial Ageing Model is discussed in Section 5.6. Sun Damage Facial Ageing Model is stated in Section 5.7. Chapter is concluded in Section 5.8.

5.1 Facial Ageing Influential Determinants

There are two ways by which facial ageing is affected: internally and externally. Intrinsic ageing of the face inevitably occurs as a consequence of physiological changes over the time and individual has almost no control over them. Intrinsic face aging process is typically slow and uncontrollable. Contrariwise, extrinsic factors, in different levels, are controllable and varied.

In the following, first, these factors will briefly be discussed, then some models are proposed according to the most important and influential ones.

5.1.1 Intrinsic Determinants

Intrinsic factors are defined by individuals genetic. Mainly, these factors cannot be easily refined. Intrinsic determinants may affect the colour of the skin, skin thickness, amount of collagen, elastin production and etc. [154]. Some of these factors are reviewed in the following.

5.1.1.1 Ethnicity

Ethnic differences in the face can explain genetically disparities seen in facial ageing progress. Some of the facial age related factors that can be differed from one ethnic to another are the amount, the composition (or colour) and production of the melanin [157], skin thickness, the amount of the collagen fibrils, natural moisturizing and etc. [158]. Since deep explanation of all of these factors is not related to this study, only some of them will be discussed.

First, let us come up with the definition of the ethnic. In this study the term ethnic is not defined as its common literal meaning which is the wide groups of populations with common culture and language. Rather, from now on in this discussion, ethnicity defines one specific population in terms of genetic similarities.

There are 3 major ethnic groups in the world according to ethnographic division from Meyers Konversations-Lexikon of 1885-90:

- Caucasian (Europeans, people of the Middle East and India)
- Mongolian or Asian (northern Mongolian, Chinese and Indo-Chinese, Japanese and Korean, Tibetan, Malayan, Polynesian, Maori, Micronesian, Eskimo, American Indian)
- Negroid (African, African Americans, African Caribbean, Australian Aborigine)

This classification is used in many age studies.

Another classification that can be very useful for the ageing studies is Fitzpatrick skin type or photo-type [159][160][161]. It depends on the amount of the melanin pigment in the skin. This classification shows the strong correlation between the skin colour with its ability to respond to UV light, that is one of the most important extrinsic factor in ageing skin, with tanning or burning reaction [157]. There are 6 different categories according to this classification, I to VI, from light to dark (see Figure 5.1).

- Type I -Pale white; blond or red hair; blue eyes; freckles. Always burns, never tans.
- Type II- White; fair; blond or red hair; blue, green or hazel eyes. Usually burns, tans minimally.
- Type III- Cream white; fair with any hair or eye color. Sometimes mild burn, usually tans.
- Type IV- Moderate brown; typical Mediterranean skin tone. Burns minimally, always tans well.
- Type V - Dark brown; Middle Eastern skin types. Very rarely burns, tans very easily.
- Type VI- Deeply pigmented dark brown to darkest brown; African descendant. Never burns, always tans [161].

Naturally, the darker the skin phenotype, the greater the skin protection against UV irradiation. The most lightly pigmented skin types have approximately half as much epidermal melanin as the most darkly pigmented skin types [162]. Therefore, there is greater probable dermal damage in the lighter ethnic groups. Accordingly, Caucasians showing earlier onset of photo-ageing compared to the other groups [163].

Moreover, the dermis (which is the thick layer of living tissue below the epidermis that forms the true skin) of black skin contains many more fibres composed of collagen fibrils and glycoproteins. People with darker skin are overall thought to have smoother and firmer skin than the ones with lighter skin in the same age.

Increasing evidence has demonstrated ethnic variability in the skin's natural moisturizing. Skin moisturizing properties can be partitioned to water loss, water content of the outermost layer of the skin and its sensitivity to exogenously factors such as dry climates and colder winter [164]. These factors have very important role in the skin ageing process. Most studies about water loss support some differences between

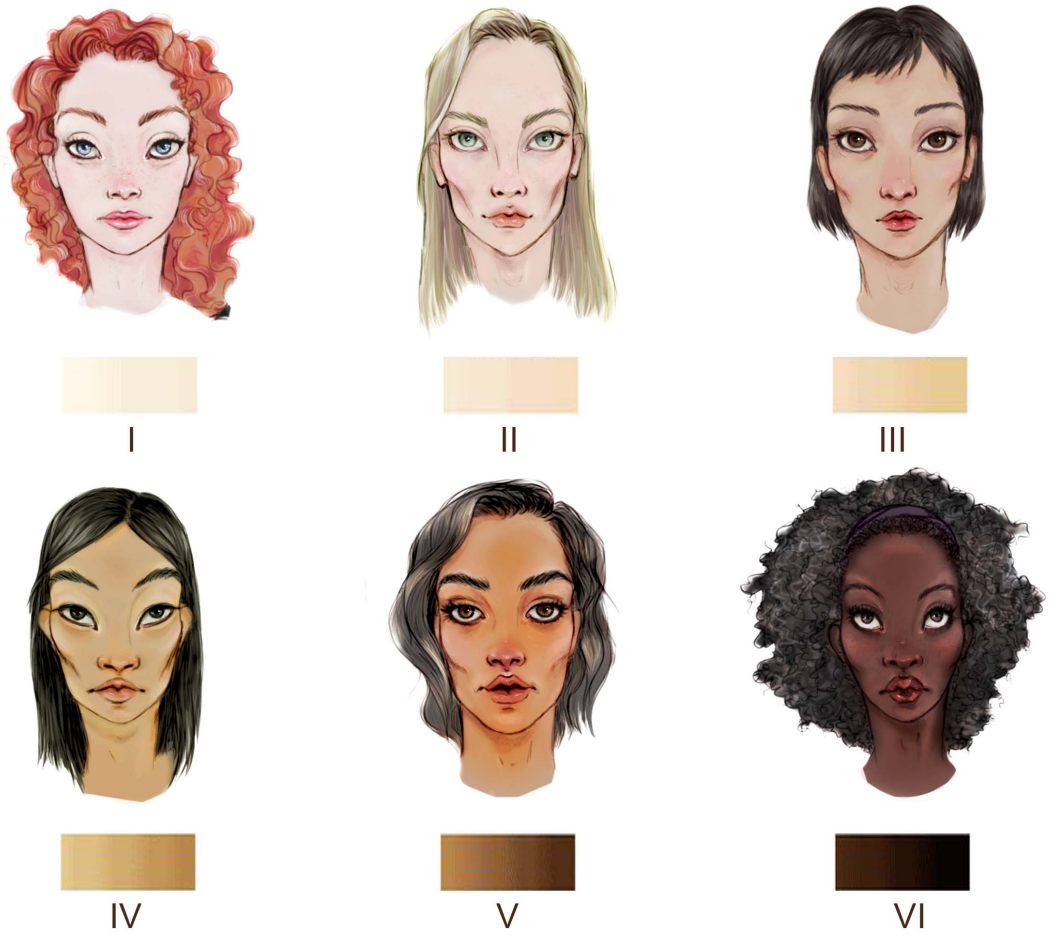

Figure. 5.1 Illustration of Fitzpatrick skin type classification.

Black, Caucasian, and Asian skin. These studies show water loss in African-American skin is significantly higher compared with Caucasian skin. These studies indicate no significant differences could be detected in water loss among Japanese (Mongolian) and German (Caucasian) women in the same age group [164].

In general, it can be said that the clinical manifestations of ageing in lighter skin types are more severe and mostly occur decades earlier than those of age-matched dark counterparts (see Figure 5.2.a).

5.1.1.2 Gender

There are many gender differences observed in human skin that can have a strong influence on gender-linked differences in facial ageing [165, pp. 113-114]. Studies indicate men's and women's skins differ in structure, biochemistry and functionality. Male skin is, in average, thicker than female skin. It contains more amount of collagen and has a tighter, firmer appearance. Sebum (a light yellow, oily substance that keeps

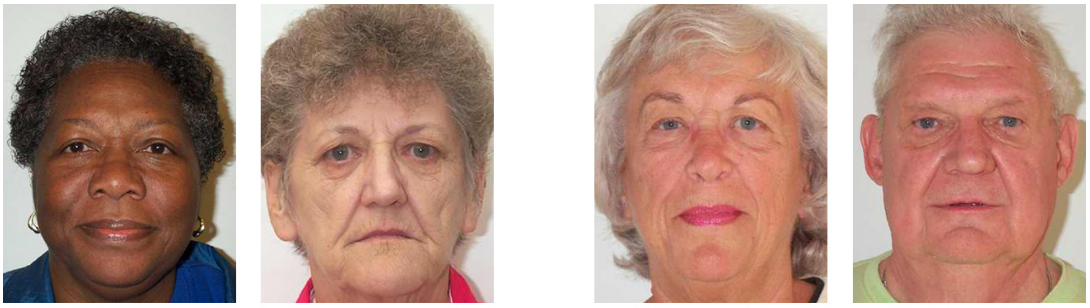

(a) (b)

Figure. 5.2 (a) 65 years old African and Caucasian women facial images to observe the difference between facial ageing marks. (b) 70 years old female and male facial images to compare the signs of ageing that consist of fine and deep wrinkles. Images are from PAL database[101].

the skin and hair moisturised) production is more in male's skin. Therefore, their skin is oilier than female skin, as a result its pH is lower and they rarely have drier skin compared to women. In men water loss is higher than women.

Some of the studies show gender-dependent differences in the degree of facial wrinkles. In general men have more deep wrinkles than women. Also, forehead wrinkles are increased by age in men compared with women (see Figure 5.2.b) [166]. At the end, male wrinkles occur later but, when they do appear, they are more pronounced.

5.1.1.3 Hormonal Changes

The human skin is the target as well as the producer of hormones [167]. These hormones have an important duty in the development and physiological functionality of the skin tissues.

Hormones are evidently involved in intrinsic ageing that is accompanied by reduced secretion of the pituitary, adrenal glands, and the gonads. Thus, with ageing, the level of hormones, such as estrogen, testosterone, dehydroepiandrosterone (DHEA) sulfate and growth hormone are decreased [168, Ch. 11] [169].

Estrogen includes a group of hormones which are chemically alike: Estrone, Estradiol (the most abundant in women of reproductive age) and Estriol. They are also referred to as primary female sex hormones. Overall, estrogen is produced in the ovaries, however, adrenal glands and fat tissues also make some estrogen, which is why men will have estrogen but at lower levels than women. One of the highest levels of estrogen receptors are seen on the facial skin, therefore it is a crucial factor in the facial ageing. A number of studies have shown that estrogens have many important beneficial and protective roles in skin physiology [170] such as improved collagen

content and quality, increased skin thickness and also improved blood supply to the skin [171].

Testosterone is a hormone supplied by the testicles and is liable for the proper development of male sexual characteristics. Females also produce testosterone, but usually in much smaller amounts. In women, testosterone is produced in the ovary, adrenal gland and the peripheral tissues from the various precursors produced in the ovaries and adrenal gland. Testosterone keeps the skin from sagging and symptoms of its loss can be dry and thin skin with poor elasticity [172].

Dehydroepiandrosterone sulfate (DHEA) is a weak male hormone produced by the adrenal glands in both men and women. It is a precursor hormone which means it has little biological effect in itself ; however, it is extremely important because it makes estrogen, progesterone, and testosterone in both men and women so its level has powerful effects on the skin [172].

Growth hormone (GH) is a small protein that is made by the pituitary gland and secreted into the bloodstream [173, pp. 136-147]. GH is essential for skin-cell repair and the prevention of skin sagging. The level of this hormone decrease as a result of ageing and indication of its drop off can be the sagging skin, loss of skin's thickness and firmness especially in cheeks and chin [174, Ch. 2,3,10].

In females, serum levels of 17β-estradiol, DHEA, progesterone, growth hormone (GH), are significantly decreased with increasing age. In males, serum levels of GH and IGF-1 decrease significantly, whereas it can decrease in late age in a part of the population. The effect of these decreases on the skin has been poorly documented, although more data are available for estrogen than for other hormones[169]. Less estrogen production that naturally occurs with age makes our skin thinner and less elastic, which leads to more wrinkling and sagging. As estrogen dips, less collagen and elastin are produced.

5.1.1.4 Anatomical Variation

Some anatomical variations have been reported in the histological structure of various sites of the skin as well as age related differences. It means different skin's regions such as forehead, upper eyelid, nasolabial area, perioral area, nose, cheek, chin, neck and volar forearm may have different level of biological parameters such as 'transepidermal water loss', skin hydration, skin surface temperature, skin pH and sebum [175, pp. 24-35]. Moreover, these measures differ from young to aged people.

Further, there are large differences in skin thickness in different body sites, ranging from 0.5 mm on the eyelids to more than 6 mm on the bottom of the feet [176]. Also, in areas of the body with high blood flow (e.g. lip, finger, nasal tip and forehead),

blood flow decreased with age compared to areas with baseline low blood flow, in which no difference was detected [177].

5.1.2 Extrinsic Determinants

Over the course of life, appearance and structure of the face will change not only because of chronological ageing and effects of intrinsic factors, but also due to several external factors that are caused by outside influences. These determinants can be: gravity, geographical area, working environment, high levels of pollution, temperature, and illnesses.

Moreover, lifestyle influence is a certain and definite factor that have impacts on health and facial ageing. Lifestyle habits includes: nutrition, sleep, exercise, drug abuse, exposure to UV light (photo-ageing), smoking, and alcohol abuse.

Addressing all the cited factors is beyond the scope of this study, but two of the most effectual determinants, drug abuse and exposure to UV light (photo-ageing) will be briefly discussed .Then, as a main part of the work, a Predictive Behavioural Face Ageing Model will be proposed, based on each lifestyle behaviour to illustrate merely a part of their devastating impact on the face age.

5.2 Primal Facial Ageing Model

To propose a facial ageing model based on any specific extrinsic factor that can affect the face age, first, a fundamental face ageing model should be constructed. Then, effects of each lifestyle factor will be added to this model. This fundamental facial ageing model is the model that makes the person's face look older up to 80 years old in the natural conditions (F-FAM) as it was completely discussed in the previous chapter.

To remind, since in the adulthood most of the changes are texture related, minor geometrical changes are required. These geometrical alterations in the face components and shape, can be done by employing the formerly extracted geometrical feature points and image warping. To manipulate the textural aspect of the face, geometrically modified faces should be fused with the Predictive Face Templates belonging to the desired age decade.

Thus, Forward Facial Ageing Model (F-FAM), which is constructed based on natural ageing process, can be used as the fundamental for any supplementary model based on any extrinsic factors. This model, from now on for Behavioural Models, is called Primal Facial Ageing Model. Derived from the equation 4.4;

$$F_{Primal}(i) = w_1 T_p(i) + w_2 \psi(f(j)) \quad , \quad \begin{cases} i > j \\ i - j = 10k \ , \ k \in \mathbb{N} \\ 0.6 < w_2 < 0.7 \\ w_1 + w_2 = 1 \end{cases} \tag{5.1}$$

$F_{Primal}(i)$ is the face which is aged to the age i by considering the natural ageing pattern and it can be the base of any Behavioural Facial Ageing Model. Note that $i > 16$, which means the input is a young adult face image.

5.3 Effectiveness Factor on Apparent Age (Δ)

The studies indicate each external or behavioural factor causes a person look years older, as we will see in the following sections. To construct the Behavioural Facial Ageing Model, an *Effectiveness Factor* must be calculated to show the average of the years that people look older than ordinary people by being exposed to each of these factors. In fact, this Effectiveness Factor is achieved by calculating the difference between the perceived or apparent age (estimated age of the individual), and the actual or chronological age (the actual number of years that individual has lived):

$$\Delta = \frac{1}{n} \sum_{m=1}^{n} (Apparent\ age - Actual\ age)_m \tag{5.2}$$

where Δ is the Effectiveness Factor, and n is the number of facial images in the dataset.

In essence, each of the lifestyle behaviour determinants has its specific Effectiveness Factor that can be statistically obtained assuming that there is a facial database of the people that are exposed to that specific factor or an existing population to performing the clinical examination.

It is worth mentioning that, undoubtedly, if someone's lifestyle contains of more than one behavioural factor, calculating the sum of these Effectiveness Factor's number to obtain the future perceived age is senseless. The solution could be defining an impact percent for each of these factors and considering the degree of its impact on the facial ageing. Of course, it requires extensive and meticulous clinical studies since it is very difficult to define a borderline for each behaviour factor impact. For example, the people who are addicted to drugs are more likely to have an alcohol abuse, or people who drink alcoholic beverages are more likely to smoke, therefore, distinguishing between the ageing effects of each behaviour is very difficult. Moreover, the number

of the years that each person is exposed to the factor is very important and can be taken into account.

5.4 Behavioural Facial Ageing Model

The statistical analysis shows that each of the negative life style habits make the individuals look a few (Δ) years older for their age. Therefore, to build a facial ageing model for each lifestyle behaviour factor, a model is constructed on the basis of the Primal Facial Ageing Model. Except that instead of using the Predictive Face Template for the same age group $T_p(i)$, the one corresponding to the age group $(i+\Delta)$ is used. It means that the facial ageing is intensified Δ years by this particular lifestyle habit and as a result the person leading this lifestyle looks Δ years older.

Aside from geometrical alterations related to the natural ageing pattern that are applied via transformation function $\psi(f(j))$, age related geometrical changes caused by the behavioural factor under discussion are applied in the face transformation function $\delta(f(j))$. For example changes in the face shape, its fatness and thinness, or changes in facial components' angles such as eyes, eyebrows and etc.

$$F_{Behavioral}(i) = w_1 T_p(i+\Delta) + w_2(\psi(f(j)) + \delta(f(j))) \tag{5.3}$$

where $F_{Behavioral}(i)$ is the affected face by one of the behavioural determinants in the age of i, $T_p(i+\Delta)$ is the Predictive Face Template that must be used instead of $T_p(i)$, so Δ is the Effectiveness Factor which shows the number of years that an affected face looks older than a normal face.

5.5 Coalesced Face Templates

Since calculated Δ for different behavioural factors is mostly less than 10, as will be seen in the following, existing Face Templates are not appropriate to use in some models. For more explanation, since Face Templates are constructed according to the different age decades, therefore if 5 years is added to the desire age, either the same Face Template or the one related to the one decade older must be used that the result with both is not accurate. Therefore, some complementary Face Templates are needed to fill the gap between the decades (25-35, 35-45, 45-55, 55-65, and 65-75 years old).

Coalesced Face Templates are constructed by using the average of the two neighbour Predictive Face Templates to cover the above mentioned issue (Figure 5.3).

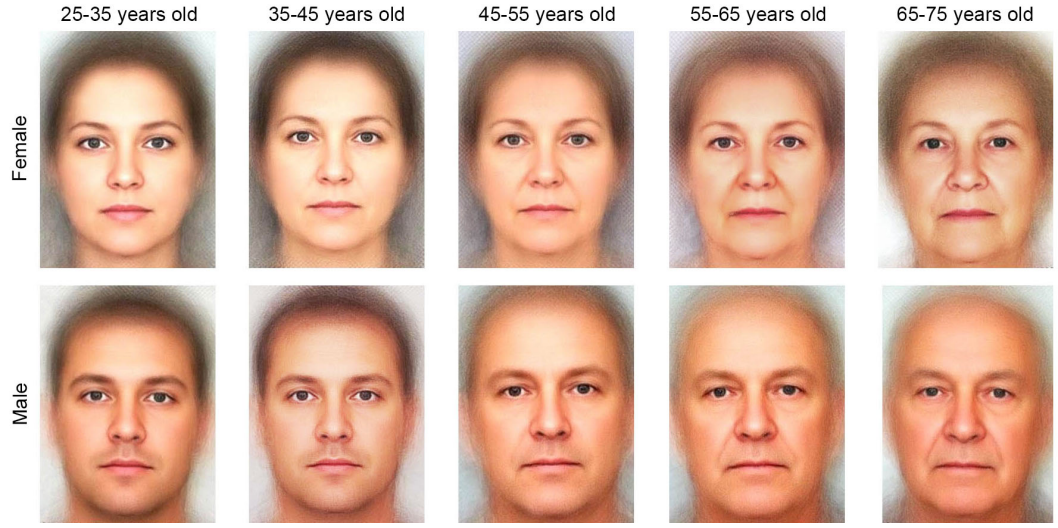

Figure. 5.3 Illustration of the Coalesced Face Templates constructed by the fusion of two neighbour Predictive Face Templates – for both genders and 5 different age decades.

5.6 Methamphetamine Addicts' Facial Ageing Model

Millions of people are trapped in a cycle of drug addiction and the number of addicts is increasing. Unfortunately, most of the people use drugs for the first time when they are teenagers [178] . Although, a lot have been discussed about drug abuse and its effects, in the accounts of drug addiction, rarely there are attempts to show the drug tolls on the face. We believe that one of the most successful ways to raise drug awareness is to show substances' catastrophic effects on a user's face over the time. Thus, we hope showing these negative devastating effects on the face, will play this important role in preventing and even advance stopping the addiction to the fatal substances [179].

Any drugs can affect users in different ways when they are continuously abused. All substances such as heroin, cocaine, crack, hallucinogen (PCP and LSD), amphetamines, marijuana and etc. can cause negative mental effects as well as serious physical tolls on the addicted person. Some of these physical effects that can touch the person's face age are: flushing and a rash of red bumps all over the skin, drop in appetite and dangerous malnutrition and as a result weight loss, significant dental diseases and grinding of teeth [180], diminished skin collagen and an appearance of premature ageing, wrinkles, and skin elasticity loss.

As regards to methamphetamine, it is often seen as one of the most visibly destructive drugs that cause facial wasting. This issue will particularly be discussed in this study and a Predictive Behavioural Model is proposed due to its abuse.

5.6.1 How Does Methamphetamine Affect Its User's Face?

According to the National Institute on Drug Abuse [181], one of the most striking effects of methamphetamine is the change in the physical appearance and consequently the face of meth users. To have a realistic face ageing model, knowing these effects is necessary. A few of them are include: acne appearance due to the dry skin, extreme itchiness due to the sensory hallucination of having bugs crawling under the skin and repetitive skin picking which causes ulcers, sores that take longer to heal, lackluster skin, loss of skin elasticity, facial musculature destruction, the pale skin colour, grayish rough texture of the skin with the coriaceous texture that causes a lot of wrinkles, abnormally quick loss of teeth as a result of dried out salivary glands and changes in salivary Ph. [180] [182], loss of appetite and as a result remarkable weight loss, and many other side effects that can make the subject appear years, or even decades older than they actually are [183].

5.6.2 Methamphetamine's Effectiveness Factor (Δ_m)

For calculating Methamphetamine's Effectiveness Factor (Δ_m), a database composed of 23 methamphetamine addicts face images are used to study the effects of meth abusing and observe the difference between an addicted face and a normal face age [184]. A statistical analysis was performed using a user study to achieve Δ_m. We asked people to estimate the age of the shown face images. By having the real and the estimated age of the given faces, Δ_m is calculated. A sample of displayed images for Δ calculation is in the Figure 5.4. The face was shown to the respondents to estimate the age of the person. For this shown face, for instance, the average of estimated age by the respondents is 29.5 and the real age is 24; thus, the average difference between perceived age and the apparent age is 5.5 years.

Of course, by increasing the number of the face images in the database, a more accurate number for Δ_m will be attained. Moreover, the number of the years that person has used the methamphetamine is surely an important factor that can be add to the model in the future.

Table 5.1. shows the average and standard deviation of the results coming from the web survey. The total number of the responses used is 100. Participants are separated by their gender since studies have indicated that visual perception is different from women to men for future possible studies in the future. Total number of Δ_m for the methamphetamine addicts is equal to 5.2 ($\approx$ 5 years).

Figure. 5.4 A sample of the images shown to the respondents for statistical calculation of Δ_m.

Table 5.1 Calculated average and standard deviation of delta for methamphetamine addicts' faces – separated by Participants' gender.

Respondents's gender	**Number of respondents**	Δ_m
Female	71	5.5 ± 3.3
Male	29	4.7 ± 2.5
Both Male and Femalle	100	5.2 ± 3.1

5.6.3 Model Construction

The statistical analysis on the methamphetamine addicts face database proves that in average, methamphetamine users look $\Delta_m \approx 5$ years older for their age. Therefore, to build a facial ageing model for the individuals with this lifestyle behaviour, a model is constructed on the basis of Behavioural Face Ageing Model. Accordingly, in this case, the Predictive Face Template corresponding to the age group $i+\Delta_m = i+5$ is used. It means that the person's age will be perceived 5 years more than her/his actual age if she/he abuses methamphetamine.

In addition, some geometrical modifications are applied in the face transformation function $\delta_m(f(j))$, for example face becomes thinner, eyes become tighter and the mouth and eyes turn a bit downward. All of these transformations are found out from meth addicts' facial images. To have more precise and accurate scale numbers for these geometrical alterations a bigger database is needed to compare all the different facial components before and after using meth.

Thus, based on Behavioural Facial Ageing Model, to model the facial ageing in meth addicts:

$$F_{Meth}(i) = w_1 T_p(i+\Delta_m) + w_2(\psi(f(j)) + \delta_m(f(j))) \tag{5.4}$$

where F_{Meth} is a meth addict face in the age of i, $T_p(i+\Delta_m)$ is the Predictive Face Template that must be used and Δ_m is the coefficient that shows the difference between a methamphetamine addict and a normal face age. Since $\Delta_m \approx 5 < 10$ the Face Template may need to be chosen from Coalesced Face Templates (T_c). Therefore;

$$F_{Meth}(i) = w_1 T_c(i+5) + w_2(\psi(f(j)) + \delta_m(f(j))) \quad , \quad \begin{cases} i > j \\ 0.6 < w_2 < 0.7 \\ w_1 + w_2 = 1 \end{cases} \tag{5.5}$$

In the end some colour adjustments such as saturation modification may be needed to give a pale look to the face.

5.6.4 Results and Evaluation

The Methamphetamine Addicts' Face Ageing Model is applied on the same database that have been employed for F-FAM testing. In this model, the input is a normal adult face image and the result is how it might look in one of the mentioned age decades (41-50 years) if the person gets addicted to the methamphetamine. Some of the results are shown in Figure 5.5.

Once more, subjective performance evaluation is employed for evaluating the results. Each person had been shown the methamphetamine addict's simulated face at the range age of 41-50 and is asked to estimate the age of the face image. The total number of estimations is 100. The calculated average and the standard deviation of the responses to results are shown in Table 5.2.

Comparison between Table 5.2 and table 4.1 can simply prove the accuracy of the proposed model. Not only the estimated age range is higher, but the obtained age difference between these two models is rather very close to the obtained Δ_m.

For more clear illustration, the average of estimated age by respondents for all the results is shown in Figure 5.6.a. This diagram demonstrates that by most of the respondents the results of the model are estimated in the expected age range. In addition, Figure 5.6.b shows the average of all estimations for each result, which for most of the results is between 45 and 55. It means that the estimated age is shifted 5 years forward. Therefore, it can be deduced that the proposed model is considerably reliable.

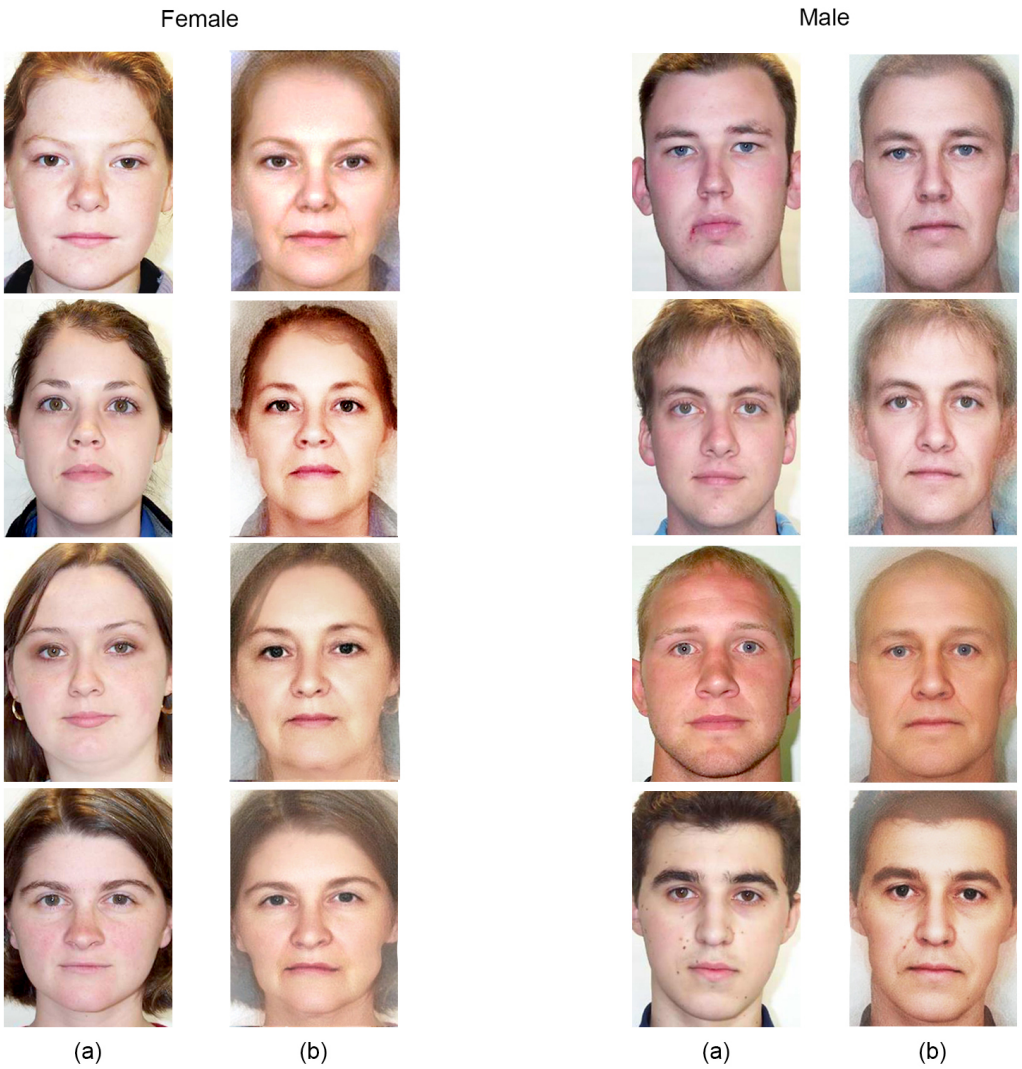

Figure. 5.5 Illustration of the results of applying Methamphetamine Addicts' Facial Ageing Model. (a) Input images (b) Outputs of applying the proposed model. The output age cluster is 41-50.

Table 5.2 Average and standard deviation of the estimated aged for 20 meth addicts' simulated faces in the age range of 41-50 – separated by gender of the participants and face images gender.

Respondents' gender	**Number of respondents**	**Estimated age of female simulated faces**	**Estimated age of male simulated faces**	**Total estimated age**
Female	47	48.1±5.5	48.8±5.6	48.5±5.1
Male	53	47.3±4.8	47.5±4.9	47.4±4.6
Both male and female	100	47.7±5.1	48.1±5.3	47.9±4.9

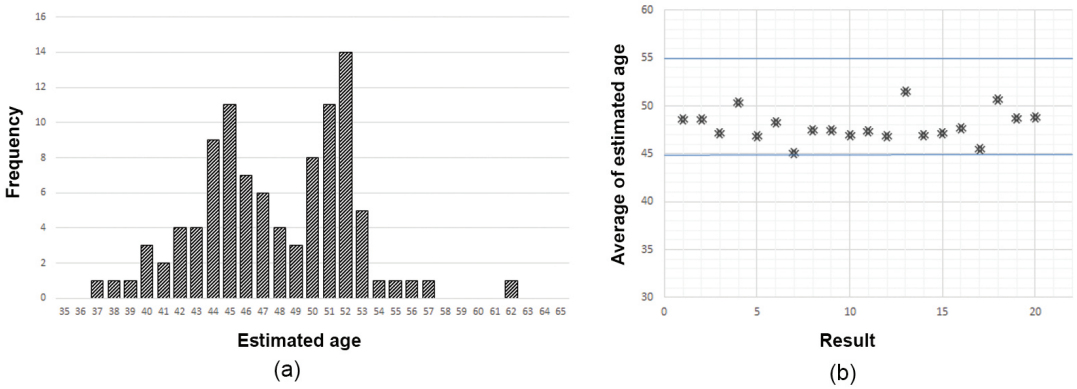

Figure. 5.6 (a) Histogram of the estimated ages by the respondants for the results of methamphetamine addicts' facial aging model. (b) Scatter diagram for average of all estimations for each result of using the Methamphetamine Addicts' Facial Ageing Model.

Figure. 5.7 Illustration of the results of applying Methamphetamine Addicts' Facial Ageing Model with sores modeling to have more realistic results. The results are in the age rang 41-50.

5.6.5 Sores Modeling

Even though the results are significantly acceptable, integration of some sores that are normally in the meth addicts' face due to the extreme itchiness, may give a more realistic appearance to the results and exhibit the terrible effects of the meth using. However, this improvement does not necessarily affect the perceived age.

To do that, different masks are created for the forehead and cheeks. Some samples of real sores from addict faces in the database are stored. Then, random pixel locations are selected on the masks, depending on the size of the sores. It has to be checked if sores can be fitted inside the mask without interfering with the borders or not. At last, a random sore from the database will be used in the specific chosen location. The number of the sores for each area can be defined. To illustrate these sores on the simulated faces, image fusion using Discrete Wavelet Transform (DWT) has been used. Some of the results of sores integration are shown in Figure 5.7.

5.7 Sun Damage Facial Ageing Model

Ultraviolet radiation can be referred as the most important environmental factor influencing the facial ageing, since studies have divided the skin ageing into two basic parts: intrinsic ageing and photo ageing [181]. The term "photo-ageing" was used for the first time in 1986 by Kligman [185] to represent the significant effects of UV light exposure on the skin ageing. The importance of photo-ageing lies on the enormous number of individuals, that intentionally (or unintentionally), are cumulatively exposed to the sun and endanger their health and face appearance. Therefore, a visual representation of its irreparable effects on the face appearance can push tan seeking people to stop extensive exposures to the sun [186].

5.7.1 Melanin, Skin Colour and Its Relation to the Sun Exposure

The natural colour of the skin has an impact on how the skin reacts to the sun and environment. In fact, this reaction is noteworthy for ageing studies since this is the intersection point between an intrinsic factor and an extrinsic factor.

Human skin colour can vary from very white that always burns to almost black that never burns. This range of colors comes from the amount and type of melanin in the skin. Melanin, the skin's brown pigment, is produced at the base of the epidermis by special cells called melanocytes [187]. These cells have photosensitive receptors that detect ultraviolet radiation from the sun and other sources. In response, they produce melanin. In general in darker skins melanocytes are more active and produce about four times as much as melanin as those in people with lighter skin. The less pigment the lighter the skin. There are two types of melanin manufactured by the skin: eumelanin and pheomelanin. People with fair skin and red hair produce more pheomelanin, and brown and black people produce more eumelanin. In general, the more eumelanin in the skin, the darker the skin. [188].

Eumelanin absorbs most of the UV radiation that is why it is considered as natural sunscreen. In other words, darkened pigmentation of the skin protects it. Pheomelanin, in contrast, acts as a photosensitizer, making the skin more sensitive to sunlight; this is necessary, for example, to synthesise vitamin D. The size and shape of eumelanin particles in the skin is related to the shape and size of the melanosomes, the organelles in melanocytes that synthesise melanin. In darker skin, the melanosomes are nearly twice as big as those in lighter skin and are individually scattered throughout the skin layers. Darker skin make more and larger melanosomes, compared to the Caucasian skin in which the smaller and more concentrated melanosomes are found. Alaluf et al. [162]

demonstrated that Caucasian skin is characterised by a low number of melanocytes, small melanosomes and light pigments, while the black skin is characterised by the presence of a higher number of melanocytes, larger melanosomes, a higher quantity of melanin and more eumelanins. Therefore, in general, Caucasian skins are very sensitive to the UV light and show the signs of photo-ageing earlier than the darker skins.

5.7.2 How Does Sun Exposure Affect the Face

"Photo-ageing causes premature ageing of the skin through cumulative exposure to ultraviolet radiation (UV) from the sun and artificial UV sources" [189].

UV rays are categorised into three types based on wavelength: UVC (100–290 nm) is largely blocked by the ozone layer and has almost no influence on skin. UVB (290–320 nm) penetrates only into the epidermis and cause sunburns. UVA (320–400 nm) penetrates into the dermis and it may be responsible for most of the long-term skin damages associated with photo-ageing, immune dysfunction, and some skin cancers [190] [191] (see Figure 5.8).

The face is continuously exposed to sunlight, so after each year, the skin will accumulate damage until the time the visible signs of ageing appear. Continuous UV exposure can lead to other changes such as pigmentation disorder that is the most visible and most specific effects of photo-ageing, loss of skin elasticity, and degradation of skin texture described as photo-induced damages [192] [193].

Many studies have been done on solar exposure and facial ageing signs. For instance one noteworthy study compared photo-ageing and chronological ageing by observing two different groups of Caucasian women: "sun-seeking" and "sun-phobic" [194]. This study shows that skin pigmentations are the most linked parameter to photo-ageing but are not very related to the age. Whatever the age is, a prevalence of pigmentation disorders occurs in individuals who regularly are exposed to the sunlight with significant differences with those who are not frequently exposed to the sun.

Concerning wrinkles and the skin texture quality, remarkable differences between the two groups appear after the age of 50. Photo-ageing is basically determined by "coarse and fine wrinkles" compared with chronological ageing that can be described with fine wrinkles [195].

In general, photo-aged women look older than women who protect themselves from the sun, especially when they are younger [194] [196]. Thus, it can be said that photo-aged skin is a good example for the term "prematurely aged skin".

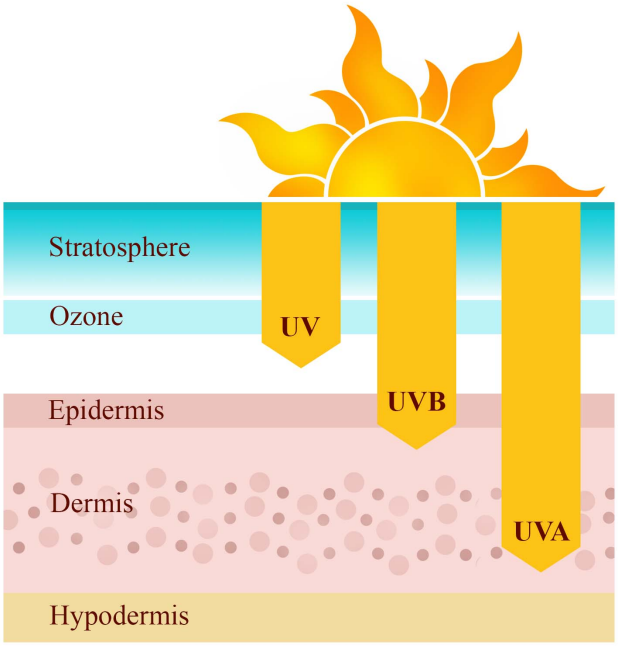

Figure. 5.8 Representation of different UV rays' penetration in the skin.

Figure 5.9 can be a good example of the UV impact on the face apparent age. Figure 5.9.a shows identical twins. This image demonstrates two people with the same DNA could look so different according to their profile. Though, the woman B has the profile of smoking and weight loss, the main factor for looking a decade older than her sister can be her cumulative exposure to the sun as she has admitted her strong interest in sunbathing. This sun exposure, in addition to causing dark skin and age spots, reduces skin's elasticity and increases wrinkles [197].

A fortiori, Figure 5.9.b is the most compelling argument for photo-ageing by showing only one face without any time differences. A 69 years old truck driver, Bill McElligott, who had spent 28 years driving on the job, has sideway sun exposure. The UVA rays transmitted through the window of his truck, have strongly damaged the left side of his face. As a result, the left side of the face looks around 20 years older than the right side [198].

5.7.3 Sun Damage Effectiveness Factor (Δ_{SD})

The measurement of the sun exposure's effect in facial ageing is very difficult, especially without the required medical and dermatological background, correct definition of the clinical factors influencing facial ageing, and only based on image data. Moreover, separating out the related factors involved in both chronological ageing and photo-

Figure. 5.9 (a) Identical twins – Age 61 — Twin B has smoked for 16 years of her life, sunbathes, and weighs 15 pounds less. Since her 20s, she has spent as much time as she could in the sun. Twin A, on the contrary, has had as little exposure to sun as possible [197]. (b) A 69-year-old man that had driven a truck for 28 years and the left side of his face had been exposed to the UVA rays transmitted through window glasses [198].

ageing is a very complex process. Many worthy studies have been done in this field by dermatologist. Of course, not using their results and starting from the scratch without the facilities and dedicated knowledge is not wise. Therefore, for the Sun Damage Effectiveness Factor (Δ_{SD}) elicitation, the result of some strong dermatology studies on the effect of sun exposure on facial ageing are used [194].

Flament et al.[194] have provided some elements for measuring the effect of UV on the skin. Their criteria and results have been used as a main approach for Sun Damage Effectiveness Factor (Δ_{SD}) extraction. The study has been performed on 298 Caucasian women (more sensitive ethnic group to the sun), aged from 30 years to 78 years. They were divided into two groups: sun-seeking (S-S) and sun-phobic (S-P). Study placed in a town with more than 110 days of sunshine every year. The women had different skin types (dry, oily, and combination) and were balanced across photo-types I to IV according to Fitzpatrick classification. Then, they were regrouped into 10-year age clusters.

Afterwards, by considering the importance of UV exposure for different items: residence location, occupation, passive UV exposure, active UV exposure, and photo-protection patterns, a score between 0 (none) and 3 (very) was given for each 10-year cluster after performing a clinical examination and after asking the sun behaviour history.

"Sun Behavioural Score History" (SBSH) is the sum of the scores for all the items. In fact, "SBSH is a key descriptor of the UV exposure level of each panelist" which is linked with age and photo-type. Therefore, the panel descriptor and labeling of S-S and S-P was made with the following thresholds: 25 for the cluster aged 30 to 39 years, 34 for the 40 to 49 years, 43 for the 50 to 59 years, 51 for the 60 to 69 years, and 60 for the cluster aged 70 to 78 years.

After that, some clinical signs like pigmentation, elastosis, vascular disorders, fine lines and wrinkles were described. Beside, five grades of photo damage from 0 to 4 were defined: 0, none; 1, minor; 2, moderate; 3, important; and 4, major. The clinical evaluation was done by using two set of photographic scales; the original skin ageing atlas [151] and the clinical scales specific for the population that have been more affected by UV exposure.

By merging the two sets of clinical measures, a mapping of facial ageing was obtained that covers four major axes: wrinkles and relief texture, lack of firmness, pigmentary disorders, and vascular alterations.

The process was ended by taking the average score of all the panelists and obtaining a clinical evaluation of each sign for each volunteer.

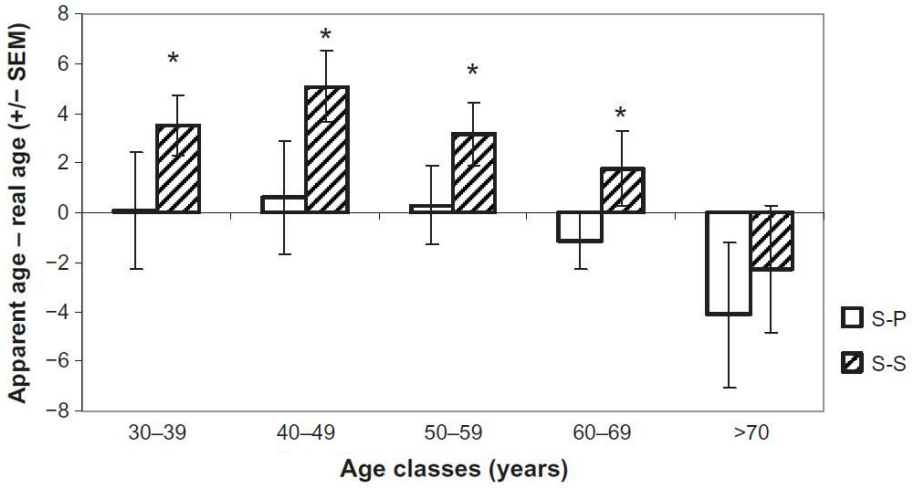

Figure. 5.10 Illustration of the difference between apparent and chronological age for the S-S and S-P groups. (Original figure is from [194]). '*' shows significant difference between bars. A positive difference means that the person looks older than her age.
Abbreviations: S-P, sun-phobic; S-S, sun-seeking; SEM, standard error of the mean.

Finally, a survey was added to the research in order to record the perceived apparent age by asking the question: "what age do you think this woman is?" from 30 people after showing them the full-face picture of the study volunteers. The effects of ageing and UV exposure were characterised by a sum of the clinical criteria divided into four clinical factors (wrinkles, sagging, pigmentary disorders, and vascular alterations).

The summary of their study on the effects of UV exposure on the face's appearance is illustrated in Figure 5.10. It can be seen that with the exclusion of the oldest cluster, S-S volunteers looked older than their chronological age.

Concerning wrinkles and skin texture quality, noteworthy differences between the two groups appear after age 50 as it can be seen in Figure 5.11.

A sum was done of all signs most affected by UV exposure by using the quantification of each volunteer which was then compared with the sum of all clinical signs established for facial ageing.

A new ratio, "Sun Damage Percentage" (SDP), was determined that represents the percentage between specific photo-ageing signs and clinical signs. By computing SDP, the effect of sun exposure on the face can be estimated. On average SDP is 80.3% $\pm$ 4.82%.

Eventually, it has been derived that "at a threshold of 80% for the SDP, women have similar apparent age to actual age. If SDP increases (82%), then apparent age becomes higher than real age, and this woman looks older. Conversely, a decrease of SDP (78%) means that the woman looks younger" (Figure.5.12) [194].

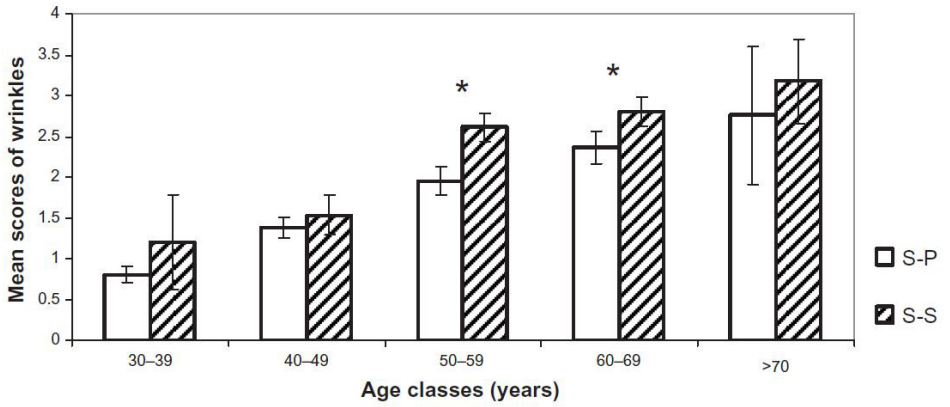

Figure. 5.11 Comparison of wrinkles and relief texture. '*' shows statistically significant difference. Abbreviations: S-P, sun-phobic; S-S, sun-seeking. Original figure is from [194].

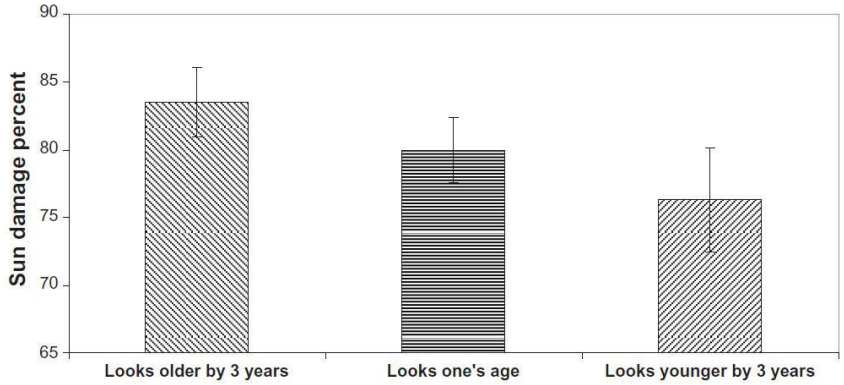

Figure. 5.12 Percentage of sun damage shows that how old a woman looks. Original figure is from [194].

On the basis of all steps mentioned above we can define the Sun Damage Effectiveness Factor (Δ_{SD}) as below:

$$\Delta_{SD} = \begin{cases} 0 & SDP = 80 \\ \pm 3 & SDP = 80 \pm 2 \end{cases} \tag{5.6}$$

where Δ_{SD} the Sun Damage Effectiveness Factor and SDP is the "Sun Damage Percentage". For the average SDP of 80%, Δ_{SD} is zero which means the apparent age and the real age are similar. If SDP increases by 2%, then apparent age becomes 3 years higher than the real age which means the person looks older. Contrariwise, a decrease of SDP by 2% means that the woman looks 3 years younger.

5.7.4 Model Construction

As discussed above, people who are continuously exposed to the sun, look $\Delta_{SD}(\approx 3)$ years older for their age. To construct the face ageing model for sun damage, in equation 5.3, $i+\Delta = i+\Delta_{SD} = i+3$. Thus, another time the Coalesced Face Template corresponding to the target age should be used. Therefore we have:

$$F_{SD}(i) = w_1 T_c(i+3) + w_2(\psi(f(j)) + \delta_{SD}(f(j))) \quad , \quad \begin{cases} i > j \\ 0.6 < w_2 < 0.7 \\ w_1 + w_2 = 1 \end{cases} \tag{5.7}$$

where, $F_{SD}(i)$ is the simulated face have been continuously exposed to the sun in age i and $T_c(i+3)$ is the Coalesced Face Template that must be used. In this study $\delta_{SD}(f(j)) = \varepsilon$ and its impact can be ignored. However we do not omit it from the model's equation as it the geometrical detailed alterations related to the Sun Damage Facial Ageing Model and it can be a part of future model improvements.

Since Δ_{SD} is close to the Δ_m, therefore, both models employ the same Face Template. As a result, the simulated faces for the same target age cluster (41-50 years old) can be very close to the meth addict's results. The differences between these two results are mainly the difference in the transformation functions $\delta_{SD}(f(j))$ and $\delta_m(f(j))$. For instance, the changes on the face geometry like face thinness and eyes angles may not be applied. However, some modifications on the texture can be added to improve the results: the appearance of the deep wrinkles and the colour of the face. For example, this time instead of a pale face, the face will be tanned.

5.7.5 Wrinkle Modeling

Facial wrinkles are not important only in terms of face age but they can also provide information about person's lifestyles and habits. For instance, facial wrinkles can represent the facial expressions or indicate some habits such as smoking or sun exposure [199]. As discussed before, there is a significant correlation between photo-ageing and the number and severity of the wrinkles, due to the damage of the elastin in skin. Therefore, to consecrate the results of Sun Damage Facial Ageing Model, some wrinkles are interpolated.

To do this, first a face image with wrinkles from the age range of $i+\Delta_{SD}$ is chosen as the wrinkle source. Then, the target face (simulated face by the equation 5.7) and the wrinkled face will share the same size. Then after, facial features are extracted for both faces and are employed to warp the wrinkled face coordinates to the target face coordinates. Finally, the image fusion is used to fuse the wrinkles to the target face. For image fusion the discrete wavelet transform (DWT) is used. To fuse $I_1(x,y)$ and $I_2(x,y)$ with wavelet transform W using fusion rule ϕ we have:

$$I(x,y) = W^{-1}(\phi(W(I_1(x,y)), W(I_2(x,y)))) \tag{5.8}$$

where W^{-1} is the inverse discrete wavelet transform (IDWT) [200]. Thus, by substituting $F_{SD(i)}$ and wrinkled face image in this equation we have;

$$F_{SDW}(i) = W^{-1}(\phi(W(F_{SD}(i)(x,y)), W(R(x,y)))) \tag{5.9}$$

where $F_{SDW}(i)$ is the simulated face after wrinkle interpolation in age i, $R(x,y)$ is the wrinkled mask image which is used as the wrinkle source.

Finally, some colour enhancement such as saturation is applied on the final image to make it more realistic as a tanned face.

5.7.6 Primary Results

The Sun Damage Facial Ageing Model is applied on the same database that had been employed for the F-FAM and Methamphetamine Addicts' Facial Ageing Model. In this model, the input is a normal adult face image and the result is how it might look in the age decade 41-50 years if the person was continuously exposed to the sun. Some of the results are shown in Figure 5.13.d

Figure 5.13 shows the input image and results of applying different models, proposed in this study, to compare.

Figure. 5.13 Illustration of the results of applying different models to compare.(a) Input images (b) Outputs of applying F-FAM (natural ageing) (c) Outputs of applying the Methamphetamine Addicts' Facial Ageing Model without considering the effect of wrinkles (d) Results of applying the Sun Damage Facial Ageing Model considering the effect of wrinkles – Note that output age range for all the results is 41-50.

Figure. 5.14 UV face image samples. Photos by Cara Phillips. [201]

5.7.7 Sun Spots Modeling

One of the most important symptoms of direct and chronic exposure to the ultraviolet rays is sun spots, also known as solar lentigines, and in some extreme cases mottled pigmentations appear on the face. While, sun damage in irreversible and cumulative, most of the times the signs of damage is invisible until the skin damage reaches a critical stage.

Ultraviolet photography is a way to show the sun damage which is hidden in normal photos. In this part of the work, we benefit from UV photos to integrate the undercover pigmentations into our model to achieve the more realistic results.

Ideal situation for using this technique is to capture photos from each subject with both ordinary camera and UV camera at the same time and with the same pose. The facial image captured using normal camera can be used as the input in the model. The output of the model, then, can be fused with the sunspots extracted from the face image captured by UV camera (named UV facial image) using wavelet transform. The results show how the person's face will look in the not too distance future in case of repeating sun exposure without protections.

Since the UV camera is not available for us, the results are achieved with available samples of the face portraits captured using UV camera. First a UV facial image is selected as the sun spot source (Figure 5.14).

Then, this UV facial image is mapped to the target face. Then after, a mask is created from the UV face image by erasing the eyes, nose and lips from the face and extracting the sunspots using wavelet transform. Finally, the image fusion using DWT is applied on two images. Some primary results are shown in Figure 5.15.

Figure. 5.15 Illustration of the results of applying Sun Damage Facial Ageing Model with the sun spots modeling to have more realistic results. The results are in the age range between 41-50.

5.8 Conclusion

In this chapter, Behavioural Facial Ageing Models are proposed. To start, various intrinsic and extrinsic determinants that affect the facial ageing process are briefly discussed. Among extrinsic factors, those lifestyle behaviours that have more effects on the face age and that avoiding them, can help to prevent premature ageing, are selected to add their effect to the ageing model.

In the proposed approach, for each lifestyle behaviour, one Effectiveness Factor (Δ) is calculated which is the difference between perceived age and actual age of the people who have that lifestyle habit. Therefore, in the ageing model Predictive Face Templates are replaced with Face Templates which are Δ years older than the target age. The geometry and colour of the face image are modeled according to the effects of each lifestyle behaviour.

The facial ageing model due to the methamphetamine abuse is proposed. $\Delta_m \approx 5$ is achieved using a survey and meth users database. Results are evaluated by subjective performance evaluation. Furthermore, Sun Damage Facial Ageing Model is presented. Its Effectiveness Factor is achieved according to the outcomes of a dermatology study on sun-seeking people. Since one of the effects of UV radiation is manifestation of the fine and deep wrinkles, to give more realistic look to the results, the effect of the wrinkles is modeled.

Outcome of the evaluation shows that results look in the desired age range. Moreover, the comparison between outcomes of the evaluation surveys on the results of natural ageing model (F-FAM) and the Behavioural Facial Ageing Models' results,

give approximately the calculated delta. It means that results are effectively realistic and are assessed in the desired age group and the presented model is accurate.

Since the serious source of the visible signs of ageing are directly linked to the environmental and behavioural factors, Behavioural Facial Ageing Models can create a revolution in the facial ageing studies. This study provides preliminary results on behavioural ageing. Of course there is a lot of space for improvement and many interesting and useful applications in biometrics and medical fields can be imagined for the future.

Chapter 6

Conclusion and Perspectives

In this final chapter, we will review the research contributions of this thesis and will discuss possible future research directions.

This thesis proposes some reliable image-based face ageing models by applying the biometric facial features. These models illustrate the individual's appearance in its past or future by using a single image as the input.

The main objectives of this work are:

1. To rejuvenate the adult face appearance down to its childhood, aiming to fill the void of childhood face modeling in the facial ageing studies.

2. To propose a model for global natural ageing process in order to predict the face in the future and provide a base model for more specific Predictive Models.

3. To attach the effects of different lifestyle behaviours to the natural facial ageing model, since there is no existing works on Behavioural Facial Ageing Models. The purpose is to show the negative impacts of high-risk behaviours on the apparent face age.

With these objectives, the thesis starts with answering the following three questions about the evolutionary trajectory of human face:

- ***What kind of changes occur in the face throughout the growth procedure and which components' changes are important for 2D facial growth modeling?***
  The work started with studying the anthropology and craniofacial morphology during childhood. After achieving the craniofacial measurements, first, those that are useful for 2D facial modeling are selected. Then, among these measurements, those which can represent a component or its distribution are kept. Some of the measurements were included in the face shape and size. Based on these studies, it is understood that significant geometrical changes happen during the formative years, but subtle changes occur in texture.

- ***What kind of changes arise in the face during ageing trajectory?***
  To begin, pathophysiology and the anatomy of facial ageing are perused. The outcomes indicate that facial ageing is associated with changes in different

structural layers of the face, namely, skeleton, muscle, fat and skin. It is also understood that how the changes in these layers affect the upper, mid and lower part of the face. A point worth noting is that although both face geometry and its texture are affected by the changes in different layers, in two-dimensional space most of them can be considered as a texture variation. In general, during adulthood most of the changes associated with texture and geometrical changes are subtle, yet effectual.

- ***What are the lifestyles most commonly linked with aspects of facial ageing and how do they affect the face's apparent age?***
  The answer to this question needs a broad study. It is difficult to differentiate between the impacts of the various lifestyle behaviours on the face. To start, based on different face ageing researches the most epidemic and ruinous behavioural factors that cause premature ageing are listed: drug abuse, sun exposure, smoking, and alcohol consumption. Then, the impacts of each lifestyle behaviour on the face were observed, and some apparent age differences between the exposed population and the healthy subjects are remarked.

Thesis Contributions

The main contributions of this thesis are as follows:

1. Backward Facial Ageing Model (B-FAM) for face image rejuvenation has been presented as the first face ageing model that covers the childhood period. This model estimates the face in its childhood by using a young adult face image.

2. Forward Facial Ageing Model (F-FAM) for natural ageing process has been proposed. This model predicts the future appearance of the face by using a young adult facial image as the input.

3. Behavioural Facial Ageing Models have been propounded based on the F-FAM. For the first time the association of lifestyle behaviours and facial ageing is considered to present the more realistic face ageing models. These models simulate the future appearance of the young adult face in case of choosing the high-risk lifestyle habits.

4. Facial Ageing Modeling Database (FAMD) is collected to model construction. This database comprises around 1600 facial images corresponding to various ages from 3 to 80 years. Moreover, using FAMD, 30 Face Templates are

constructed for different age clusters that can be used as the face prototypes in different age studies.

5. Face Time-Machine Database (FaceTiM V1.0) containing 246 images from 112 subjects, is created mainly to test and evaluate the results.

The focus of the B-FAM is on the geometrical aspects of the face. Face components and face contour have been modified non-linearly pursuant to a reliable Geometrical Model. Then, texture has been adapted by fusing the geometrically changed face and the created Reconstructive Face Template matched with the target age.

The EER of the objective evaluation performed in 112 results of B-FAM is 21.5%. By increasing the number of the results a more accurate number could be achieved. The conditions of the enrolled reference images surely influence the evaluation outcome. Because some of them do not have the same pose, expression and light condition similar to the achieved results that are used as the probe image. Hence, by the replacement of more appropriate images as the reference, the EER may decrease. Of course, the face recognition system's performance has an impact on this number.

The outcome of the first protocol of subjective performance evaluation applied on the results of B-FAM, which is to determine the similarity percentage of the simulated results and the references, deduce that 78.57% of the respondents observed more than 65% of similarity. For the second protocol which is to match the adult face images with simulated images from their childhood, the average number of the correct answers is 93.56%.

From the performance evaluations made on the results of B-FAM, it can be deduced that while the results have the appearance and characteristics of a typical child's face, the personal identity characteristics of the original input adult face are preserved.

Based on our experience, reconstructing a child face from an adult face image is more challenging compared to predicting an aged adult face using a young adult image. Not only the skin texture should be adapted to the target age, but also the craniofacial morphology of the face should be dramatically changed. B-FAM's attribute is that the estimated face images convey the perception of childness which is very difficult to achieve.

Therefore, it can be concluded that obtained results of B-FAM are reasonably persuasive and the model is remarkably accurate.

The main focus of the F-FAM is on the textural attributes of the face since most of the face transformations in ageing trajectory are associated with the facial texture. Yet, the impact of geometrical changes cannot be denied. In the presented approach,

the texture is estimated by mapping the relative Predictive Face Template to the geometrically changed face.

In F-FAM the impact of wrinkles are not considered. However, the results demonstrate that even without simulating the fine wrinkles and only with the effects of muscle reduction and subtle geometrical alterations, the face age will change.

Subjective performance evaluation performed on 20 results of this model shows 65% of the participants believe that the results of the model are estimated in the target age range. Hence, we can conclude the results are sensible and the F-FAM is accurate.

The main intention of the Behavioural Facial Ageing Models is to prevent people specially the youth from choosing the unsafe lifestyle habits. Two Behavioural Models are proposed: Methamphetamine Addicts' Facial Ageing Model and Sun Damage Facial Ageing Model.

The most important and challenging phase of constructing the Behavioural Models construction is the calculation of the Δ, which needs an extensive study on the population under the influence of that specific behaviour. Gathering a population with the same lifestyle profile or collecting their facial images as a database is a big challenge. In addition, sometimes survey participants do not provide their accurate and complete lifestyle profile. Moreover, in some cases the behaviours overlap and distinguishing between their impacts is tough.

Subjective evaluation applied on 20 results of the Methamphetamine Addicts' Facial Ageing Model indicates that 80% of participants estimate the age of simulated results in the expected age range. It shows that the results are convincing. Moreover, comparison between the results of the subjective evaluations performed on the natural ageing model and Methamphetamine Addicts' Facial Ageing Model can simply prove the precision of the model. The estimated age difference by respondents is rather very close to the obtained Effectiveness Factor (Δ).

In these proposed models the effects of the non-facial factors that can influence the individual's apparent age, such as hair style, facial hair and makeup are not considered.

In addition, one of the challenges for facial ageing modeling, specifically for the Reconstructive Modeling, is the actions affecting the natural procedure of the face growth such as cosmetic surgeries and heavy makeup. It is noticeable that the more natural the input face is, the more realistic the results will be.

Ageing modeling database collection is a challenging and tough task. In addition to the challenges common with the other face related databases, like lighting conditions, pose, image quality, occlusion, etc. some other limitations such as facial expressions, make up, cosmetic surgeries and all the alteration that can affect the apparent age, may have an effect on the image modality. For instance, facial expressions that change the

facial components shape and measures make the image useless for an accurate ageing study. Finding the images from the same subject, at different ages, with the proper quality and pose is very difficult. Not all the images found on the internet are suitable for constructing a reliable model since, in addition to all the conditions mentioned above, there is no certainty about the exact age of the person, and also they vary in expressions and pose. Moreover, there are many legal restrictions for collecting face images especially from children.

To conclude, we can say that the proposed models in this study are remarkably accurate to estimate a realistic facial appearance of an individual in the target age. While the simulated face images have the physiognomy, geometrical and textural characteristics of the target age, the personal identity and details of the input face images are retained.

Perspectives

In the course of this study, some challenges have been faced and questions raised which lead us to further improvement and future works. These future perspectives are presented below:

Ethnic–Based Ageing Models: In this study, the database used in geometrical measurements and the Face Template construction is a mix of different ethnics; while, there are clearly distinct differences between face and its components' shape across ethnicities. For example, in the East Asians and the Sub-Saharan Africans the nose is much boarder compared to other ethnicities; it is more prominent and longer in the Middle Eastern and the Southern European populations. The eyes are farther apart and the face is broader in the East-Asians. Moreover, as discussed before, there are also ethnic differences in skin and its ageing progress. These information can lead us to more realistic models in terms of geometry, texture, and time or region of wrinkles manifestation. More clear data can be achieved by having a facial ageing database specific to each ethnicity, though collecting such databases is a very challenging task. Hence, Ethnic-based Geometrical Model and Face Templates can be constructed which for sure can be very beneficial for ageing studies.

Personalised Wrinkle Model: Facial wrinkle manifestation is linked with facial expression and face mimic. In fact the muscles shrink during facial emotions causing the development of the lines and wrinkles, so with the passage of time these wrinkles become permanent even when the face relaxes. Therefore, we can personalise the

wrinkle model for each person by recording the wrinkles caused by different emotions and applying these wrinkles on the face with different intensity for different age ranges.

Smokers and Alcoholics Facial Ageing Models: Smoking is the most preventable cause of morbidity that is responsible for millions of deaths a year worldwide [202]. Moreover, appearing much older is an explicit and perhaps the most socially distressing effect of smoking. Unfortunately, the lifetime smoking almost always begins by the time kids graduate from high school [203]. It seems that, the demonstration of the health risks associated with smoking had no potency to quit it. We hope that presenting Smoker's Facial Ageing Model can benefit the young generation's sensitivity to their face appearance to convince them not to start smoking. This ageing model can also become a powerful motivator for older smokers to quit.

Furthermore, studies show that alcohol accelerates the face ageing process since it dehydrates the body by forcing the kidneys to work double times to remove the over-plus water from the system and leaves body's organs [204]. As the skin is the body's largest external organ, so it dries from inside out and deep facial wrinkles will appear more quickly. It also changes the blood flow in accordance with the skin because alcohol causes small blood vessels to widen as a result of the rising blood pressure and therefore more blood flows to the surface [205]. Therefore, alcohol intake causes flushed face, redness and sometimes puffiness in the face and under the eyes which can become permanent with long-term drinking habits. Moreover, alcohol limits the absorption of vitamins specially vitamin 'A' that plays a significant role in the production of collagen, amino acids, and minerals of which the deficiency can affect the face's muscles, skin and its youthful looking. Hence, Alcoholics' Facial Ageing Model can also be used to visualise the effects of alcohol on the face and prevent the alcohol intake specially in young generation.

Moreover, since the duration of the exposure to each behavioural habit is very important, for proposing an accurate Behavioural Model, the number of the years of exposure can be considered as a factor in the model.

Effects of the Healthy Lifestyle: In this study we proposed models based on risky lifestyle behaviours, as modeling the destructive effects of these behaviours can be effective in preventing people not to choose them. Showing the positive effects of a healthy lifestyle, such as a healthy diet and physical activity, to slow the ageing process can also be persuasive in choosing these lifestyle habits.

Slope of Ageing Speed: As the speed of ageing is different from one person to another,

we have found a way to approximate the slope of ageing speed in each person and model the face in its future based on that. First we estimate the face of people in their current age using their previous facial images. So by comparing the current facial image and the simulated face we can understand if the speed of ageing in one person is slower than normal, faster than normal or normal. So we can simulate the face in the upcoming years according to the achieved slope of ageing.

3D Morphable Models: In this study we have proposed different 2D models for facial ageing. This work can be a base for 3D facial ageing modeling that its development has already been started by our biometrics team at Lissi laboratory [206].

The Morphable 3D Facial Backward and Forward Modeling and simulation method is the extension of mesh and texture modeling from 2D to 3D domain and gives the additional capability of compensating for pose and lighting variations.

Having the power to modify a three-dimension facial image in order to transform the face to its older or younger appearance, requires precise three-dimensional models including Geometrical Mesh Model and Textural Model. This model represents a 3D object using a collection of points in the 3D space, connected by various geometric entities of 3D file formats each of which corresponds to the texture material from the 3D face image. Figure 6.1 shows the primary results of the Backward 3D Facial Model.

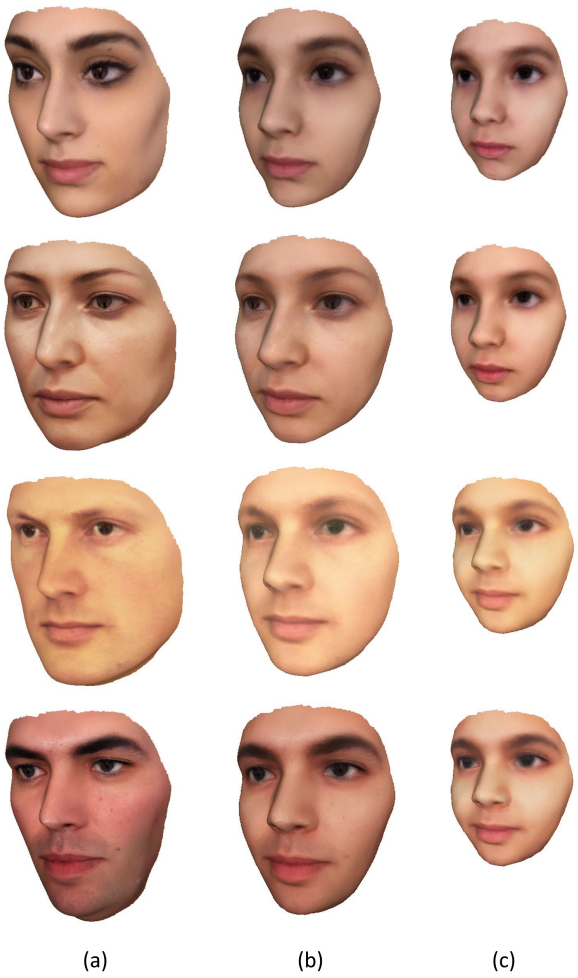

Figure. 6.1 Primary results of the Backward 3D Facial Model. (a) Input 3D face (b) Result in the age of 12-13. (c) Result in the age of 3-4.

Bibliography

[1] Ramanathan, R. Chellappa, and S. Biswas, "Age progression in human faces: A survey," *Journal of Visual Languages and Computing*, vol. 15, pp. 3349–3361, 2009.

[2] R. Shaw, M. McIntyre, and W. Mace, "The role of symmetry in event perception," in *Perception: Essays in honor of James J. Gibson*, R. B. MacLeod and H. L. Pick, Eds. Ithaca, NY, US: Cornell University Press, 1974, p. 317.

[3] J. B. Pittenger and R. E. Shaw, "Aging faces as viscal-elastic events: implications for a theory of nonrigid shape perception," *Journal of Experimental Psychology. Human Perception and Performance*, vol. 1, no. 4, pp. 374–382, Nov. 1975.

[4] D. W. Thompson, *On growth and form*. Cambridge:University Press;New York:Macmillan, 1945.

[5] J. T. Todd, L. S. Mark, R. E. Shaw, and J. B. Pittenger, "The perception of human growth," *Scientific American*, vol. 242, no. 2, pp. 132–134, Feb. 1980.

[6] L. S. Mark, J. T. Todd, and R. E. Shaw, "Perception of growth: a geometric analysis of how different styles of change are distinguished," *Journal of Experimental Psychology. Human Perception and Performance*, vol. 7, no. 4, pp. 855–868, Aug. 1981.

[7] L. S. Mark and J. T. Todd, "The perception of growth in three dimensions," *Perception & Psychophysics*, vol. 33, no. 2, pp. 193–196, Feb. 1983.

[8] V. Bruce, M. Burton, T. Doyle, and N. Dench, "Further experiments on the perception of growth in three dimensions," *Perception & Psychophysics*, vol. 46, no. 6, pp. 528–536, Dec. 1989.

[9] A. J. O'Toole, T. Vetter, H. Volz, and E. M. Salter, "Three-dimensional caricatures of human heads: distinctiveness and the perception of facial age," *Perception*, vol. 26, no. 6, pp. 719–732, 1997.

[10] A. J. O'Toole, T. Price, T. Vetter, J. C. Bartlett, and V. Blanz, "3d shape and 2d surface textures of human faces: the role of 'averages' in attractiveness and age," *Image and Vision Computing*, vol. 18, no. 1, pp. 9–19, Dec. 1999.

[11] L. G. Farkas, M. D., Ed., *Anthropometry of the Head and Face*, 2nd ed. New York: Raven Pr, Jan. 1994.

[12] Y. H. Kwon and N. d. V. Lobo, "Age Classification from Facial Images," *Computer Vision and Image Understanding*, vol. 74, no. 1, pp. 1–21, Apr. 1999.

[13] M. Kass, A. Witkin, and D. Terzopoulos, "Snakes: Active contour models," *International Journal of Computer Vision*, vol. 1, no. 4, pp. 321–331, 1988.

[14] W.-B. Horng, C.-P. Lee, and C.-W. Chen, "Classification of Age Groups Based on Facial Features," *Tamkang journal of science and engineering 4(3)*, pp. 183–192, Sep. 2001.

[15] S. Izadpanahi and . Toygar, "Geometric feature based age classification using facial images," in *IET Conference on Image Processing (IPR 2012)*, Jul. 2012, pp. 1–5.

[16] Y. Fu, G. Guo, and T. S. Huang, "Age Synthesis and Estimation via Faces: A Survey," *IEEE Transactions on Pattern Analysis and Machine Intelligence*, vol. 32, no. 11, pp. 1955–1976, Nov. 2010.

[17] A. Lanitis, C. Draganova, and C. Christodoulou, "Comparing different classifiers for automatic age estimation," *IEEE Transactions on Systems, Man, and Cybernetics, Part B (Cybernetics)*, vol. 34, no. 1, pp. 621–628, Feb. 2004.

[18] T. F. Cootes, G. J. Edwards, and C. J. Taylor, "Active appearance models," in *Computer Vision — ECCV'98*, ser. Lecture Notes in Computer Science, H. Burkhardt and B. Neumann, Eds., Jun. 1998, pp. 484–498.

[19] K. Luu, K. Ricanek, T. D. Bui, and C. Y. Suen, "Age estimation using Active Appearance Models and Support Vector Machine regression," in *2009 IEEE 3rd International Conference on Biometrics: Theory, Applications, and Systems*, Sep. 2009, pp. 1–5.

[20] K. Luu, T. D. Bui, C. Y. Suen, and K. Ricanek, "Spectral Regression based age determination," in *2010 IEEE Computer Society Conference on Computer Vision and Pattern Recognition - Workshops*, Jun. 2010, pp. 103–107.

[21] K. Luu, T. D. Bui, C. Y. Suen, and R. K., "Combined local and holistic facial features for age-determination," in *2010 11th International Conference on Control Automation Robotics Vision*, Dec. 2010, pp. 900–904.

[22] X. Geng, Z.-H. Zhou, Y. Zhang, G. Li, and H. Dai, "Learning from Facial Aging Patterns for Automatic Age Estimation," in *in 14th ACM International Conference on Multimedia*, ser. MM '06. New York, NY, USA: ACM, 2006, pp. 307–316.

[23] X. Geng, Z.-h. Zhou, S. Member, K. Smith-miles, and S. Member, "Automatic Age Estimation Based on Facial Aging Patterns," *IEEE Trans. Pattern Analysis and Machine Intelligence*, vol. 29, no. 12, pp. 2234–2240, 2007.

[24] Y. Fu, Y. Xu, and T. S. Huang, "Estimating Human Age by Manifold Analysis of Face Pictures and Regression on Aging Features," in *2007 IEEE International Conference on Multimedia and Expo*, Jul. 2007, pp. 1383–1386.

[25] Y. Fu and T. S. Huang, "Human Age Estimation With Regression on Discriminative Aging Manifold," *IEEE Transactions on Multimedia*, vol. 10, no. 4, pp. 578–584, Jun. 2008.

[26] G. Guo, Y. Fu, C. R. Dyer, and T. S. Huang, "Image-Based Human Age Estimation by Manifold Learning and Locally Adjusted Robust Regression," *IEEE Transactions on Image Processing*, vol. 17, no. 7, pp. 1178–1188, Jul. 2008.

[27] X. Geng, C. Yin, and Z. H. Zhou, "Facial Age Estimation by Learning from Label Distributions," *IEEE Transactions on Pattern Analysis and Machine Intelligence*, vol. 35, no. 10, pp. 2401–2412, Oct. 2013.

[28] N. Burson and T. D. Schneider, "Method and apparatus for producing an image of a person's face at a different age," U.S. Patent US4 276 570 A, Jun., 1981.

[29] D. M. Burt and D. I. Perrett, "Perception of age in adult Caucasian male faces: computer graphic manipulation of shape and colour information," *Biological Sciences*, vol. 259, no. 1355, pp. 137–143, Feb. 1995.

[30] D. A. Rowland and D. I. Perrett, "Manipulating facial appearance through shape and color," *IEEE Computer Graphics and Applications*, vol. 15, no. 5, pp. 70–76, Sep. 1995.

[31] I. Pitanguy, F. Leta, D. Pamplona, and H. I. Weber, "Defining and measuring aging parameters," *Applied Mathematics and Computation*, vol. 78, no. 2, pp. 217–227, Sep. 1996.

[32] F. R. Leta, A. Conci, D. Pamplona, and I. Itanguy, "Manipulating facial appearance through age parameters," in *Proc. Ninth Brazilian Symposium on Computer Graphics and Image Processing*, 1996, pp. 167–172.

[33] I. Pitanguy, D. Pamplona, H. I. Weber, F. Leta, F. Salgado, and H. N. Radwanski, "Numerical modeling of facial aging," *Plastic and Reconstructive Surgery*, vol. 102, no. 1, pp. 200–204, Jul. 1998.

[34] B. Tiddeman, M. Burt, and D. Perrett, "Prototyping and Transforming Facial Textures for Perception Research," *IEEE Comput. Graph. Appl.*, vol. 21, no. 5, pp. 42–50, Sep. 2001.

[35] B. Tiddeman, M. Stirrat, and D. Perrett, "Towards Realism in Facial Image Transformation: Results of a Wavelet MRF Method," *Computer Graphics Forum*, vol. 24, no. 3, pp. 449–456, Sep. 2005.

[36] A. Lanitis, C. Taylor, and T. Cootes, "Toward automatic simulation of aging effects on face images," *IEEE Transactions on Pattern Analysis and Machine Intelligence*, vol. 24, no. 4, pp. 442–455, Apr. 2002.

[37] C. M. Scandrett, C. J. Solomon, and S. J. Gibson, "A person-specific, rigorous aging model of the human face," *Pattern Recognition Letters*, vol. 27, no. 15, pp. 1776–1787, Nov. 2006.

[38] N. Ramanathan and R. Chellappa, "Modeling Age Progression in Young Faces," in *2006 IEEE Computer Society Conference on Computer Vision and Pattern Recognition (CVPR'06)*, ser. CVPR '06, vol. 1. Washington, DC, USA: IEEE Computer Society, Jun. 2006, pp. 387–394.

[39] N. Ramanathan and C. R, "Modeling shape and textural variations in aging faces," in *2008 8th IEEE International Conference on Automatic Face Gesture Recognition*, Sep. 2008, pp. 1–8.

[40] K. Waters, "A Muscle Model for Animation Three-dimensional Facial Expression," in *14th Annual Conference on Computer Graphics and Interactive Techniques*, ser. SIGGRAPH '87. New York, NY, USA: ACM, 1987, pp. 17–24.

[41] J. Suo, F. Min, S. Zhu, S. Shan, and X. Chen, "A Multi-Resolution Dynamic Model for Face Aging Simulation," in *IEEE Conference on Computer Vision and Pattern Recognition, 2007. CVPR '07*, Jun. 2007, pp. 1–8.

[42] Z. Xu, H. Chen, and S.-C. Zhu, "A high resolution grammatical model for face representation and sketching," in *2005 IEEE Computer Society Conference on Computer Vision and Pattern Recognition (CVPR'05)*, vol. 2, Jun. 2005, pp. 470–477.

[43] S. Ubaid, S. Das, and M. Imthiyas, "Human age prediction and classification using facial image," *International Journal on Computer Science and Engineering*, vol. 5, p. 357, 2013.

[44] I. Kemelmacher-Shlizerman, S. Suwajanakorn, and S. Seitz, "Illumination-Aware Age Progression," in *2014 IEEE Conference on Computer Vision and Pattern Recognition (CVPR)*, Jun. 2014, pp. 3334–3341.

[45] X. Shu, J. Tang, H. Lai, L. Liu, and S. Yan, "Personalized Age Progression with Aging Dictionary," in *2015 IEEE International Conference on Computer Vision (ICCV)*, Dec. 2015, pp. 3970–3978.

[46] A. Bastanfard, O. Bastanfard, H. Takahashi, and M. Nakajima, "Toward anthropometrics simulation of face rejuvenation and skin cosmetic," *Computer Animation and Virtual Worlds*, vol. 15, no. 3-4, pp. 347–352, Jul. 2004.

[47] G. Guo, "Digital anti-aging in face images," in *2011 International Conference on Computer Vision*, Nov. 2011, pp. 2510–2515.

[48] D. Bitouk, N. Kumar, S. Dhillon, P. Belhumeur, and S. K. Nayar, "Face swapping: automatically replacing faces in photographs," *ACM Transactions on Graphics (TOG)*, vol. 27, no. 3, p. 39, 2008.

[49] T. F. Cootes and C. J. Taylor, "Active Shape Models – "Smart Snakes"," in *British Machine Vision Conference*, vol. 92, 1992, pp. 266–275.

[50] K.-W. Wan, K.-M. Lam, and K.-C. Ng, "An accurate active shape model for facial feature extraction," *Pattern Recognition Letters*, vol. 26, no. 15, pp. 2409–2423, Nov. 2005.

[51] S. K. Zhou and D. Comaniciu, "Shape regression machine," in *Biennial International Conference on Information Processing in Medical Imaging*, vol. 20, 2007, pp. 13–25.

[52] N. Wang, X. Gao, D. Tao, H. Yang, and X. Li, "Facial feature point detection: A comprehensive survey," *Neurocomputing*, 2017.

[53] P. D. Sozou, T. F. Cootes, C. J. Taylor, E. C. Di Mauro, and A. Lanitis, "Non-linear point distribution modelling using a multi-layer perceptron," *Image and Vision Computing*, vol. 15, no. 6, pp. 457–463, Jun. 1997.

[54] D. Cristinacce, T. Cootes, and I. Scott, "A multi-stage approach to facial feature detection," in *British Machine Vision Conference*, vol. 1, 2004, pp. 231–240.

[55] S. Lucey, Y. Wang, M. Cox, S. Sridharan, and J. F. Cohn, "Efficient Constrained Local Model Fitting for Non-Rigid Face Alignment," *Image and vision computing*, vol. 27, no. 12, pp. 1804–1813, Nov. 2009.

[56] S. W. Chew, P. Lucey, S. Lucey, J. Saragih, J. F. Cohn, and S. Sridharan, "Person-independent facial expression detection using Constrained Local Models," in *2011 IEEE International Conference on Automatic Face & Gesture Recognition (FG 2011)*, Mar. 2011, pp. 915–920.

[57] C. Lindner, P. A. Bromiley, M. C. Ionita, and T. F. Cootes, "Robust and Accurate Shape Model Matching Using Random Forest Regression-Voting," *IEEE Transactions on Pattern Analysis and Machine Intelligence*, vol. 37, no. 9, pp. 1862–1874, Sep. 2015.

[58] P. N. Belhumeur, D. W. Jacobs, D. J. Kriegman, and N. Kumar, "Localizing parts of faces using a consensus of exemplars," *IEEE transactions on pattern analysis and machine intelligence*, vol. 35, no. 12, pp. 2930–2940, Dec. 2013.

[59] X. Yu, J. Huang, S. Zhang, W. Yan, and D. N. Metaxas, "Pose-Free Facial Landmark Fitting via Optimized Part Mixtures and Cascaded Deformable Shape Model," in *2013 IEEE International Conference on Computer Vision*, Dec. 2013, pp. 1944–1951.

[60] T. F. Cootes, G. V. Wheeler, K. N. Walker, and C. J. Taylor, "View-based active appearance models," *Image and Vision Computing*, vol. 20, no. 9–10, pp. 657–664, Aug. 2002.

[61] J. Gonzalez-Mora, F. D. l. Torre, R. Murthi, N. Guil, and E. L. Zapata, "Bilinear Active Appearance Models," in *2007 IEEE 11th International Conference on Computer Vision*, Oct. 2007, pp. 1–8.

[62] G. Tzimiropoulos and M. Pantic, "Optimization Problems for Fast AAM Fitting in-the-Wild," in *2013 IEEE International Conference on Computer Vision*, Dec. 2013, pp. 593–600.

[63] S. Lucey, R. Navarathna, A. B. Ashraf, and S. Sridharan, "Fourier Lucas-Kanade algorithm," *IEEE transactions on pattern analysis and machine intelligence*, vol. 35, no. 6, pp. 1383–1396, Jun. 2013.

[64] S. Rivera and A. Martinez, "Learning Deformable Shape Manifolds," *Pattern recognition*, vol. 45, no. 4, pp. 1792–1801, Apr. 2012.

[65] H. Yang and I. Patras, "Sieving Regression Forest Votes for Facial Feature Detection in the Wild," in *2013 IEEE International Conference on Computer Vision*, Dec. 2013, pp. 1936–1943.

[66] J. M. Saragih, S. Lucey, and J. F. Cohn, "Deformable Model Fitting by Regularized Landmark Mean-Shift," *International Journal of Computer Vision*, vol. 91, no. 2, pp. 200–215, Jan. 2011.

[67] M. B. Stegmann, R. Fisker, B. K. Ersbøll, H. H. Thodberg, and L. Hyldstrup, "Active Appearance Models: Theory and Cases," in *9th Danish Conf. Pattern Recognition and Image Analysis*, 2000, pp. 49–57.

[68] L. Liang, F. Wen, Y.-Q. Xu, X. Tang, and H.-Y. Shum, "Accurate Face Alignment using Shape Constrained Markov Network," in *2006 IEEE Computer Society Conference on Computer Vision and Pattern Recognition (CVPR'06)*, vol. 1, Jun. 2006, pp. 1313–1319.

[69] S. Cosar, M. Cetin, and A. Ercil, "A Robust Facial Feature Point Tracker using Graphical Models," in *2007 5th International Symposium on Image and Signal Processing and Analysis*, Sep. 2007, pp. 550–555.

[70] P. Luo, "Hierarchical Face Parsing via Deep Learning," in *Conference on Computer Vision and Pattern Recognition (CVPR)*, ser. CVPR '12, Washington, DC, USA, 2012, pp. 2480–2487.

[71] T. Cootes, A. Hill, C. Taylor, and J. Haslam, "Use of active shape models for locating structures in medical images," *Image and Vision Computing*, vol. 12, no. 6, pp. 355–365, Jul. 1994.

[72] T. Cootes, E. Baldock, and J. Graham, "An introduction to active shape models," in *Image processing and analysis*, 2000, pp. 223–248.

[73] T. F. Cootes, G. J. Edwards, and C. J. Taylor, "Active Appearance Models," *IEEE Transactions on Pattern Analysis and Machine Intelligence (TPAMI)*, vol. 23, no. 6, pp. 681–685, Jun. 2001.

[74] C. Goodall, "Procrustes Methods in the Statistical Analysis of Shape," *Journal of the Royal Statistical Society. Series B (Methodological)*, vol. 53, no. 2, pp. 285–339, 1991.

[75] J. Saragih and R. Goecke, "A Nonlinear Discriminative Approach to AAM Fitting," in *2007 IEEE 11th International Conference on Computer Vision*, Oct. 2007, pp. 1–8.

[76] B. D. Lucas and T. Kanade, "An Iterative Image Registration Technique with an Application to Stereo Vision," in *7th International Joint Conference on Artificial Intelligence - Volume 2*, ser. IJCAI'81. San Francisco, CA, USA: Morgan Kaufmann Publishers Inc., 1981, pp. 674–679.

[77] S. Baker and I. Matthews, "Lucas-Kanade 20 Years On: A Unifying Framework," *International Journal of Computer Vision*, vol. 56, no. 3, pp. 221–255, Feb. 2004.

[78] D. Hunter, "Synthesis of facial ageing transforms using three-dimensional morphable models," PhD. thesis, University of St. Andrews, Scotland, 2009.

[79] I. Matthews and S. Baker, "Active Appearance Models Revisited," *International Journal of Computer Vision*, vol. 60, no. 2, pp. 135–164, Nov. 2004.

[80] G. D. Hager and P. N. Belhumeur, "Efficient Region Tracking With Parametric Models of Geometry and Illumination," *The IEEE Transactions on Pattern Analysis and Machine Intelligence (TPAMI)*, vol. 20, no. 10, pp. 1025–1039, Oct. 1998.

[81] E. E. Catmull, "A Subdivision Algorithm for Computer Display of Curved Surfaces." PhD. Thesis, The University of Utah, 1974.

[82] A. Gustafsson, "Interactive Image Warping," M.A. Thesis, Helsinky University of Technology, May 1993.

[83] G. Wolberg, *Digital Image Warping*, 1st ed. Los Alamitos, CA, USA: IEEE Computer Society Press, 1994.

[84] P. S. Heckbert, "Fundamentals of Texture Mapping and Image Warping," M.A. Thesis, University of California at Berkeley, Berkeley, CA, USA, 1989.

[85] R. MacCracken and K. I. Joy, "Free-form Deformations with Lattices of Arbitrary Topology," in *The 23rd Annual Conference on Computer Graphics and Interactive Techniques*, ser. SIGGRAPH '96. New York, NY, USA: ACM, 1996, pp. 181–188.

[86] T. W. Sederberg and S. R. Parry, "Free-form Deformation of Solid Geometric Models," in *The 13th Annual Conference on Computer Graphics and Interactive Techniques*, ser. SIGGRAPH '86. New York, NY, USA: ACM, 1986, pp. 151–160.

[87] S.-Y. Lee, K.-Y. Chwa, and S. Y. Shin, "Image Metamorphosis Using Snakes and Free-form Deformations," in *The 22Nd Annual Conference on Computer Graphics and Interactive Techniques*, ser. SIGGRAPH '95. New York, NY, USA: ACM, 1995, pp. 439–448.

[88] T. Beier and S. Neely, "Feature-based Image Metamorphosis," in *The 19th Annual Conference on Computer Graphics and Interactive Techniques*, ser. SIGGRAPH '92. New York, NY, USA: ACM, 1992, pp. 35–42.

[89] F. L. Bookstein, "Principal warps: thin-plate splines and the decomposition of deformations," *IEEE Transactions on Pattern Analysis and Machine Intelligence*, vol. 11, no. 6, pp. 567–585, Jun. 1989.

[90] S. Schaefer, T. McPhail, and J. Warren, "Image Deformation Using Moving Least Squares," in *ACM transactions on graphics (TOG)*, ser. SIGGRAPH '06, vol. 25. New York, NY, USA: ACM, 2006, pp. 533–540.

[91] D. Levin, "The Approximation Power of Moving Least-squares," *Mathematics of Computation of the American Mathematical Society*, vol. 67, no. 224, pp. 1517–1531, Oct. 1998.

[92] T. Igarashi, T. Moscovich, and J. F. Hughes, "As-rigid-as-possible Shape Manipulation," in *ACM transactions on graphics (TOG)*, ser. SIGGRAPH '05. New York, NY, USA: ACM, 2005, pp. 1134–1141.

[93] B. K. P. Horn, "Closed-form solution of absolute orientation using unit quaternions," *JOSA A*, vol. 4, no. 4, pp. 629–642, Apr. 1987.

[94] A. Lanitis, "FG-NET (Face and Gesture Recognition Network) Database," 2004.

[95] K. Ricanek Jr. and T. Tesafaye, "MORPH: A Longitudinal Image Database of Normal Adult Age-Progression," in *The 7th International Conference on Automatic Face and Gesture Recognition*, ser. FGR '06. Washington, DC, USA: IEEE Computer Society, 2006, pp. 341–345.

[96] A. Midori Albert and K. Jr. Ricanek, "The MORPH Database: Investigating the Effects of Adult Craniofacial Aging on Automated Face-Recognition Technology," *Research and Technology - Forensic Science Communications*, vol. 10, no. 2, Apr. 2008.

[97] P. J. Phillips, H. Moon, S. A. Rizvi, and P. J. Rauss, "The FERET evaluation methodology for face-recognition algorithms," *IEEE Transactions on Pattern Analysis and Machine Intelligence*, vol. 22, no. 10, pp. 1090–1104, Oct. 2000.

[98] K. Ueki, T. Hayashida, and T. Kobayashi, "Subspace-based age-group classification using facial images under various lighting conditions," in *7th International Conference on Automatic Face and Gesture Recognition (FGR06)*, Apr. 2006, pp. 6 pp.–48.

[99] M. Nakano and M. Fukumi, "Age and Gender Recognition Using Facial Edge Information," in *the First World Congress of the International Federation for Systems Research: The New Roles of Systems Sciences For a Knowledge-based Society*, Kobe, Nov. 2005.

[100] A. Bastanfard, M. A. Nik, and M. M. Dehshibi, "Iranian Face Database with age, pose and expression," in *2007 International Conference on Machine Vision*, Dec. 2007, pp. 50–55.

[101] M. Minear and D. C. Park, "A lifespan database of adult facial stimuli," *Behavior Research Methods, Instruments, & Computers: A Journal of the Psychonomic Society, Inc*, vol. 36, no. 4, pp. 630–633, Nov. 2004.

[102] Y. Fu and N. Zheng, "M-Face: An Appearance-Based Photorealistic Model for Multiple Facial Attributes Rendering," *IEEE Transactions on Circuits and Systems for Video Technology*, vol. 16, no. 7, pp. 830–842, Jul. 2006.

[103] B. Yao, X. Yang, and S.-C. Zhu, "Introduction to a Large-scale General Purpose Ground Truth Database: Methodology, Annotation Tool and Benchmarks," in *The 6th International Conference on Energy Minimization Methods in Computer Vision and Pattern Recognition*, ser. EMMCVPR'07. Berlin, Heidelberg: Springer-Verlag, 2007, pp. 169–183.

[104] A. C. Gallagher and T. Chen, "Clothing cosegmentation for recognizing people," in *2008 IEEE Conference on Computer Vision and Pattern Recognition*, Jun. 2008, pp. 1–8.

[105] B. Ni, Z. Song, and S. Yan, "Web Image Mining Towards Universal Age Estimator," in *17th ACM International Conference on Multimedia*, ser. MM '09. New York, NY, USA: ACM, 2009, pp. 85–94.

[106] R. Rothe, R. Timofte, and L. V. Gool, "DEX: Deep EXpectation of Apparent Age from a Single Image," in *2015 IEEE International Conference on Computer Vision Workshop (ICCVW)*, Dec. 2015, pp. 252–257.

[107] D. S. Ma, J. Correll, and B. Wittenbrink, "The Chicago face database: A free stimulus set of faces and norming data," *Behavior Research Methods*, vol. 47, no. 4, pp. 1122–1135, Dec. 2015.

[108] G. Panis, A. Lanitis, N. Tsapatsoulis, and T. F. Cootes, "Overview of research on facial ageing using the FG-NET ageing database," *IET Biometrics*, vol. 5, no. 2, pp. 37–46, 2016.

[109] "Face Time-Machine Database (FaceTiM V.1.0)." [Online]. Available: http://www.amine-nait-ali.org/facetim

[110] J. Hall, J. Allanson, K. Gripp, and A. Slavotinek, *Handbook of Physical Measurements*. Oxford University Press, Nov. 2006.

[111] J. C. Kolar and E. M. Salter, *Craniofacial Anthropometry: Practical Measurement of the Head and Face for Clinical, Surgical,and Research Use*. Springfield, Ill., U.S.A: Charles C Thomas Pub Ltd, Mar. 1997.

[112] A. Bukis and R. Simutis, "Face Orientation Normalization Using Eye Positions," *Computer Technology and Application*, vol. 4, no. 10, 2013.

[113] "Francis Galton and Composite Portraiture." [Online]. Available: http://galton.org

[114] D. I. Perrett, K. J. Lee, I. Penton-Voak, D. Rowland, S. Yoshikawa, D. M. Burt, S. P. Henzi, D. L. Castles, and S. Akamatsu, "Effects of sexual dimorphism on facial attractiveness," *Nature*, vol. 394, no. 6696, pp. 884–887, Aug. 1998.

[115] E. Farazdaghi and A. Nait-ali, "Backward Face Ageing Model (B-FAM) for Digital Face Image Rejuvenation," *IET Biometrics*, May 2017.

[116] E. Farazdaghi, F. M. Z. Heravi, L. Chatelain, and A. NAIT-ALI, "Reverse facial ageing model for youthful appearance restoration from adult face images," in *2016 6th European Workshop on Visual Information Processing (EUVIP)*, Oct. 2016, pp. 1–6.

[117] P. Sharma, A. Arora, and A. Valiathan, "Age Changes of Jaws and Soft Tissue Profile," *The Scientific World Journal*, p. e301501, Nov. 2014.

[118] S. Premkumar, *Textbook of Craniofacial Growth*. JP Medical Ltd, Jun. 2011.

[119] R. K. Harley, G. A. Lawrence, L. D. Sanford, and R. Burnett, *Visual impairment in the schools: (3rd Ed.)*. Charles C Thomas Publisher, Jan. 2000.

[120] R. S. Snell and M. A. Lemp, *Clinical Anatomy of the Eye*, 2nd ed. Malden, MA, USA: Wiley-Blackwell, Dec. 1997.

[121] J. D. Subtelny, "A longitudinal study of soft tissue facial structures and their profile characteristics, defined in relation to underlying skeletal structures," *American Journal of Orthodontics*, vol. 45, no. 7, pp. 481–507, Jul. 1959.

[122] S. R. Coleman and R. Grover, "The Anatomy of the Aging Face: Volume Loss and Changes in 3-Dimensional Topography," *Aesthetic Surgery Journal*, vol. 26, pp. S4–S9, Jan. 2006.

[123] D. H. Enlow, R. E. Moyers, and W. W. Merow, *Handbook of facial growth*. Saunders, 1975.

[124] D. F. Huelke, "An Overview of Anatomical Considerations of Infants and Children in the Adult World of Automobile Safety Design," *Annual Proceedings / Association for the Advancement of Automotive Medicine*, vol. 42, pp. 93–113, 1998.

[125] C. J. Lux, C. Conradt, D. Burden, and G. Komposch, "Three-dimensional analysis of maxillary and mandibular growth increments," *The Cleft Palate-Craniofacial Journal: Official Publication of the American Cleft Palate-Craniofacial Association*, vol. 41, no. 3, pp. 304–314, May 2004.

[126] A. D. Dixon, D. A. N. Hoyte, and O. Ronning, *Fundamentals of Craniofacial Growth*. CRC Press, Apr. 1997.

[127] C. Solomon and T. Breckon, "Morphological Processing," in *Fundamentals of Digital Image Processing*. John Wiley & Sons, Ltd, 2010.

[128] F. Y. Shih, *Image Processing and Mathematical Morphology: Fundamentals and Applications*. CRC Press, Mar. 2009.

[129] F. Cherifi, B. Hemery, R. Giot, M. Pasquet, and C. Rosenberger, "Performance Evaluation Of Behavioral Biometric Systems," in *Book on Behavioral Biometrics for Human Identification: Intelligent Applications*. IGI, 2009, p. 21.

[130] A. Jain, P. Flynn, and A. A. Ross, *Handbook of Biometrics*. Springer Science & Business Media, Oct. 2007.

[131] *Technical Document About FAR, FRR and EER Version 1.0*. SYRIS Technology Corp., 2004.

[132] R. Fitzgerald, M. H. Graivier, M. Kane, Z. P. Lorenc, D. Vleggaar, W. P. Werschler, and J. M. Kenkel, "Update on Facial Aging," *Aesthetic Surgery Journal*, vol. 30, no. 1_Supplement, pp. 11S–24S, Jul. 2010.

[133] B. Mendelson and C.-H. Wong, "Changes in the Facial Skeleton With Aging: Implications and Clinical Applications in Facial Rejuvenation," *Aesthetic Plastic Surgery*, vol. 36, no. 4, pp. 753–760, Aug. 2012.

[134] J. E. Pessa, "An algorithm of facial aging: verification of Lambros's theory by three-dimensional stereolithography, with reference to the pathogenesis of midfacial aging, scleral show, and the lateral suborbital trough deformity," *Plastic and Reconstructive Surgery*, vol. 106, no. 2, pp. 479–488; discussion 489–490, Aug. 2000.

[135] R. B. Shaw Jr, E. B. Katzel, P. F. Koltz, M. J. Yaremchuk, J. A. Girotto, D. M. Kahn, and H. N. Langstein, "Aging of the facial skeleton: aesthetic implications and rejuvenation strategies," *Plastic and reconstructive surgery*, vol. 127, no. 1, pp. 374–383, 2011.

[136] D. M. Kahn and R. B. Shaw, "Aging of the bony orbit: a three-dimensional computed tomographic study," *Aesthetic Surgery Journal*, vol. 28, no. 3, pp. 258–264, Jun. 2008.

[137] B. Jahan-Parwar and K. Blackwell, "Facial Bone Anatomy: Overview, Mandible, Maxilla," Jun. 2013. [Online]. Available: http://emedicine.medscape.com/article/835401-overview.

[138] J. E. Pessa, V. P. Zadoo, K. L. Mutimer, C. Haffner, C. Yuan, A. I. DeWitt, and J. R. Garza, "Relative maxillary retrusion as a natural consequence of aging: combining skeletal and soft-tissue changes into an integrated model of midfacial aging," *Plastic and Reconstructive Surgery*, vol. 102, no. 1, pp. 205–212, Jul. 1998.

[139] R. B. Shaw and D. M. Kahn, "Aging of the midface bony elements: a three-dimensional computed tomographic study," *Plastic and Reconstructive Surgery*, vol. 119, no. 2, pp. 675–681; discussion 682–683, Feb. 2007.

[140] J. E. Pessa, D. E. Slice, K. R. Hanz, T. H. Broadbent, and R. J. Rohrich, "Aging and the shape of the mandible," *Plastic and Reconstructive Surgery*, vol. 121, no. 1, pp. 196–200, Jan. 2008.

[141] S. Eremia, Ed., *Office-Based Cosmetic Procedures and Techniques*, 1st ed., ser. Chapter 1. Cambridge ; New York: Cambridge University Press, Feb. 2010.

[142] A. E. Wulc, A. E. Wulc, P. Sharma, C. N. Czyz, and C. N. Czyz, "The Anatomic Basis of Midfacial Aging," in *Midfacial Rejuvenation*, M. E. Hartstein, A. E. Wulc, and D. E. Holck, Eds. Springer New York, 2012, pp. 15–28.

[143] H. H. Publishing, "The aging eye: when to worry about eye, eyelid problems." [Online]. Available: https://www.health.harvard.edu/healthbeat/the-aging-eye-when-to-worry-about-eye-eyelid-problems.

[144] J. H. Liu and F. E. Bartun, "The aging face: rhytidectomy and adjunctive procedures," *Selected readings in plastic surgery*, vol. 6, no. C3, 2001.

[145] J. M. Stuzin, "Restoring facial shape in face lifting: the role of skeletal support in facial analysis and midface soft-tissue repositioning," *Plastic and Reconstructive Surgery*, vol. 119, no. 1, pp. 362–376; discussion 377–378, Jan. 2007.

[146] E. C. Naylor, R. E. B. Watson, and M. J. Sherratt, "Molecular aspects of skin ageing," *Maturitas*, vol. 69, no. 3, pp. 249–256, Jul. 2011.

[147] J. Calleja-Agius, Y. Muscat-Baron, and M. P. Brincat, "Skin ageing," *Menopause International*, vol. 13, no. 2, pp. 60–64, Jun. 2007.

[148] C. Castelo-Branco, M. Duran, and J. González-Merlo, "Skin collagen changes related to age and hormone replacement therapy," *Maturitas*, vol. 15, no. 2, pp. 113–119, Oct. 1992.

[149] J. M. Waller and H. I. Maibach, "Age and skin structure and function, a quantitative approach (II): protein, glycosaminoglycan, water, and lipid content and structure," *Skin research and technology: official journal of International Society for Bioengineering and the Skin (ISBS) [and] International Society for Digital Imaging of Skin (ISDIS) [and] International Society for Skin Imaging (ISSI)*, vol. 12, no. 3, pp. 145–154, Aug. 2006.

[150] S. Luebberding, N. Krueger, and M. Kerscher, "Age-related changes in skin barrier function - quantitative evaluation of 150 female subjects," *International Journal of Cosmetic Science*, vol. 35, no. 2, pp. 183–190, Apr. 2013.

[151] R. Bazin and E. Doublet, *Skin aging atlas. Volume 1,*. Paris: Éd. Med'com, 2007.

[152] R. Klette, *Concise Computer Vision: An Introduction into Theory and Algorithms*. Springer Science & Business Media, Jan. 2014.

[153] R. J. Schalkoff, *Digital image processing and computer vision*. John Wiley & Sons Australia, Limited, 1989.

[154] M. A. Farage, K. W. Miller, P. Elsner, and H. I. Maibach, "Intrinsic and extrinsic factors in skin ageing: a review," *International Journal of Cosmetic Science*, vol. 30, no. 2, pp. 87–95, Apr. 2008.

[155] H. Rexbye, I. Petersen, M. Johansens, L. Klitkou, B. Jeune, and K. Christensen, "Influence of environmental factors on facial ageing," *Age and Ageing*, vol. 35, no. 2, pp. 110–115, Mar. 2006.

[156] K. Sveikata, I. Balciuniene, and J. Tutkuviene, "Factors influencing face aging. Literature review," *Stomatologija*, vol. 13, no. 4, pp. 113–116, 2011.

[157] A. V. Rawlings, "Ethnic skin types: are there differences in skin structure and function?" *International Journal of Cosmetic Science*, vol. 28, no. 2, pp. 79–93, Apr. 2006.

[158] N. A. Vashi, M. Buainain De Castro Maymone, and R. V. Kundu, "Aging Differences in Ethnic Skin," *The Journal of Clinical and Aesthetic Dermatology*, vol. 9, no. 1, pp. 31–38, Jan. 2016.

[159] S. Sachdeva, "Fitzpatrick skin typing: Applications in dermatology," *Indian Journal of Dermatology, Venereology and Leprology*, vol. 75, no. 1, p. 93, 2009.

[160] M. A. Pathak, "In memory of Thomas Bernhard Fitzpatrick," *The Journal of Investigative Dermatology*, vol. 122, no. 2, pp. xx–xxi, Feb. 2004.

[161] T. B. Fitzpatrick, "Soleil et peau [Sun and skin]," *Journal de Médecine Esthétique*, vol. 2, pp. 33–34, 1975.

[162] S. Alaluf, D. Atkins, K. Barrett, M. Blount, N. Carter, and A. Heath, "Ethnic variation in melanin content and composition in photoexposed and photoprotected human skin," *Pigment Cell Research / Sponsored by the European Society for Pigment Cell Research and the International Pigment Cell Society*, vol. 15, no. 2, pp. 112–118, Apr. 2002.

[163] D. A. Weigand, C. Haygood, and J. R. Gaylor, "Cell layers and density of Negro and Caucasian stratum corneum," *The Journal of Investigative Dermatology*, vol. 62, no. 6, pp. 563–568, Jun. 1974.

[164] D. C. Wan, V. W. Wong, M. T. Longaker, G. P. Yang, and F.-C. Wei, "Moisturizing Different Racial Skin Types," *The Journal of Clinical and Aesthetic Dermatology*, vol. 7, no. 6, pp. 25–32, Jun. 2014.

[165] Z. D. Draelos, *Cosmetics and Dermatologic Problems and Solutions, Third Edition*. CRC Press, Sep. 2011.

[166] K. Tsukahara, M. Hotta, O. Osanai, H. Kawada, T. Kitahara, and Y. Takema, "Gender-dependent differences in degree of facial wrinkles," *Skin research and technology: official journal of International Society for Bioengineering and the Skin (ISBS) [and] International Society for Digital Imaging of Skin (ISDIS) [and] International Society for Skin Imaging (ISSI)*, vol. 19, no. 1, pp. e65–71, Feb. 2013.

[167] C. C. Zouboulis, "Human skin: an independent peripheral endocrine organ," *Hormone Research*, vol. 54, no. 5-6, pp. 230–242, 2000.

[168] B. A. Gilchrest and J. Krutmann, *Skin Aging*. Springer Science & Business Media, Apr. 2006.

[169] T. J. Phillips, Z. Demircay, and M. Sahu, "Hormonal effects on skin aging," *Clinics in Geriatric Medicine*, vol. 17, no. 4, pp. 661–672, vi, Nov. 2001.

[170] M. J. Thornton, "The biological actions of estrogens on skin," *Experimental Dermatology*, vol. 11, no. 6, pp. 487–502, Dec. 2002.

[171] M. P. Brincat, "Hormone replacement therapy and the skin," *Maturitas*, vol. 35, no. 2, pp. 107–117, May 2000.

[172] P. Smith, "A comprehensive look at hormones and the effects of hormone replacement," in *14th Annual International Congress on Anti-Aging Medicine*, Orlando, Fla, Apr. 2005.

[173] M. Sulindro and M. Lam, *How To Stay Young and Live Longer*, 2nd ed. Pasadena, CA: Academy of Anti Aging Research, Sep. 2001, 136–147.

[174] R. Klatz and C. Kahn, *Grow Young With Hgh: The Amazing Medically Proven Plan to : Lose Fat, Build Muscle, Reverse the Effects of Aging, Strengthen the Immune System, Improve Sexual Performance*, 1st ed. New York: Harpercollins, Apr. 1997.

[175] M. A. Farage, K. W. Miller, and H. I. Maibach, *Textbook of Aging Skin*. Springer Science & Business Media, Dec. 2009.

[176] M. Gray, "Preventing and managing perineal dermatitis: a shared goal for wound and continence care," *Journal of Wound, Ostomy, and Continence Nursing: Official Publication of The Wound, Ostomy and Continence Nurses Society*, vol. 31, no. 1 Suppl, pp. S2–9; quiz S10–12, Feb. 2004.

[177] J. M. Waller and H. I. Maibach, "Age and skin structure and function, a quantitative approach (I): blood flow, pH, thickness, and ultrasound echogenicity," *Skin research and technology: official journal of International Society for Bioengineering and the Skin (ISBS) [and] International Society for Digital Imaging of Skin (ISDIS) [and] International Society for Skin Imaging (ISSI)*, vol. 11, no. 4, pp. 221–235, Nov. 2005.

[178] N. I. o. D. Abuse, "Nationwide Trends." [Online]. Available: https://www.drugabuse.gov/publications/drugfacts/nationwide-trends

[179] E. Farazdaghi and A. Nait-Ali, "Face aging predictive model due to methamphetamine addiction," in *2016 International Conference on Bio-engineering for Smart Technologies (BioSMART)*, Dec. 2016, pp. 1–4.

[180] H. Shekarchizadeh, M. R. Kahmi, S. Z. Mohebbi, H. Ekhtiari, and J. I. Virtanen, "Oral Health of Drug Abusers: A Review of Health Effects and Care," *Iranian Journal of Public Health*, vol. 42, no. 9, pp. 929–940, Sep. 2013.

[181] "www.drugabuse.gov."

[182] M. Cretzmeyer, J. Walker, J. A. Hall, and S. Arndt, "Methamphetamine use and dental disease: results of a pilot study," *Journal of Dentistry for Children (Chicago, Ill.)*, vol. 74, no. 2, pp. 85–92, Aug. 2007.

[183] A. Mandal, "Opioid Side Effects," *News Medical Life Sciences*, Apr. 2010. [Online]. Available: http://www.news-medical.net/health/Opioid-Side-Effects.aspx

[184] "www.facesofmeth.us."

[185] L. H. Kligman, "Photoaging. Manifestations, prevention, and treatment," *Dermatologic Clinics*, vol. 4, no. 3, pp. 517–528, Jul. 1986.

[186] E. Farazdaghi and A. Nait-Ali, "Facial ageing model considering sun exposure effects," in *2017 2nd International Conference on Bio-engineering for Smart Technologies (BioSMART)*, Paris, Aug. 2017.

[187] D. Gawkrodger and M. R. Ardern-Jones, *Dermatology E-Book: An Illustrated Colour Text*. Elsevier Health Sciences, Jul. 2016.

[188] N. G. Jablonski, *Living Color: The Biological and Social Meaning of Skin Color*, 1st ed. University of California Press, Sep. 2012.

[189] R. Yin, Q. Chen, and M. R. Hamblin, *Skin Photoaging*. Morgan & Claypool Publishers, 2015.

[190] "Ultraviolet (UV) Radiation." [Online]. Available: https://www.cancer.org/cancer/cancer-causes/radiation-exposure/uv-radiation.html

[191] B. A. Gilchrest, "A review of skin ageing and its medical therapy," *The British Journal of Dermatology*, vol. 135, no. 6, pp. 867–875, Dec. 1996.

[192] L. Baumann, "Skin ageing and its treatment," *The Journal of Pathology*, vol. 211, no. 2, pp. 241–251, Jan. 2007.

[193] J. Uitto, "Understanding premature skin aging," *The New England Journal of Medicine*, vol. 337, no. 20, pp. 1463–1465, Nov. 1997.

[194] F. Flament, R. Bazin, S. Laquieze, V. Rubert, E. Simonpietri, and B. Piot, "Effect of the sun on visible clinical signs of aging in Caucasian skin," *Clinical, Cosmetic and Investigational Dermatology*, vol. 6, pp. 221–232, 2013.

[195] C. Griffiths, "The clinical identification and quantification of photodamage," *British Journal of Dermatology*, vol. 127, no. S41, pp. 37–42, 1992.

[196] F. Flament, R. Bazin, H. Qiu, C. Ye, S. Laquieze, V. Rubert, A. Decroux, E. Simonpietri, and B. Piot, "Solar exposure(s) and facial clinical signs of aging in Chinese women: impacts upon age perception," *Clinical, Cosmetic and Investigational Dermatology*, vol. 8, pp. 75–84, 2015.

[197] B. Guyuron, D. J. Rowe, A. B. Weinfeld, Y. Eshraghi, A. Fathi, and S. Iamphongsai, "Factors contributing to the facial aging of identical twins," *Plastic and reconstructive surgery*, vol. 123, no. 4, pp. 1321–1331, 2009.

[198] J. R. Gordon and J. C. Brieva, "Unilateral Dermatoheliosis," *New England Journal of Medicine*, vol. 366, no. 16, p. e25, Apr. 2012.

[199] H. C. Okada, B. Alleyne, K. Varghai, K. Kinder, and B. Guyuron, "Facial changes caused by smoking, a comparison between smoking and nonsmoking identical twins," *Plastic and Reconstructive Surgery*, vol. 132, no. 5, pp. 1085–1092, Nov. 2013.

[200] N. Nahvi and D. Mittal, "Medical Image Fusion Using Discrete Wavelet Transform," *International Journal of Engineering Research and Applications*, vol. 4, no. 9, pp. 165–170.

[201] C. Phillips, "Ultraviolet Beauties." [Online]. Available: http://www.cara-phillips.com/ultraviolet-beauties/

[202] A. Morita, "Tobacco smoke causes premature skin aging," *Journal of Dermatological Science*, vol. 48, no. 3, pp. 169–175, Dec. 2007.

[203] M. J. Elders, *Preventing Tobacco Use Among Young People: A Report of the Surgeon General*. DIANE Publishing, Mar. 1997.

[204] "Alcohol and Your Kidneys," *The National Kidney Foundation*, Dec. 2015. [Online]. Available: https://www.kidney.org/atoz/content/alcohol

[205] S. MacMahon, "Alcohol consumption and hypertension." *Hypertension*, vol. 9, no. 2, pp. 111–121, Feb. 1987.

[206] F. M. Z. Heravi, M. Eslahi, E. Farazdaghi, and A. Nait-Ali, "A Morphable Model to simulate rejuvenation trajectory of 3d face images: Preliminary results," in *2016 International Conference on Bio-engineering for Smart Technologies (BioSMART)*, Dec. 2016, pp. 1–4.